PRODUCTION AND PHYSICOCHEMICAL CHARACTERISATION OF BIO-OIL FROM THE PYROLYSIS OF JATROPHA CURCAS WASTE

SEYED AMIRMOSTAFA JOURABCHI, BEng.

THESIS SUBMITTED TO THE UNIVERSITY OF NOTTINGHAM FOR THE DEGREE OF DOCTOR OF PHILOSOPHY

MAY 2015

ABSTRACT

The increasing use of fossil fuels and the impending depletion of their reserves worldwide are driving alternative energy sources as one of the foremost consideration for research in energy, fuel, and power technology. Additionally, the increasing rate of harmful emissions especially carbon dioxide from the increased usage of fossil fuels have led to the need for more environmentally friendly replacement fuels. Presently, bio-oil originating from biomass has been proposed as an alternative fuel to fossil diesel. The aim of this research project is to optimally produce bio-oil in terms of quantity and quality from Jatropha curcas waste by using conventional and fast pyrolysis methods. Jatropha curcas shrub, which can be planted economically in tropical regions like Malaysia, is typically planted as a source of inedible oil for biodiesel production. The leftover pressed cake after oil extraction is an agricultural waste, which can be upgraded into fuel via pyrolysis. In this project, the pyrolysis parameters to achieve optimum quantity and quality of bio-oil from Jatropha curcas waste were determined. To achieve this, two fixed-bed pyrolysis rigs for conventional and fast pyrolysis processes were designed and fabricated, and a corresponding Design of Experiment was performed. By considering yield, calorific value, water content and acidity, the results from both methods were mathematically modelled after comparison and the optimum parameters for both methods were determined. The validated models of conventional and fast pyrolysis showed that optimum combined quantity and quality of bio-oil occur at reaction temperatures of 800 K and 747 K respectively but at the same nitrogen linear velocity of 0.0078 cm/s. At these optimum conditions, conventional and fast pyrolysis yield 50.08 wt% and 40.08 wt% of bio-oil with gross calorific values of 15.12 MJ/kg and 16.92 MJ/kg, water contents of 28.34 wt% and

28.02 wt%, and pH values of 6.77 and 7.01, respectively. The produced bio-oils from both rigs at their optimum points were dehydrated, and the physicochemical characteristics of the dehydrated bio-oils from both rigs were compared to standard specifications for burner biofuels. Based on ASTM D7554-10 standard for burner biofuel specifications, by reducing the sulphur contents, both dehydrated bio-oils can be used as burner fuel without any further processes. Finally, both 10% of optimised and dehydrated bio-oils emulsified in 90% diesel were tested and compared to EN590, the European standards for diesel used in commercial diesel engines and ASTM D6751-01, the standard biodiesel specifications. In addition to sulphur content, if the water content of both of these emulsified dehydrated bio-oils are removed, they can be commercially used as diesel fuel in diesel engines because their solid content, kinematic viscosity, ash content, flash point, cetane number and copper corrosion strip test results are within the range of EN590 standard.

LIST OF PUBLICATIONS

1. M. S. Z. Gui , S. A. Jourabchi, H. K. Ng and S. Gan, "Comparison of the Yield and Properties Of Bio-Oil Produced By Slow and Fast Pyrolysis of Rice Husks and Coconut Shells" Applied Mechanics And Materials 625, 626–629, Trans Tech Publications, Switzerland 2014.
2. S. A. Jourabchi, S. Gan and H. K. Ng "Pyrolysis of Jatropha curcas Pressed Cake for Bio-oil Production in a Fixed-Bed System" Energy Conversion and Management 78, 518–526, 2014.
3. S.A. Jourabchi, S. Gan and H. K. Ng. "Investigation of pyrolysis parameters on the yield and quality of bio-oil from Jatropha curcas wastes" Developments in Sustainable Chemical and Bioprocess Technology, 81–87, Springer, United State of America, 2013.
4. S.A. Jourabchi, S. Gan and H. K. Ng. "Pyrolysis of Jatropha curcas wastes to produce bio-oil" Fuelling the future: advances in science and technologies for energy generation, transmission and storage, 93–97, BrownWalker Press, 2012.
5. S.A. Jourabchi, S. Gan and H. K. Ng. "Production and physico-chemical characterisation of bio-oil from the pyrolysis of Jatropha curcas wastes" Proceedings of the 14th Asia Pacific Confederation of Chemical Engineering Congress (APCChE), 882–883, Singapore, 2012.

ACKNOWLEDGEMENTS

In the name of God that gave me this opportunity to learn a piece of his unlimited knowledge. Quran (2:32): They told God, "Exalted are You; we have no knowledge except what You have taught us. Indeed, it is You who is the Knowing, the Wise.".

This thesis entirely is presented to my late father (Seyed Ali Jourabchi) and mother's (Parvin Sadat Hoseini Far) souls. God bless their souls. With their encouragement and motivation, I have been guided to be a curious person with a thirst for knowledge.

My greatest gratitude goes to my supervisors, Professor Dr. Gan Suyin and Professor Dr. Ng Hoon Kiat. They were not only my supervisors, but I have felt closer than a family to them. Their motivation, encouragement, guidance and support have been unlimited towards me. I hope one day I can be as good a lecturer and a researcher just like them. That is my goal.

I would like to thank the previous Dean of Engineering, Professor Dr. Michael Cloke who listened to me and trusted in me by offering a scholarship for my PhD study.

I would like to thank my wife, Rosita who has been patient throughout our adventurous life especially for the past ten years that she moved to Malaysia with me and sacrificed her life back in Iran to support me in this study. I really appreciate that.

Also, I would like to thank my son, Ali who has been the fun of my life all the time. His patience, sacrifices and jokes also made me happy and kept my spirit to finish what I have started. I wish him all the best in his life.

In addition, I would like to thank my three lovely sisters (Zahra, Masoumeh and Niusha) who have supported me throughout my life. Without their help and sacrifices, the journey of PhD was impossible for me.

Finally, I would like to thank all other people who have helped me in my PhD at the University of Nottingham Malaysia and United Kingdom Campuses. These include laboratory technicians, other respected lecturers, and other staff; without their help, this study would not have been possible.

TABLE OF CONTENTS

LIST OF FIGURES

LIST OF TABLES

NOMENCLATURE

ABBREVIATIONS

^{13}C NMR	^{13}C Nuclear Magnetic Resonance
AES	Auger Electron Spectroscopy
ASTM	American Standard Test Method
BS	British Standard
CCTED	Collision Cell Technology with Energy Discrimination
CP/MAS	Cross-Polarization/Magic Angle Spinning
CPDB	Conventional Pyrolysis Dehydrated Bio-oil
CPDB BO10	emulsion of 9.5 wt% of Conventional Pyrolysis Dehydrated Bio-oil and 0.5 wt% methanol in 90 wt% diesel
DDJO	De-waxed and De-gammed Jatropha curcas Oil
DoE	Design of Experiment
DSC	Differential Scanning Calorimetric
ECHA	European Chemical Agency
EDS	Energy-Dispersive Spectroscopy
EDX	Energy-Dispersive X-ray spectroscopy
EN	European Standards

ENSYN Environmental Synthesiser (Trade mark name)

FFA Free Fatty Acid

FPDB Fast Pyrolysis Dehydrated Bio-oil

FPDB BO10 emulsion of 9.5 wt% of Fast Pyrolysis Dehydrated Bio-oil and 0.5 wt% methanol in 90 wt% diesel

HPL High Pressure Liquefaction

HYPZ High Yield Production Zone

ICP-MS Inductively Coupled Plasma Mass Spectrometry

IQT Ignition Quality Tester

JME Jatropha Methyl Ester

LLE Liquid-Liquid Extraction

LTC Low Temperature Conversion

ME Methyl Ester

MP Malaysian Plan

MIG Metal Inert Gas (welding method)

MOA Ministry of Agriculture and Agro-Based Industry Malaysia

MSDS Materials Safety Data Sheet

NEG Net Energy Gain

NER Net Energy Ratio

NREL National Renewable Energy Laboratory

REACH Registration, Evaluation and Authorization of Chemicals

RMS Root Mean Square

TCD-IR Thermo Conductivity Detector Infra-Red

TGA Thermo-Gravimetric analysis

TIG Tungsten Inert Gas (welding method)

XPS X-ray Photoelectron Spectroscopy

XRD X-Ray Diffraction Analysis

UK United Kingdom

UN United Nations

UNFCCC United Nations Framework Convention on Climate Change

CHEMICAL FORMULAE, UNITS AND SYMBOLS

^{o}C Celsius (temperature unit)

μ Dynamic viscosity

ρ Density

V^{0} Volumetric flow rate of fluid

Al Aluminium

C Carbon

Ca Calcium

CO Carbon monoxide

CO_2 Carbon dioxide

C_p Specific heat capacity at constant pressure

Fe Iron

G Giga

Gt Giga tonne

h Convection heat transfer coefficient

H_2 Hydrogen

hr Hour(s)

k Thermal conductivity

K Potassium

K Kelvin (temperature unit)

m^o Mass flow rate

Mg Magnesium

min Minute(s)

N_2 Nitrogen

Na Sodium

NO_x Nitrogen oxides

O_2 Oxygen

P Phosphorus

P_r Prandtl number

R_e Reynolds number

s Second(s)

S Sulphur

Si Silicon

x^o Linear velocity

CHAPTER 1 INTRODUCTION

1.1 Background

1.1.1 Fossil Fuels

Over the last hundred years, a seventeen-fold increase in energy consumption has resulted in increasing use of fossil fuels and depletion of fossil fuels reserves worldwide [1–2]. Based on the International Energy Agency report in 2011 [3], more than 75% of the world's total primary energy supply originates from non-renewable fossil fuels such as coal, oil and natural gas. However, the political and economic instability of many of the fossil fuels producing countries have caused fuel price fluctuation and an overall increase in fuel cost with time.

The usage of fossil fuels as the main source of energy has resulted in the accumulation of greenhouse gases in the atmosphere. For instance, while the annual carbon dioxide (CO_2) emission globally is about 22 Gt, its potential emission from available fossil fuel resources in China alone can reach up to a total of 225 Gt [4]. Figure 1 - 1 shows that CO_2 emission per capita has increased dramatically in the last 40 years in two developing countries (over 250% and 350% increase in Iran and Malaysia respectively). The same source indicated that global emission of CO_2 per capita has increased from 3.08 to 4.89 tonnes per capita from 1960 to 2010 [5]. By considering the growth of human population declared by the United Nations (UN), which is approximately 3.5 billion in 1970 and close to 7 billion people in 2009, it can be deduced that the CO_2 emission has more than doubled during the past 40 years [6].

The current energy scenario coupled with the increasing amount of greenhouse gases, particularly CO_2, and pollutant emissions from the combustion of fossil fuels have led to

intense research on sustainable and environmentally-friendly alternative fuels such as biodiesel, bio-ethanol and biomass.

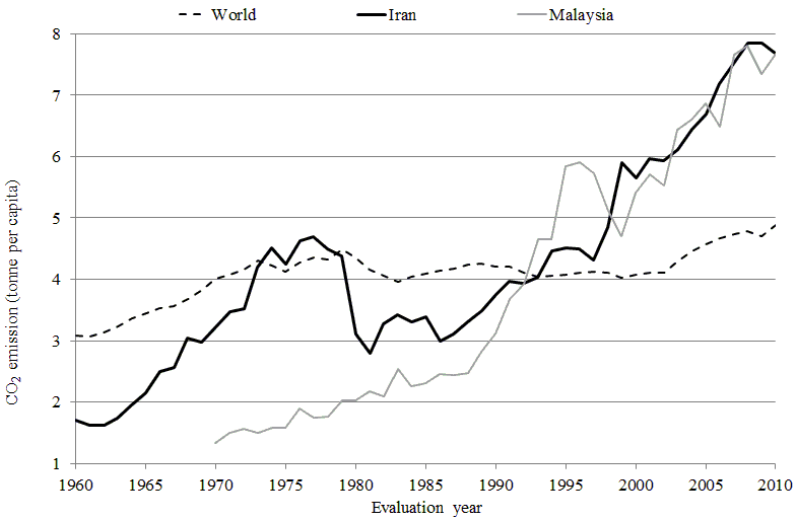

Figure 1 - 1 CO_2 emission globally and in two developing countries [5]

1.1.2 Biomass

Biomass based on its availability and its status as a waste product is one of the prime sources of renewable energy worldwide. Biomass originates from plants or their by-products that are produced completely or partly by photosynthesis such as forestry residues, agricultural bi-products or animal wastes that can be used as a source of energy [7]. In the year 2002 alone, 117 billion tonnes in oven dry weight of plant biomass was produced around the world including 80 billion tonnes of forest residues, which is equivalent to 40 billion tonnes of petroleum fuel [8]. Only in Korea, more than 2.4 million tonnes of furniture waste has been produced in the past three years [9]. Biomass already contributes approximately 14% of the total energy source worldwide and up to 50% in developing countries [10–11]. It was also the third biggest energy source after coal oil and natural gas in the year 2000 [12].

Not only can biomass be considered based on its availability, but as a fuel, it offers the advantages of reducing nitrogen oxides (NO_x) and sulphur oxides (SO_x) emissions due to its low nitrogen (N) and sulphur (S) contents [7, 11]. The lower metal content in biomass as compared to fossil fuels is also another advantage [13]. Furthermore, due to its renewable origin, its greenhouse effect is lesser or can be assumed to be zero [11]. Figure 1 - 2 shows how a sample biomass utilisation cycle produces a variety of fuels while achieving a zero net CO_2 emission [14].

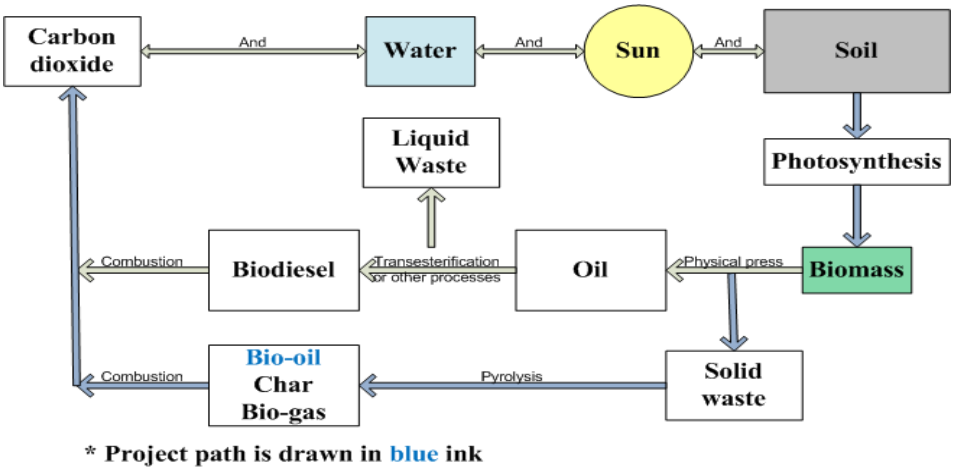

Figure 1 - 2 Sample biomass utilisation cycle. Adapted from [14]

In the United Kingdom (UK), the government has initiated a long term plan for reduction of CO_2 emission up to 20%, 60% and 80% by the years 2010, 2050 and 2100, respectively by using different kinds of green energy including biomass to generate electricity [15]. Parallel to the UK, renewable energy initiatives were first introduced in 5th Malaysia Plan (MP) in 1986 in Malaysia. In the Second National Communication to the UNFCCC (United Nations Framework Convention on Climate Change), the Ministry of Natural Resources and Environment of Malaysia announced in 2010 that

from 1995, during the 7th MP till the 9th MP, RM 154 million (Ringgit Malaysia) for 176 university research and industrial projects have been supported utilising renewable energy resources such as biomass, solar, mini-hydro, winds and oceans [16].

1.1.3 Pyrolysis Bio-oil

Pyrolysis, which is a thermochemical decomposition process that occurs at elevated temperatures in the absence of oxygen gas, is considered as one of the ways in utilising biomass as a source of energy. Biomass pyrolysis produces gas and liquid products, and leaves a solid residue known as char. The liquid product is a fuel termed as bio-oil. Based on practicality in various applications, especially in storage, liquid fuel is a highly safe and desirable form in comparison to gaseous or solid fuels [17]. In addition, it can be stored and transported more efficiently compared to the original biomass. That is a key reason why biodiesel was developed to be used in a variety of applications especially in diesel engines. Nevertheless, the sources of most biodiesels are edible plant feedstock. Using inedible sources of fuel is now more important to prevent undesirable economic effects on food prices globally. In light of the current scenario, bio-oil has thus been proposed as a fuel, which mitigates the problems faced by biodiesel. Presently, bio-oil produced from the pyrolysis of biomass can be used directly, or after further physicochemical processes to heat up boilers, or even drive diesel engines or turbines [17–18]. During the combustion of bio-oil, its net zero CO_2 as well as lesser NO_x and/or SO_x emissions as compared to fossil fuels makes it a potential liquid fuel replacement [19].

1.1.4 Jatropha curcas

In this study, the feedstock of interest is Jatropha curcas, a drought-free and inedible crop, which can be planted economically in tropical and sub-tropical regions [20]. Its

seed is a source of oil that is used currently for commercial biodiesel production. Locally in Malaysia, the Ministry of Agriculture and Agro-Based Industry (MOA) has identified Jatropha curcas as a new emerging crop and is emphasising more research on this crop, from development of suitable varieties to production technologies for maximum biofuel yield. With the introduction of Jatropha curcas planting schemes under the Bionas Agropolitan Technology Corridor Development, and with more than 420,000 tonnes of Jatropha curcas pure biodiesel being exported from the leading Bionas Group yearly (in 2012), it is evident that more research on this crop is necessary to maximise the benefits of growing Jatropha curcas [21].

In terms of Jatropha curcas biodiesel usage in engines, research has demonstrated that diesel engine could run without any modifications using a 10% mixture of de-waxed and degummed Jatropha curcas oil in normal diesel while blends up to 50% could be used by preheating the fuel up to 333 K [22]. Another study also proved that Jatropha curcas oil either preheated or in low blend concentrations, resulted in combustion performance and emission characteristics close to that of mineral diesel in a single-cylinder, direct injection diesel engine [23].

Nevertheless, the extraction of oil for the purpose of biodiesel production only takes up to 18 wt% of the dry fruit, but it has been reported that the remaining Jatropha curcas fruit after biodiesel production has the potential of fuel production with twice the energy content as compared to biodiesel [22]. A research study carried out in Thailand which models the future scenario up to 20 years reported that Jatropha curcas plantation for the purpose of biodiesel can have a Net Energy Ratio (NER)[1] of up to 1.42 [24]. The same study also reported that the NER can be improved by up to 6.03, if Jatropha curcas is utilised holistically. Different parts of the Jatropha curcas shrub can

[1] $\text{NER}=\frac{\text{The total energy content of bio-fuels that is being produced}}{\text{The total energy consumed for production of bio-fuels from initial plantation to final product}}$

be utilised in a number of thermochemical processes [24]. For example, it has been shown that Jatropha seed husk could successfully be used as feedstock for open core down draft gasifier to generate producer gas [25]. For pyrolysis, approximately 50 wt% of its nutshell can be transformed into bio-oil, and even its wood and leaves can be valorised for fuel extraction [19].

The pressed cake remaining after oil extraction is considered as waste. This waste has the potential to be used as a source of bio-oil production [12]. In one study, thermo-gravimetric analysis (TGA) and a fixed-bed quartz reactor were used to determine a suitable degradation model and to investigate the effect of operating conditions on product distribution [12]. It was found that the main thermal decomposition occurred over the temperature range of 523 K to 723 K, and could be described by the three-parallel reactions model. The temperature and hold time within the fixed-bed quartz reactor influenced the yields of gas, liquid and char products, although full optimisation was not carried out. Similarly, parametric studies of fast and flash pyrolysis of Jatropha oil cake in electrically heated reactors using nitrogen (N_2) have been carried out [26]. Maximum oil yield of 64.25 wt% was obtained at a particle size of 1.0 mm, a pyrolysis temperature of 773 K, and a N_2 flow rate of 1.75 m^3/h. The obtained pyrolysis oil had a calorific value of 19.66 MJ/kg, and could be used as a source of low-grade fuel directly or upgraded to a higher quality bio-fuel. Meanwhile, another investigation on the use of the Low Temperature Conversion (LTC) process at temperatures between 653 and 693 K to pyrolyse Jatropha curcas fruit and cake has been carried out [27]. It was documented in this work that binary mixtures of diesel and pyrolysis oil containing up to 10% pyrolysis oil were very effective while binary mixtures containing between 10% and 20% pyrolysis oil were not very effective because of the higher viscosity and sulphur content.

1.2 Problem Statement

To date, while a number of research studies have indicated the potential of Jatropha curcas wastes as pyrolysis feedstock, full optimisation of pyrolysis parameters to maximise not only bio-oil yield, but also quality is lacking. In addition to calorific value, which can be considered as one of the most important specification of any fuel other important characteristics of bio-oil such as water content and acidity need to be considered for optimisation purpose [28–29]. Furthermore, on fixed-bed reactor setup, the main parameter that has been investigated in the literature is limited to reaction temperature. In contrast, fast pyrolysis which is distinguished by a high heating rate of biomass followed by a high cooling rate of the volatiles, has been the scope of many studies, especially for the production of bio-oil [17]. Hence, the parameters associated with this method also need to be investigated and optimised for Jatropha curcas waste. Apart from optimisation of both methods, investigating both conventional and fast pyrolysis methods provides an opportunity to compare the yield and quality of the final products for both methods. Finally, in view of future commercialisation, the physicochemical properties of the optimised Jatropha curcas bio-oil need to be determined and compared with current available fuel standards.

1.3 Research Aim and Objectives

The aim of this research project is to optimally produce bio-oil in terms of quantity and quality from Jatropha curcas pressed cake by using conventional and fast pyrolysis methods. The specific objectives are as defined below:

- Characterisation of Jatropha curcas pressed cake to verify its viability as a biomass source for this research project.

- Design and fabrication of two laboratory-scale pyrolysis reactors (for conventional and fast pyrolysis methods), and their respective condensers.
- Development and validation of empirical correlations to relate yield and key specifications of the produced bio-oil to pyrolysis parameters for both conventional and fast pyrolysis methods based on the Performed Design of experiment.
- Determination of the optimum parameters for best combined quantity and quality of bio-oil using the developed mathematical models for both pyrolysis methods.
- Physicochemical characterisation of the optimised bio-oil products and comparing the final produced fuel quality with current fuel standards.

1.4 Thesis Outline

This thesis comprises eight chapters in total. The content of each of the chapters is briefly described in the following:

Chapter 1 Introduction: This chapter sets the background to the research project. An overview of fossil fuels and their negative impacts, as well as the need for biomass as a renewable energy source is presented. The chapter next describes pyrolysis bio-oil and its benefits, and Jatropha curcas as the feedstock of interest in this work. The problem statement is then discussed followed by the research aim and objectives.

Chapter 2 Literature Review: This chapter is a review of related research works on bio-oil, its production and characterisation, as well as pyrolysis systems. The chapter starts with an overview of bio-oil and physicochemical characterisation including the available standards for this new bio-fuel. Next, the chapter expands on the Jatropha curcas plant itself and its applications, followed by a review of available resources on

Jatropha curcas bio-oil. Then, the chapter discusses the pyrolysis process, its parameters, different types of pyrolysis and available pyrolysis systems. The chapter concludes by highlighting the area of needed research based on current available papers.

Chapter 3 Reactor Design and Fabrication: This chapter focuses on the design of the conventional and fast pyrolysis rigs. Descriptions of the design parameters including reactor material, heat transfer, reaction temperature, and N_2 velocity are firstly given. The design calculations for fixed-bed conventional and fast pyrolysis rigs are then presented followed by the test results of seven different design setups. Also, the chapter reports on the fabrication of both conventional and rapid heating (fast) pyrolysis rigs.

Chapter 4 Jatropha curcas Pressed Cake Physicochemical Characterisation: In this chapter, physicochemical characterisation of the Jatropha curcas pressed cake is reported. Thermo Gravimetric Analysis (TGA) and Differential Scanning Calorimetry (DSC) tests were used to model the conventional pyrolysis rig which is later used in Chapter 5 for calculation of energy balance in pyrolysis process. Additionally, organic and inorganic elements and other important organic compounds were also measured by using a variety of methods. All results are reported and a brief conclusion of the findings finalises the chapter.

Chapter 5 Parametric Investigation of Conventional Fixed-bed Pyrolysis and Rapid Heating Fast Pyrolysis: This chapter focuses on both conventional and fast pyrolysis processes by using fixed-bed and rapid heating pyrolysis rigs respectively. After describing and carrying out the Design of Experiments (DoE) methodology, the results from both rigs are presented and discussed. In addition, this chapter also compares the results obtained from the two different reactor setups. Apart from that, by

simulating the pyrolysis in TGA/DSC unit the energy balance for the conventional pyrolysis method is also investigated in this chapter.

Chapter 6 Empirical Correlations Development and Process Optimisation: In this chapter, mathematical models for conventional and fast pyrolysis processes' results from Chapter 5 are developed. Subsequently, the optimum experimental parameters for the production of bio-oil are determined by normalisation method using the developed mathematical models and validated against experimental tests.

Chapter 7 Bio-oil Physicochemical Characterisation: This chapter describes the physicochemical characterisation of the optimally produced bio-oils. The results are compared to standard specifications of diesel, biodiesel and burner biofuels, and each of the specifications is discussed separately.

Chapter 8 Conclusions: The final chapter of this thesis presents the main outcomes of the study which are in line with the specific objectives. The chapter concludes by suggesting potential areas of research for future work.

CHAPTER 2 LITERATURE REVIEW

2.1 Bio-oil

Bio-oil is a dark brown highly oxygenated liquid with a pungent odour, originating as one of the end products of biomass pyrolysis especially fast pyrolysis [17–18, 26]. Historically bio-oil originated from the ancient Egyptians. At the time of the Pharaohs in Egypt, pyrolysis was used to produce tar that was used to seal Egyptian boats and to cover and preserve their dead bodies [17–18].

High Pressure Liquefaction (HPL) and fast pyrolysis are two conventional thermo-chemical processes for producing bio-oil out of biomass, but the HPL process which produces only 30 wt% bio-oil has been suppressed by almost 80 wt% production in the fast pyrolysis process currently [30]. Bio-oil has a variety of names such as pyrolysis oil, pyrolysis liquid, bio-crude oil, wood liquid, wood oil, liquid smoke, wood distillates, pyroligneous acid, liquid wood, pyrolytic tar or even tar [17]. Recently bio-oil is being used instead of light and heavy oil, in pilot, commercial and even industrial scale boilers around the world [14]. In the UK, Omrod diesel has tested bio-oil on a dual fuel diesel engine at medium velocity with satisfying results [15].

Table 2 - 1 is a list of biomass and their respective bio-oil yields based on different pyrolysis conditions. It can be observed that up to 65 %wt of biomass has the potential to produce bio-oil and a variety of biomass sources can be used in obtaining bio-oil. It need to be mentioned that in this research study (the whole thesis) it is assumed that $T_K=273+T_C$ and the decimal figures for this exchange of the temperature units are neglected.

Table 2 - 1 Different biomass and their bio-oil yields from pyrolysis processes

Biomass	Pyrolysis process	Pressurized	Inert fluid		Temperature K	Yield (%wt)	Reference
			type	Velocity ($\frac{cm}{s}$)			
Sunflower cake	Conventional	No	N_2	1.78	823	48.69	[7]
Sawdust	Fast			1.66	698	65	[9]
Cotton straw				6.6	823	35	[13]
Cottonseed cake				3.3	823	35	[31]
Wheat straw	Conventional	40 psi		0.87	773	37.6	[32]
Rice straw	Fast	No			683 – 783	50	[33]
Sesame stalk				6.63	823	37.2	[34]
Olive cake				1.75	823	39.4	[35]
Olive residue				1.36	823	38.12	[36]
Alfalfa stem					673 – 773	53	[37]
Hazelnut shell	Conventional			1.75	773	23.1	[38]

Data extracted from sources and processed

2.1.1 Physicochemical Properties of Bio-oil

Bio-oil consists of approximately 200 organic materials and can be used not only as a fuel, but also as a feedstock for the production of different chemical components [39]. It also contains up to thousands of different components within the five main categories of alcohols, phenolics, ketones, aldehydes, and organic acids [26]. Acids, aldehydes, alcohols and ketones are the products from cellulose and hemicellulose of biomass, while phenolics and cyclic oxygenates are the products from lignin [40].

One of the most critical objectives of pyrolysis is the production of bio-oil such that its hydrocarbons lie within the range of conventional hydrocarbons fuels [41]. To achieve that, uncomplicated reaction steps can be performed such as thermally induced separation, polymerisation, further cracking and aromatisation [41]. Bio-oil is acidic with a pH within the range of 2 to 4 depending on the source and water content [4]. Normally, formic and acetic acids reduce the pH of the produced bio-oil [40]. The bio-oil product specifications are strongly correlated to the biomass type. As an example, soybean bio-oil stands out from most bio-oils with a pH of 5 to 7 which is not acidic at all [42].

For comparison purpose, Table 2 - 2 shows a comparison of the analysis of physicochemical properties of two bio-oils extracted from wood using two different processes against conventional diesel fuel. The processes are the ablative process developed by the National Renewable Energy Laboratory (NREL) and the rapid thermal process from Environmental Synthesiser (ENSYN).

Table 2 - 2 Physicochemical properties of two bio-oil analysis comparing to diesel fuel [43]

Physicochemical property	Unit	NREL	ENSYN	Diesel fuel
Water content	(wt%)	16.9	26.3	-
Calorific value	(MJ/kg)	17.0	16.3	44.0
Air/Fuel ratio*	-	6.45	5.62	14.50
C	(wt%)	58.25	57.95	87
H		7.40	7.23	13
N		1.52	1.64	-
O (calculated)		32.83	33.19	-

* Stoichiometric combustion

Both ENSYN and NREL bio-oils have been tested on a diesel engine and the results focussed specifically at ignition delay [43]. The results showed that the lower water content in the NREL bio-oil was the most important parameter in achieving better performance on the diesel engine as compared to the ENSYN bio-oil [43]. Bio-oil has the potential to attract water because of its high oxygen content leading to a high polarity [40]. In addition to water content, the lack of homogenous heat transfer to biomass in a pyrolysis bed can prevent high calorific volatiles cracking resulting in a high calorific value char and a low calorific value bio-oil [40].

Vegetable oils are unlimited sources of biofuel as they have similar energy content as diesel. If bio-oil is the product of direct pyrolysis of vegetable oil, its components are chemically similar to conventional diesel [44–45]. In Table 2 - 3, the physicochemical properties of bio-oil produced by direct pyrolysis of rapeseed oil are tabulated and for each property, the relevant ASTM test method used is included. To find the bio-oil empirical formula, Electron-Impact Mass Spectrometry method with low energy is one

of the most effective ways by projecting molecular weight distribution without any sample preparation prior to testing [46].

Table 2 - 3 Physicochemical properties of bio-oil produced from pyrolysis of rapeseed oil [45]

Physicochemical property	Unit	ASTM	Result
Density at 303 K	kg/m^3	D 1298	918
Water content	wt%	D 1744	-
Viscosity at 323 K	cSt	D 88	43
Flash point	K	D 93	359
Conradson residue	wt%	D 189	0.05
Calorific value	MJ/kg	D 3286	38.4
C	wt%	D 482	74.04
H		D 3177	10.29
N		-	3.97
O (by difference)		-	11.70

Emulsions of bio-oil in conventional diesel upgrade the bio-oil quality for practical applications [47]. Apart from experimental measurements, the characteristics of bio-oil emulsions in diesel can also be predicted using mathematical models as reported in one study for cetane number as shown in Figure 2 - 1 [47].

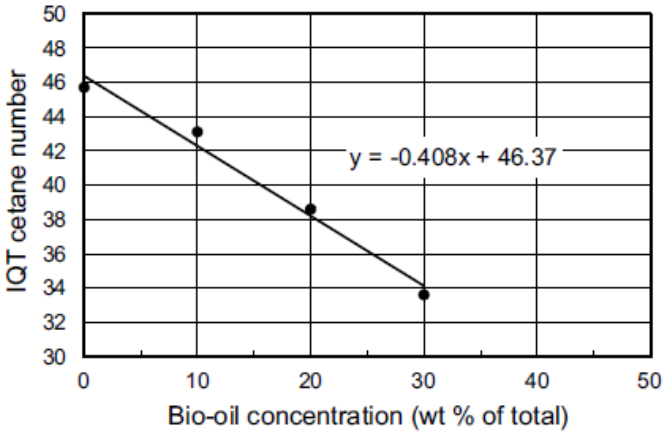

Figure 2 - 1 Cetane number of bio-oil and diesel emulsions [47]

Normally, due to the unpredictable combustion quality of bio-oil, experimentally determining the cetane number is not an easy task, but as can be observed in Figure 2 - 1, by using the emulsions and mathematical interpolation, the cetane number of bio-oil emulsions can be predicted [47].

2.2 Bio-oil Standardisation

Bio-oil is an alternative fuel which was only recently produced on a commercial scale. Thus, similar to conventional fuel, standardisation of its quality is necessary [28]. Instead of modifying diesel engines or gas turbines to suit bio-oil usage, the more logical way is to produce a bio-oil that can be used in existing applications without any modifications [47]. As an example, bio-oil viscosity is not only higher than conventional fuels, but also increases with aging, hence different methods may be required to test the bio-oil, and new standards needed to categorise its quality level [28]. As a general comparison, the typical bio-oil physicochemical properties are compared to American mineral oil in Table 2 - 4. For each physicochemical property of bio-oil, a standard testing method has been introduced and the compiled test methods are tabulated in this table.

Table 2 - 4 Comparison of physicochemical properties of typical bio-oil and mineral oil [28]

Physicochemical property	Unit	Test method	Typical bio-oil	Mineral oil
Water	wt%	ASTM E 203	20 – 30	0.5 max
Solid		Filtering	0.5 max	-
Ash		ASTM D 482	0.2 max	0.1 max
Sulphur		-	0.05 max	varies
Nitrogen		-	0.4 max	-
Stability	-	-	unstable	-
Viscosity at 313 K	cSt	ASTM D 455	15 – 35	5.5 – 24
Density at 288 K	kg/m^3	ASTM D 4052	1100 – 1300	-
Flash point	K	ASTM D 93	277 – 383	328 min
Pour point	K	ASTM D 97	264 – 237	267 min
Calorific value	MJ/kg	ASTM D 240	13 – 18	-
pH	-	-	2 – 3	-
Distillability	-	-	Not distillable	-

By the year 2009, standard physicochemical properties for biofuels as an ASTM burner fuel have been published in ASTM D7544 as shown in Table 2 - 5 [28–29]. The Registration, Evaluation, and Authorization of Chemicals (REACH) has been established in EU and the European Chemical Agency (ECHA) is managing all the REACH mentioned processes [28]. The Materials Safety Data Sheet (MSDS) has been

initiated for the registration of bio-oil products under CAS 94114-43-9 category [28]. For the approval of standard bio-oil as burner fuel, the testing of solid content of bio-oil is expected to be improved [28]. Currently, work on other bio-oil standards for turbine and diesel engine applications is being carried out.

Table 2 - 5 Physicochemical properties specifications for pyrolysis liquid biofuels in ASTM D7544 [28]

Physicochemical property	Test method	Specification	Units
Gross calorific value	D240	15 min	MJ/kg
Water content	E203	30 max	mass %
Pyrolysis solids content	Annex A1	2.5 max	mass %
Kinematic viscosity at 40°C	D445[a]	125 max	mm^2/s
Density at 20°C	D4052	1.1–1.3	kg/dm^3
Sulphur content	D4294	0.05 max	mass %
Ash content	D482	0.25 max	mass %
pH	E70-07	Report	
Flash point	D93 B	45 min	°C
Pour point	D97	–9 max	°C

2.3 Bio-oil from Jatropha curcas

2.3.1 Jatropha curcas

Jatropha curcas as shown in Figure 2 - 2 is a non-edible, fast-growing shrub with high resistance to drought and is simple to cultivate [20, 25, 48–49]. Jatropha curcas can be found in Southeast Asia, India, Central and South America, and Africa [20, 25, 48-49]. It belongs to a group of shrub species having more than 70 genotypes such as Jatropha gossypiifolia and Jatropha pohliana [20, 48]. Physic nut, ratanjyoti, bagbherebdra, big purge nut, Barbados purging nut, black vomit nut, Habb-El-Mueluk, pinoncillo and purging nut are all different names in different regions worldwide for Jatropha curcas [50]. This species originates from the Caribbean and was used by the Mayas for many years; thereafter, it was taken to Africa by the Portuguese and distributed to different countries in Africa and Asia [48]. Today, it can be found in most tropical and subtropical regions around the world [20]. Depending on the species and

weather, it can grow up to approximately 3 to 8 meters high [50]. Having over 60 wt% oil in its kernel has made this shrub a source for fuel in addition to being a feedstock for the production of soap, lubricant and wood coating [50].

Figure 2 - 2 Plant, leaves, fruits and seeds of Jatropha curcas [51]

2.3.2 Cultivation Viability

Economically, the area of cultivation of a plant for large scale production should be considered when choosing an appropriate biomass for pyrolysis [49]. For any project related to large scale bio-fuel extraction from Jatropha curcas, the plantation method and potential cultivation zone are essential. In an interview conducted with the staff of Bionas Company (Malaysia) on February 2010, it was stated that tentative plantation could be carried out in any climate without freezing temperatures [21]. The plant starts producing limiting amount of fruits from its second year of life and this can reach up to 5 kg production for each tree in its fifth year of life up to 50 years [25]. Normally, 35 to 50 wt% of each fruit is contributed by the shell while the seed contributes 50% to 65 wt% [25]. Each fruit has an average length of 2.5 cm and approximately 422 fruits or 1600 seeds have a mass of 1 kg [22, 25]. After drying, the shell and seed of Jatropha curcas fruit have weight percentages of approximately 37.5% and 62.5%, respectively

of which the kernel has a share of 58 wt% of the seed with husk forming the balance (Figure 2 - 3) [22].

Figure 2 - 3 Jatropha curcas fruit and its compositions [22]

Jatropha curcas propagation can be carried out through seeding or cuttings [50]. Defining areas worldwide with the potential of high yield production is important in cultivating this plant. Table 2 - 6 lists the regions around the world with medium to high yields of Jatropha curcas production [52].

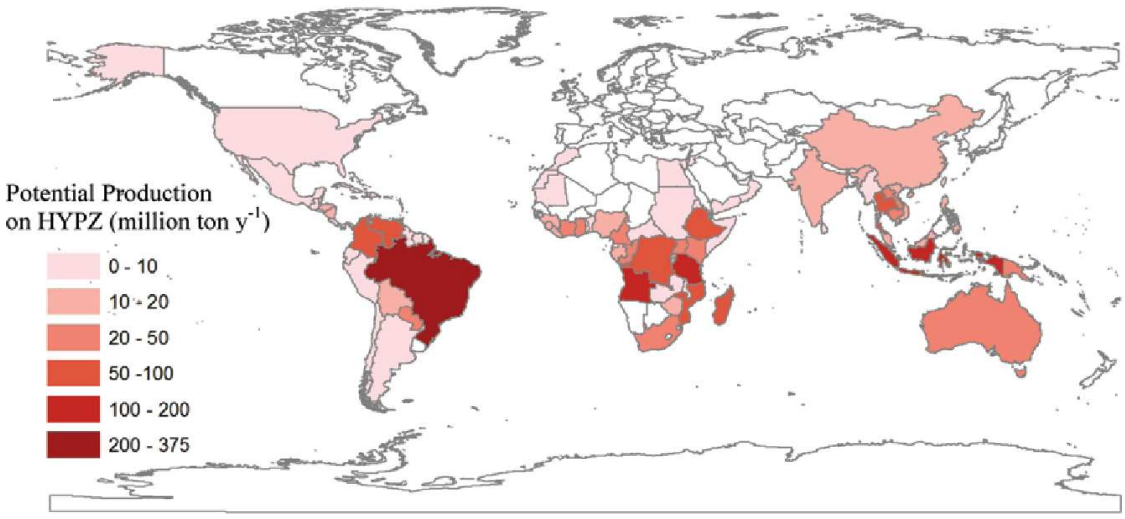

Figure 2 - 4 Jatropha Curcas potential production of high yield production zone (HYPZ) [52]

Table 2 - 6 Potential area and dry seed production of high-yield Jatropha curcas producing zones at global, regional and national levels [52]

Area	Production	Area
	10^6 ton/year	10^4 km^2
Global	1955.7	604.2
Continents		
Africa	904.8	
South America	575.5	
Asia	368.6	113.5
North America	83.3	25.3
Oceania	23.5	7.5
National level (top 10 countries)		
Brazil	374.8	116.2
Angola	145.1	45.9
Indonesia	127.3	38.4
Tanzania	112.3	34.9
Zaire	87.0	27.4
Ethiopia	65.4	20.5
Madagascar	63.0	19.3
Columbia	60.4	18.4
Thailand	54.4	16.9
Venezuela	53.0	15.9

By using computer modelling and considering the climate around the globe, the potential plantation areas of Jatropha curcas can be graphically shown as in Figure 2 - 4. Malaysia is in the zone with the potential of producing 10 to 20 million ton of dry seed in one year, which is classified as a High Yield Production Zone (HYPZ).

2.3.3 Jatropha curcas Applications

Some applications, especially biodiesel, have high impacts on bio-oil research and development because the source of bio-oil is often the waste product of biodiesel production. A summary of practical applications of Jatropha curcas can be seen in Figure 2 - 5. Through bio-refinery, a variety of products can be expected from Jatropha curcas for the commercial market as depicted in Figure 2 - 6.

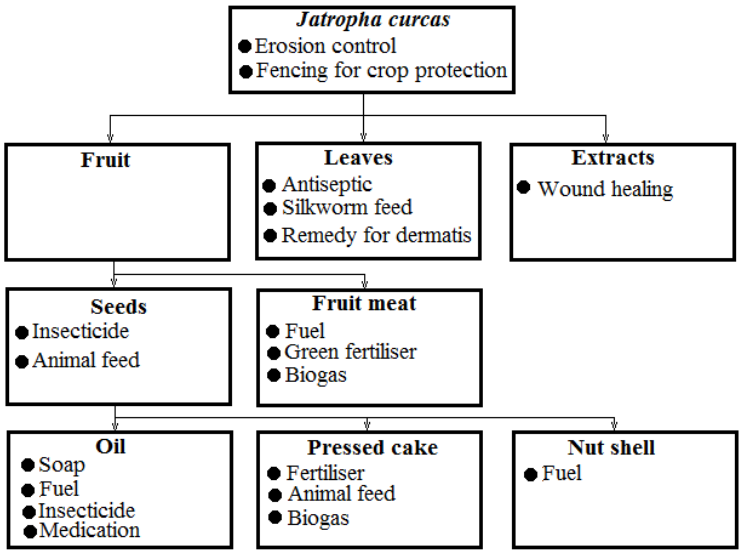

Figure 2 - 5 Practical applications of Jatropha curcas [26]

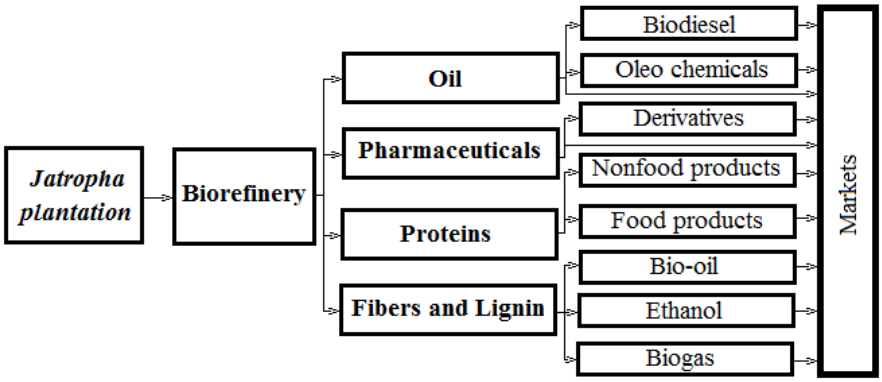

Figure 2 - 6 Simplified bio-refinery potential of Jatropha curcas [26]

Biodiesel is mono-alkyl ester of fatty acid chemically and physically extracted from different animal fats and vegetable oils such as palm, soybean, sunflower, rapeseed and canola [44, 53–54]. Direct usage of vegetable oil in diesel engine as fuel without modification can cause injector coking, extra carbon deposit, engine oil gelling; and oil ring sticking [44]. The common biodiesel production process is termed as transesterification. Methanol or ethanol can be used as the reactant, but based on its lower price; methanol is widely used for biodiesel production [14, 53]. Typical sources for biodiesel include rapeseed, canola, soybean, sunflower and palm oil, but a variety of

sources are being studies currently such as animal fat, waste cooking oil, almond, andiroba, babassu, barley, camelina, coconut, copra, cumaru, cynara, cardunculus, fish oil, groundnut, Jatropha curcas, karanja, laurel, Lesquerella fendleri, Madhuca indica, microalgae, oat, piqui, poppy seed, rice, rubber seed, sesame, sorghum, tobacco seed and even wheat [14, 44]. Biodiesel produced from vegetable oil is a potential renewable, non-toxic replacement for conventional diesel by having lower sulphur and aromatic contents and flash point, and higher biodegradability as compared to diesel fuel [14, 45, 55].

Biodiesel as a fuel has been officially recognised, and both ASTM and European standards (EN) have introduced standard biodiesel specifications for commercial usage as pure biodiesel or as blends with conventional diesel [14]. Table 2 - 7 and Table 2 - 8 list the specifications of ASTM D 6752-02 and EN14214 standards, respectively.

Table 2 - 7 Biodiesel specifications according to ASTM D 6752-02 [20]

Physicochemical property	ASTM method	Limits	Units
Flash point	D 93	130 min	^{o}C
Water and sediment	D 2709	0.050 max	% volume
Kinematic viscosity at 40^{o}C	D 445	1.9–6.0	mm^{2}/s
Sulphated ash	D 874	0.020 max	wt %
Total sulphur	D 5453	0.05 max	wt %
Copper strip corrosion	D 130	No. 3 max	-
Cetane number	D 613	47 min	-
Cloud point	D 2500	Report	^{o}C
Carbon residue	D 4530	0.050 max	wt %
Acid number	D 664	0.80 max	mg KOH/g
Free glycerine	D 6584	0.020	wt %
Total glycerine	D 6584	0.240	wt %
Phosphorus	D 4951	0.0010	wt %
Vacuum distillation end point	D 1160	360^{o}C max, at 90% distilled	^{o}C

As the feedstock used in this research is Jatropha curcas waste after oil extraction from the seed for biodiesel production, the specifications of Jatropha curcas methyl ester (JME) is indirectly, but still closely related to the present research. By using low cost feedstock such as inedible oils, waste cooking oil and animal fat, the price of biodiesel can be reduced [53]. Other oils like castor oil have been used for many years

in countries such as Brazil [20]. The final biodiesel produced from castor oil has high substandard density and viscosity because of its methyl and ethyl ricinoleic esters' solubility in alcohol [20]. This problem has led the Brazilians to be pioneers in finding a suitable replacement for castor oil, i.e. Jatropha [20]. Jatropha curcas oil was also used as a diesel replacement in Madagascar, Cape Verde and Benin during World War II [53].

Table 2 - 8 Biodiesel specifications according to EN14214 [14]

Physicochemical property	Units	Lower limit	Upper limit	Method
Ester content	% (m/m)	96.5	-	pr EN 14103 d
Density at 15°C	kg/m^3	860	900	EN ISO 3675/EN ISO 12185
Viscosity at 40°C	mm^2/s	3.5	5.0	EN ISO 3104
Flash point	°C	>101	-	ISO CD 3679e
Sulphur content	mg/kg	-	10	-
Tar remnant (at 10% distillation remnant)	% (m/m)		0.3	EN ISO 10370
Cetane number	-	51.0	-	EN ISO 5165
Sulphated ash content	% (m/m)	-	0.02	ISO 3987
Water content	mg/kg		500	EN ISO 12937
Total contamination			24	EN 12662
Copper band corrosion (3 hr at 50°C)	rating	Class 1	Class 1	EN ISO 2160
Oxidation stability at 110 °C	hr*	6	-	pr EN 14112 k
Acid value	mg KOH/g	-	0.5	pr EN 14104
Iodine value	-		120	pr EN 14111
Linoleic acid methyl ester	% (m/m)		12	pr EN 14103 d
Polyunsaturated (≥4 double bonds) methyl ester			1	-
Methanol content			0.2	pr EN 141101
Monoglyceride content			0.8	pr EN 14105m
Diglyceride content			0.2	pr EN 14105m
Triglyceride content			0.2	pr EN 14105m
Free glycerine			0.02	pr EN 14105m / pr EN 14106
Total glycerine			0.25	pr EN 14105m
Alkali metals (Na + K)	mg/kg		5	pr EN 14108 / pr EN 14109
Phosphorus content			10	pr EN 14107p

* Hour (hr)

Ideal vegetable oils for biodiesel need to have a high percentage of monounsaturated fatty acids, and a low percentage of saturated and polyunsaturated fatty acids [53]. It can be deduced from Table 2 - 9 that by being rich in oleic fatty acid and having only 0.2% linolenic acid as compared to the limit of 12% specified in EN 14214, Jatropha curcas oil is a good potential for biodiesel production although the medium percentage of linoleic fatty acid makes the product less stable against oxidation [53]. The standard iodine value for biodiesel based on EN 14214 is 120 $\frac{g\ I_2}{100g}$, and as can be observed in

Table 2 - 10, unprocessed Jatropha curcas oil has only an iodine value of 103.62 $\frac{g\ I_2}{100g}$ [53].

Table 2 - 9 Comparison of fatty acids composition of Jatropha curcas oil to other typical vegetable oils [53]

Fatty acid	Jatropha curcas	Palm kernel	Sunflower	Soybean	Palm
Oleic 18:1	44.7	15.4	21.1	23.4	39.2
Linoleic 18:2	32.8	2.4	66.2	53.2	10.1
Palmitic 16:0	14.2	8.4	-	11.0	44.0
Stearic 18:0	7.0	2.4	4.5	4.0	4.5
Palmitoleic 16:1	0.7	-	-	-	-
Linolenic 18:3	0.2	-	-	7.8	0.4
Arachidic 20:0	0.2	0.1	0.3	-	-
Margaric 17:0	0.1	-	-	-	-
Myristic 14:0	0.1	16.3		0.1	1.1
Caproic 6:0	-	0.2		-	-
Caprylic 8:0		3.3			-
Lauric 12:0		47.8			0.2
Capric 10:0		3.5			-
Saturated	21.6	82.1	11.3	15.1	49.9
Monounsaturated	45.4	15.4	21.1	23.4	39.2
Polyunsaturated	33	2.4	66.2	61.0	10.5

Table 2 - 10 Physicochemical properties of biodiesel produced from Jatropha curcas oil [53]

Physicochemical property	Units	Value
Density at 15°C	g/cm^3	0.8826
Kinematic viscosity at 40°C	cSt	4.016
Water content	w/w%	0.003
Conradson carbon residue	w/w%	0.0223
Pour point	°C	–5
Flash point	°C	117
Copper strip corrosion	1a	1a
Ash content	w/w%	Not detected
Calorific value	MJ/kg	41.72

The physicochemical specifications of Jatropha curcas biodiesel as can be observed in Table 2 - 11 are comparable and within the range of diesel engine application acceptance although further testing for in-depth clarification of practical performance is still required [20–21].

The oil extracted from Jatropha curcas seed by expeller can be recovered up to 97 wt% as biodiesel through transesterification, and it can be directly used in slow velocity diesel engines or other diesel applications [12, 22]. Before transesterification of Jatropha curcas oil, it can be de-waxed and de-gummed to improve its quality through

refrigeration, centrifuge, heating, agitation, addition of phosphoric acid and distilled water as the oil has a high viscosity of $4.9 \times 10^{-2}\ Pa\ .s$ [22]. Experimental tests have indicated that de-acidification of Jatropha curcas oil can be economically performed via liquid-liquid extraction (LLE) using aqueous ethanol as solvent to extract free fatty acid (FFA) with limited reduction of neutral oil [54].

Table 2 - 11 Physicochemical properties of Jatropha curcas oil and biodiesel [20]

Jatropha curcas			
Specification	Unit	Oil	Biodiesel
Oil content	w/w %	31.6	Not applied
Acid value	Mg KOH/g	8.45	Not applied
Ash content	w/w %	-	-
Calorific value	MJ/kg	40.31	41.72
Conradson carbon residue	w/w %	0.5396	0.0223
Copper strip corrosion	-	1a	1a
Density at 15 °C	g/cm^3	0.9215	0.8826
Flash point	°C	Not applied	117
Kinematic viscosity at 40°C	cSt	30.687	4.016
Pour point	°C	–2	–5
Water content	w/w %	0.052	0.003

In Table 2 - 12, the physicochemical properties of diesel, refined Jatropha curcas oil and Jatropha curcas biodiesel are tabulated. Based on the properties, a blend of 20% of de-waxed and de-gummed Jatropha curcas Oil (DDJO) in diesel did not affect the engine performance noticeably, and by preheating the fuel till 60 °C, up to 50% of this treated oil could be added to diesel to run the diesel engine without problems [22]. Different blends of JME blended with diesel were tested and the results showed that the brake thermal efficiency of JME was higher than diesel which was attributed to the oxygen content of JME [22].

Table 2 - 12 Physicochemical properties of Jatropha curcas fuels as compared to diesel [22]

Physicochemical property	Unit	JME*	DDJO**	Diesel
Viscosity	cSt	8.818	48.956	4.438
Density at 38 °C	Kg/m^3	857.3	891.80	788.96
Flash point	°C	144	245	66
Cloud point	°C	11	16	09
Carbon residue	wt%	0.02	0.20	0.03
Free fatty acid	wt%	0.08	1.43	-
Calorific value	kcal/kg	8076	8765	10’404

*Jatropha curcas methyl ester **De-waxed and degummed Jatropha curcas oil

2.3.3.1 Non-fuel Applications of Jatropha curcas

In South America, Africa and India, different parts of this plant have been modified and applied as herbal medication for years. Gubitz et al. [48] produced a comprehensive article on the medicinal and other non-fuel uses of this plant. For instance, Africans use the seed for expelling intestine worms, preventing constipation while the leaves are used as an anti-haemorrhagic agent and even as treatment for malaria. They boil leaves, seeds and bark in water, and the extracted juice is used as a laxative medicine while a leaf decoction is processed to produce herbal cream for rheumatism and skin inflammation. The root decoction of Jatropha is used against syphilis and pneumonia in addition as a purgative, vermifuge and even abortifacient syrup. Meanwhile, Mexicans use the latex to resolve digestion problems, fungal infections and bee sting. Different Jatropha extracts can also be used in replacement of harmful chemical pesticides to control pests such as vector snail, golden snail, corn beetle, bean beetle, housefly and cotton pest. Its natural strong structure, high resistance to disease and pests, as well as its fatal poisonous effects on herbivores are reasons that Jatropha can be used as a natural fence especially for cultivation and farming zones [48, 56]. The strong root of the shrub can also prevent further erosion in deserted lands [56]. Jatropha curcas flowers attract honeybees and the plant can be used for honey farming [56]. Herbal drugs from Jatropha shrubs have been tested and used to treat cancerous cells [57]. Finally, Jatropha curcas oil can be used in alkyl resin, shoe polish, varnish, liquid soap, shampoo, candle, and cosmetics production [53].

2.3.4 Bio-oil Potential of Jatropha curcas

Although production of biodiesel from Jatropha curcas seeds has been the focus of research for a number of years, the oil extraction covers only up to 18 wt% of the dry fruit, while the other components of the fruit can be used as combustibles [22]. The

remaining Jatropha curcas fruit after biodiesel production has the potential of fuel production with twice the energy content as compared to its biodiesel energy [22]. Approximately 50 wt% of its nut shell can be transformed into bio-oil and even its wood and leaves can be valorised for fuel extraction [26]. After seed oil extraction, the biomass waste can be used as a potential source for bio-oil production via pyrolysis, although the full details of optimisation and efficiency are not currently available. Comparing Jatropha curcas seed to rice husk, olive and cotton cocoon shell in terms of conventional pyrolysis product yield, it has been shown that more char, less gas and comparably equal bio-oil yields can be obtained using Jatropha curcas [12]. According to this study, the chemical analysis of Jatropha curcas pressed cake waste is tabulated in Table 2 - 13. Having a high volatile matter of 79.20 wt% and a low ash content of only 1.5 wt% makes Jatropha curcas a highly desirable feedstock for thermochemical processes especially pyrolysis [12].

In one study, thermo-gravimetric analysis (TGA) and a fixed-bed quartz reactor were used to determine a suitable degradation model and to investigate the effect of operating conditions on product distribution [12].

Table 2 - 13 Chemical analysis of pressed cake waste of Jatropha curcas [12]

Jatropha curcas pressed cake					
Proximate analysis	wt%	Elemental analysis	wt%	Component analysis	wt%
Volatiles	79.20	Carbon	52.30	Hemicelluloses	17.47
Fixed carbon	18.86	Hydrogen	6.50	Cellulose	56.31
Ash	1.50	Nitrogen	5.20	Lignin	23.91
Moisture	0.44	Potassium	3.84	Other	2.32
		Calcium	2.00		
		Phosphorus	1.98		
		Magnesium	1.21		
		Sulphur	0.58		
		Chlorine	0.21		
		Oxygen	26.18		

It was found that the main thermal decomposition occurred over the temperature range of 523 K to 723 K, and could be described by the three-parallel reactions model.

The temperature and hold time within the fixed-bed quartz reactor influenced the yields of gas, liquid and char products, although full optimisation was not carried out. Similarly, a parametric study of flash pyrolysis of Jatropha oil cake in an electrically heated fluidised bed reactor using N_2 has been carried out [27]. Maximum oil yield of 64.25 wt% was obtained at a particle size of 1.0 mm, a pyrolysis temperature of 773 K, and a N_2 flow rate of 1.75 m^3/hr. The obtained pyrolysis oil had a calorific value of 19.66 MJ/kg, and could be used as a source of low-grade fuel directly or upgraded to a higher quality bio-fuel. Meanwhile, another investigation on the use of the Low Temperature Conversion (LTC) process at temperatures between 653 and 693 K to pyrolyse Jatropha curcas fruit and cake has been carried out [58]. It was documented in this work that binary mixtures of diesel and pyrolysis oil containing up to 10% pyrolysis oil were very effective while binary mixtures containing between 10% and 20% pyrolysis oil were not very effective because of the higher viscosity and sulphur content.

A recent study on production of Jatropha curcas bio-oil from its pressed cake seed confirms the viability of this biomass source for biofuel production [59]. In this study bio-oil was distilled for improvement of calorific value, water content, viscosity and density. They also further reduced the water content by using sodium sulphate and alumina [59].

2.3.4.1 Potential Energy Source

In 2008, a 20-year predictive study on the usage of Jatropha curcas as an energy source has been carried out in Thailand [24]. The schematic life cycle of this plan is shown in Figure 2 - 7. The total calculation of the energy input and output of the system are summarised for 1 hectare of land in Figure 2 - 8 and Figure 2 - 9, respectively. The

results showed that the net energy gain (NEG[2]) and NER of JME and its by-products for 1 hectare of land are 4720 GJ and 6.03 GJ, accordingly, and half of the NEG originated from the pressed cake fuel potential [24]. Even by considering only the seed cake as a source of energy, the NER of approximately 3 still shows more than 200% rise in energy balance of the system.

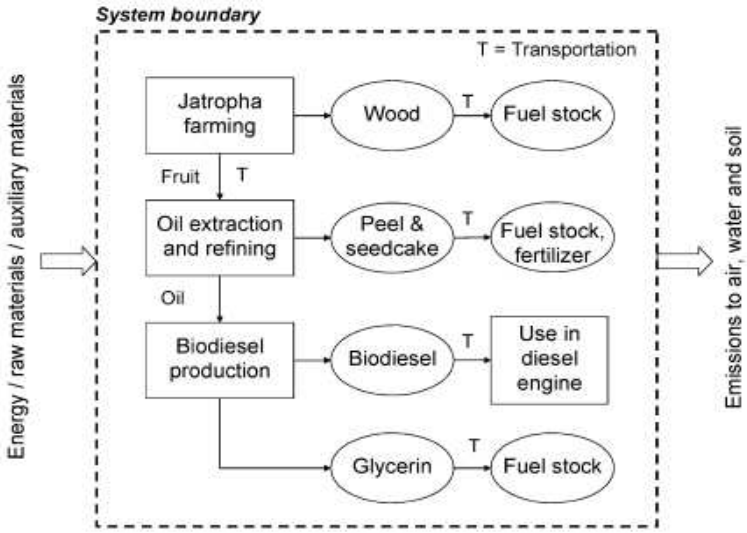

Figure 2 - 7 Jatropha curcas life cycle for the aim of bio-energy [24]

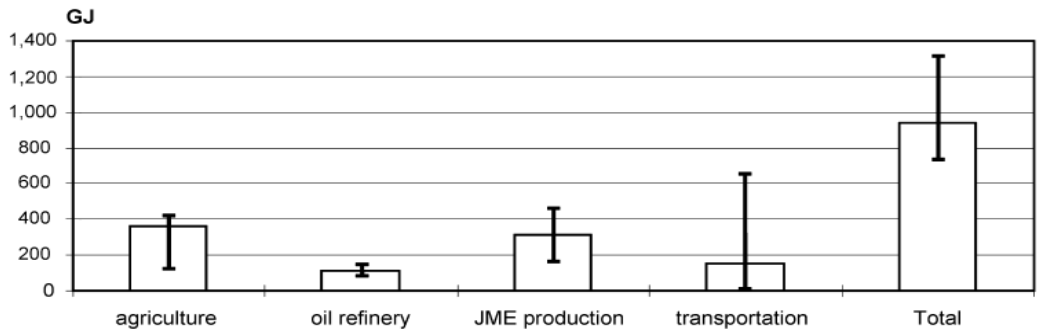

Figure 2 - 8 Energy consumption for Jatropha curcas and its products [24]

[2] Net Energy Gain=(The energy content of bio-fuels produced and their by-products)

-(The total energy consumed for production of the bio fuels from plantation to final products)

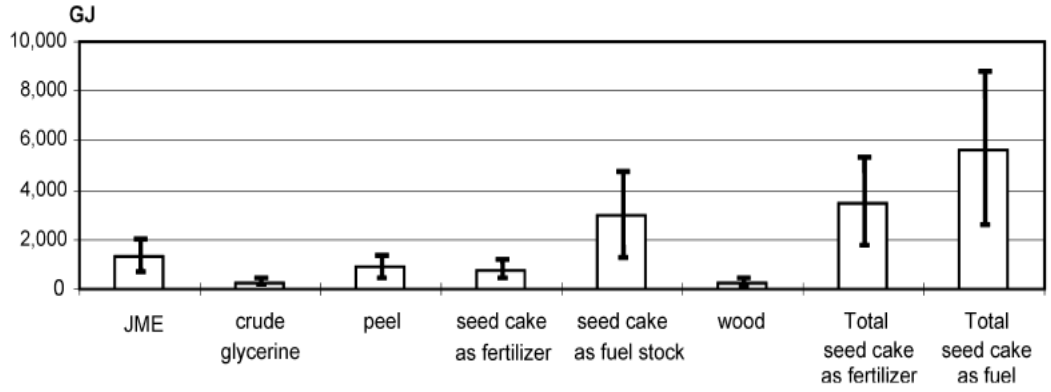

Figure 2 - 9 Energy production from JME and its by-products [24]

2.4 Pyrolysis

Biomass can be converted to energy via either biochemical processes such as fermentation or anaerobic digestion, or thermo-chemical processes [40]. Thermo-chemical conversion offers some advantages over biochemical transformations such as opportunities for distributed pre-processing, separation and usage of both carbohydrate and lignin, and integration into existing petroleum refineries [60–61]. The three main methods of thermo-chemical conversion of biomass into energy are direct combustion, gasification and pyrolysis [7]. Pyrolysis is the initial step in the conversion of solid biomass into higher value fuels in liquid and gas forms or even solid char which may be followed by further catalytic upgrading [1, 10]. Pyrolysis technology based on its co-product yields is the most favourable process and is more economical than gasification [62]. It can be scaled down or up for different purposes without any complications [63]. Figure 2 - 10 shows a schematic diagram of a pyrolysis plant.

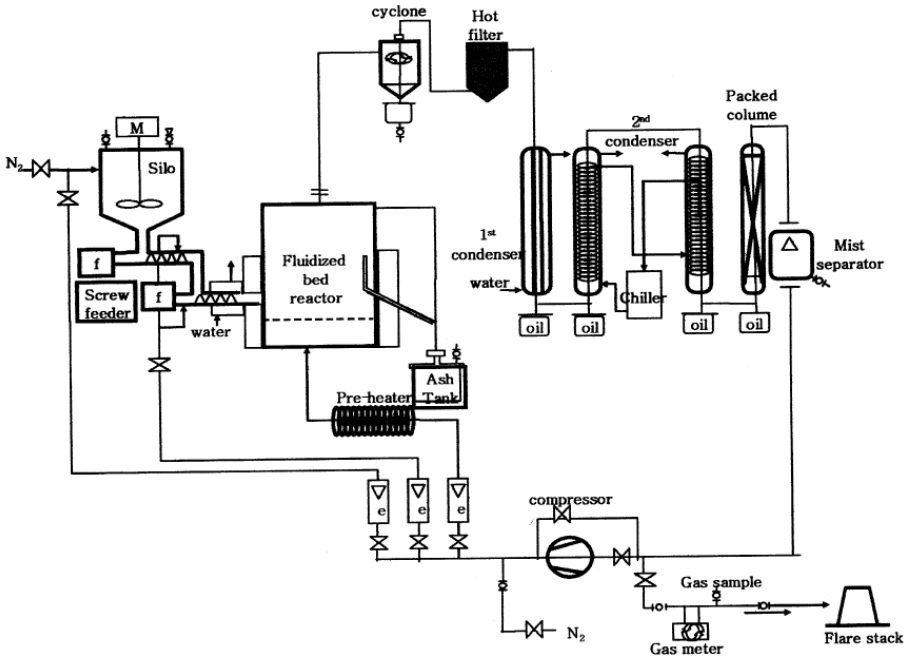

Figure 2 - 10 Schematic of a pyrolysis plant [33]

The details of the pyrolysis process as summarised from various references are as follows [8–10, 17, 42, 53, 49, 64–67]:

- The biomass is dried until its water content is below 10%. It should be dried at a temperature of $378^{o}K$ for 24 hr before pyrolysis. Effective drying of biomass before pyrolysis can improve the quality of bio-oil by reducing acid and water content, and increasing the calorific value of the end product. An experimental research on hardwood showed that drying at $200^{o}C$ for 90 min improved the bio-oil by increasing its pH value, reducing its water content down to 20% and improving its calorific value up to 20 $\frac{MJ}{kg}$ [8]. In another work, distilled water was used to soak the biomass before drying as a simple pre-treatment to improve the bio-oil yield by reducing the alkali metal content [33].
- The dried biomass is ground to desirable particle size. The reviewed papers indicated that experiments performed on various seeds and nuts used grain sizes

from 0.6 mm to 1.8 mm in diameter, although it has been reported that grain size has negligible effects on the yield and quality of the products [17].

- Heat is transferred to the biomass in the absence of oxygen by using an inert gas, normally N_2, as an initial step. Hydro-pyrolysis is a type of pyrolysis whereby the inert gas used is hydrogen. By using hydrogen, the bio-oil yield can be increased by 10% based on the reduction in oxygen content of the product. Steam pyrolysis is used to enhance tar yield by reducing absorption of tar vapour by char.
- Volatiles are initially separated from the solid using high temperature resulting in char creation. Further heat transfer occurs from the hot volatile fluid into the colder solid to separate more volatiles from solid. Condensation of part of the volatiles produces bio-oil.
- The remaining gas which consists of hydrogen, CO2, carbon monoxide and methane can be trapped as another potential fuel source, or can be circulated and burned on the spot to generate energy for the pyrolysis process.
- Depend on the feedstock, temperature, heating rate and pyrolysis experimental setup, different kinds of fuels and chemicals with a variety of compositions can be obtained although some cases show that particle size within the range of 0.4 mm to 1.8 mm, and inert gas flow rate within the range of 100 cc/min to 600 cc/min have negligible effects on production yields [17].

2.4.1 Pyrolysis Parameters

The parameters affecting pyrolysis processes include the reactor configuration itself, heating rate, final temperature, inert gas type, inert gas flow rate, heat transfer rate, grain size and biomass type with biomass type being the most important if the main aim to produce bio-oil [8–10, 17, 42, 53, 49, 64–67]. Details of the most important parameters are discussed in Chapter 3 along with the design methodology used in this research.

Some of these parameters are interrelated, and an example of this is grain size which affects the heat transfer rate to biomass.

2.4.2 Pyrolysis Systems and Reactors

Based on the heating rate and temperature, pyrolysis processes can be divided into two main categories of conventional and fast pyrolysis systems. For each category, various reactor configurations are available as described below.

2.4.2.1 Conventional Pyrolysis and Reactor

Conventional pyrolysis or slow pyrolysis is the process of slowly heating dried and ground biomass in the absence or lack of oxygen in favour of extracting bio-oil, gas and char [17]. There are no exact measurements or standard reference to show how much time is needed for this process to be classified as conventional or slow [17, 65]. These arbitrary names have been given to in light of the development of fast pyrolysis to differentiate between the two systems. Recent researches show that lignin oligomers in bio-oil resulting from lignin of biomass during fast pyrolysis can be transformed as secondary chemical reaction into undesirable mono-phenols based on the slow process of heating the pyrolysis bed [66].

The most common reactor for conventional pyrolysis is the fixed-bed reactor. The main part consists of a heating element and a fixed-bed. By using inert gas such as N_2 or a vacuum process, the biomass is heated up and the outlet gas is quenched for bio-oil production while the remaining gas can be used for different purposes. The char will remain in the bed and can be extracted after the process finishes.

2.4.2.2 Fast Pyrolysis and Reactors

Fast pyrolysis is defined as the process in which the biomass is heated at a high heating rate within a short period of time in the absence of oxygen [17]. Fast pyrolysis

is typically used to minimise char production although in some cases of conventional pyrolysis, the char production can be as low as 25 wt% with a bio-oil yield of more than 66 wt% of the original biomass [17, 39]. Reducing the residence time of volatiles prevents further cracking and reactions, and result in a higher yield of bio oil [4]. The heating rate is the most crucial parameter in fast pyrolysis [13]. A higher heating rate is suitable for higher bio-oil yield with lower water content by breaking the chemical bridges and fast cross-linking reactions with a variety of activation energies [13]. Table 2 - 14 shows various pyrolysis technologies along with their residence time, heating rate and temperature. For high yields of bio-oil, not only is a high heat transfer rate desirable according to Table 2 - 14, but reactor configuration is also the core of fast pyrolysis. For the past twenty years, many reactor configurations have been tested and they can be categorised into four main types, i.e. fluidised bed, transported and circulating fluidised bed, vacuum, and ablative reactors [17]. The most important reactor types as described in [17] are summarised below.

Table 2 - 14 Pyrolysis technologies and their characteristics [17]

Pyrolysis technology	Residence time	Heating rate	Temperature (°C)	Products
carbonization	days	very low	400	charcoal
conventional	5–30 min	low	600	oil, gas, char
fast	0.5–5 s	very high	650	bio-oil
flash-liquid	<1 s	high	<650	bio-oil
flash-gas	<1 s	high	<650	chemicals, gas
ultra	<0.5 s	very high	1000	chemicals, gas
vacuum	2–30 s	medium	400	bio-oil
hydro-pyrolysis	<10 s	high	<500	bio-oil
methanol-pyrolysis	<10 s	high	>700	chemicals

Table 2 - 14 is covering number of available pyrolysis methods and many other specifications were used in latest researchers work but the boundaries are not clearly clarified [65]. Apart from that, place of the measuring items such as temperature and heating rate are inconsistent in different literature and an standardisation seems

necessary for future works for clarification of the type of pyrolysis (slow, fast and flash) [65].

- **Fluidised bed reactor**

In Figure 2 - 11 Fluidised bed pyrolysis reactor, the configuration of a fluidised bed pyrolysis reactor is shown. The reactor contains sand for active and fast heat transfer to the biomass grains. The sand is fluidised because of hot inlet gas pressure while the biomass particles passing through the mixture of hot sand and gas because of their lower density as compared to sand. After separation of char in a cyclone, the gas undergoes a quenching process [17]. The quenching process can be performed in multiple phases, but the product of each is bio-oil and the by-product is incondensable gas. This gas can be recycled into the bed after combustion, or can be trapped and used for a variety of purposes such as hydrogen fuel production. This reactor gives good control over temperature, and its scalability is easily modifiable making it one of the best for bio-oil production although small biomass grain size is needed and heat transfer at large-scale still needs to be well-defined.

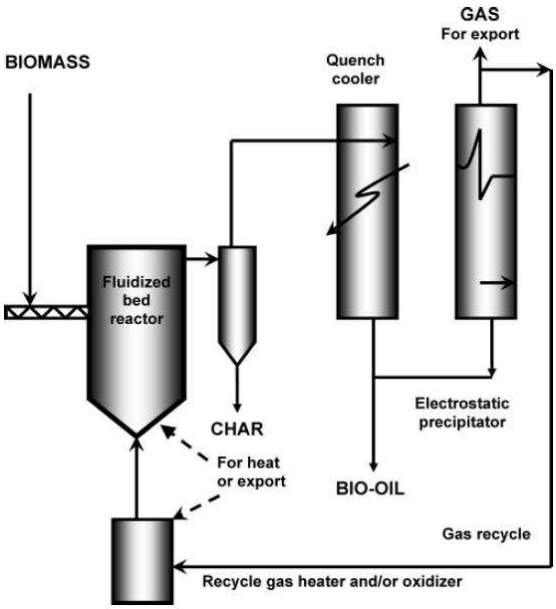

Figure 2 - 11 Fluidised bed pyrolysis reactor [17]

- **Circulating Fluidised Bed Reactor**

This configuration is similar to the fluidised bed, but to reduce char residence time, a higher pressure gas flow is used. The mixture of sand and char, as shown in Figure 2 - 12, is sent to a combustor and after the char is burnt, the remaining sand is recycled back into the bed. The advantages of this set up compared to fluidised bed include more abrasion of char by using a higher velocity of gas and biomass as well as a higher production rate due to the higher velocity. There are some disadvantages such as more diluted char particles in the bio-oil based on the high velocity particles, accumulated ash in the bed because of char recycling and lower heat transfer by emphasizing more on convection heat transfer especially at large-scale.

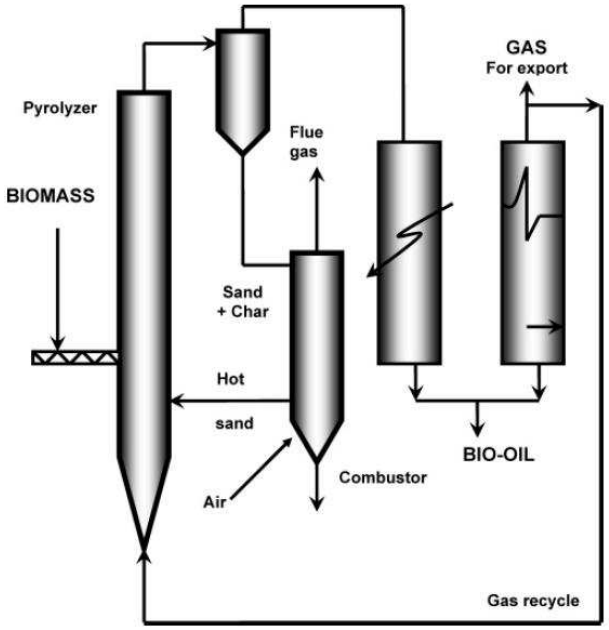

Figure 2 - 12 Circulating fluidised bed pyrolysis reactor [17]

- **Vacuum Reactor**

In the vacuum reactor as shown in Figure 2 - 13, the bed is vacuumed by using a pump while the biomass is heated up using convection heat transfer with modified

placement of biomass within bed. According to the configuration, vacuum reactors cannot be categorised as fast pyrolysis reactors because the residence time of the biomass within the bed is similar to fixed-bed reactors in conventional pyrolysis. Nonetheless, the reason for classifying vacuum reactors under fast pyrolysis is due to the short residence time of the gas within the bed. The short residence time of volatiles in the bed prevents further decomposition hence not only the final bio-oil product has a molecular structure similar to the original biomass structure, but the bio-oil yield is higher . Although a large particle size and a low heating temperature can be used in operation with no inert gas requirement, inefficient heat and mass transfers with a big volume of machinery is needed for bio-oil yields ranging from 35 wt% to 50 wt% only.

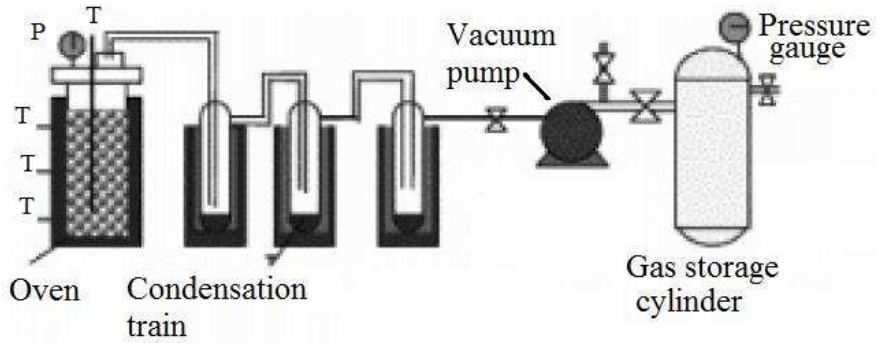

Figure 2 - 13 Vacuum pyrolysis reactor [17]

- **Ablative Reactor**

The ablative reactor consists of heated walls in which small biomass particles are rubbed against by pressure as shown in Figure 2 - 14. This pressure can be produced by a centrifugal force or mechanical power. Volatiles separated from the char lubricate the surface of the reactor walls and aids in the movement of biomass along the wall. Additionally, the walls are heated to volatilise the biomass for condensation. Fast separation of volatiles, high constant production, ability to use large biomass particles, relatively lower operation temperature, and no inert gas requirement are the advantages

of this reactor set up. In contrast,, the heat transfer from wall to grains limits the reaction rate and the reactor has a high cost especially for scaling up.

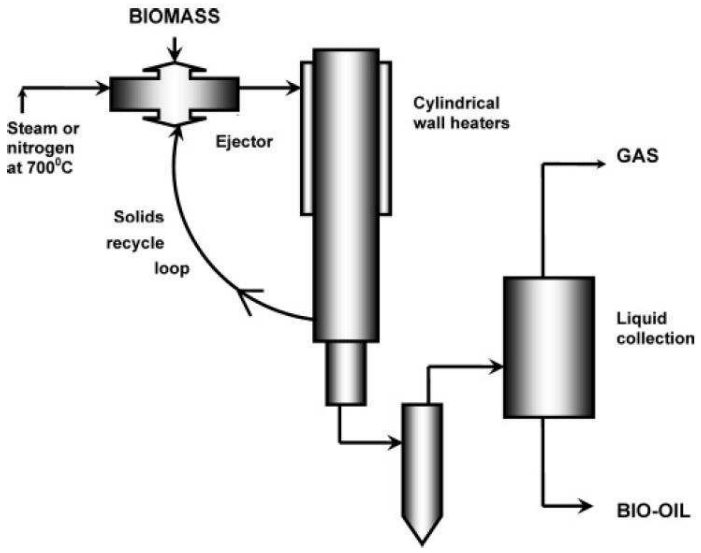

Figure 2 - 14 Ablative pyrolysis reactor [17]

2.4.3 Viability of Pyrolysis

2.4.3.1 Energy Approach

To determine the viability and energy efficiency of pyrolysis, an energy balance has been carried out on fast pyrolysis of switchgrass with a maximum bio-oil yield of 60.7% [68]. The results of this study are tabulated in Table 2 - 15 with the corrected energy taking into account of the bio-oil that is trapped within the system [68]. The viability of the process can be observed clearly, even without the correction factor; up to 68.2% energy can be utilised and recovered in addition to a high volume of switchgrass being converted into a high quality fuel with condensed volume.

Table 2 - 15 Energy balance and recovery in fast pyrolysis of switchgrass [68]

Energy in (MJ/h)			Energy out (MJ/h)		
Item	Actual	Corrected	Item	Actual	Corrected
N_2	0.05	0.05	Reactor heat loss	3.61	3.61
Switch grass	39.83	39.83	N_2	0.00	0.00
Heaters	7.66	7.66	Bio-oil	24.85	31.07
			Char	5.52	5.52
			Bio-gas	2.03	2.03
			Condenser heat loss	11.54	5.31
Total	47.54	47.54	Total	45.54	47.54

Energy recovered (%)	No utilisation		Product utilisation	
	Actual	Corrected	Actual	Corrected
Bio-oil	52.3	65.4	62.2	77.8
Bio-oil + char	63.9	77.1	66.8	80.5
Bio-oil+ char + bio-gas	68.2	81.3	68.2	81.3

Another study on energy balance of pyrolysis process using corn cobs and stover showed that with 60% bio-oil yield and a heating value of $20\ \frac{MJ}{kg}$, the energy density of the bio-oil is up to 32 times of the energy density of the biomass [69].

2.4.3.2 Entropy Approach

One study on entropy and energy balance for continuous pyrolysis process indicated that this process decreases entropy by over 4% as shown in Table 2 - 16 [70].

Table 2 - 16 Energy and entropy balance in continuous fast pyrolysis process [70]

Process	Inflow		Process	Outflow	
	Energy	Entropy		Energy	Entropy
Item	kJ/min	kJ/min.K	Item	kJ/min	kJ/min.K
Biomass	772.236	2.59	Char	434.511	0.591
N_2	0.933	0.003	N_2	24.248	0.035
Heat (reactor wall)	23.523	0.032	Heat loss (reactor)	71.428	0.1751
Increased potential*	467.419	–0.8614	Bio-oil	531.103	0.772
			Gas	152.821	0.222
Total	746.692	1.872		1214.111	1.795

*Increased potential stored in char, bio-oil and gas due to chemical reaction

The irreversible part of the process occurs during quenching. Using alternative methods for heat release in the condenser can reduce the level of irreversibility to have a significant negative entropy process. One of the most effective methods is using

absorption refrigeration system for the purpose of cooling down the condenser, either completely or partially.

2.5 Concluding Remarks

Reviewed literature indicates conclusive information and current developments for pyrolysis processes, Jatropha curcas plant, and bio-oil. The comprehensive information on fuel production from Jatropha curcas is mainly limited to biodiesel production at the moment. Although recent research (in parallel time to this research work) on production and quality of bio-oil from Jatropha curcas has been found and reviewed, parametric investigation on pyrolysis process has not been performed. Investigation on the quality and improvement of bio-oil from Jatropha curcas pressed cake is also performed in this latest research but standard measurements and comparison was not used in the direction of using bio-oil commercially. In conclusion, based on the available literature, more conclusive research on the production of bio-oil from Jatropha curcas is lacking. This project intends to develop and optimise Jatropha curcas bio-oil production in terms of both yield and quality by reviewing pyrolysis parameters, as well as provide comprehensive understanding of bio-oil specifications and potential applications. Also specific comparison between fast and slow pyrolysis bio-oils by using similar beds need to be investigated as it is lacking for Jatropha curcas waste as source of biomass. The findings will contribute towards commercialisation of biofuel production from the wastes of this plant in tropical regions.

CHAPTER 3 REACTOR DESIGN AND FABRICATION

3.1 Introduction

Conventional pyrolysis is the foundation upon which all other pyrolysis methods are based on whereas fast pyrolysis targets the production of bio-oil. The major advantage of conventional pyrolysis lies in its simplicity in experimental setup, which allows investigation of pyrolysis processes in limited facilities. The purposes of using a fixed-bed reactor were twofold. First, the pyrolysis process can be modelled by using a TGA unit operating at the same heating rate as the designed fixed-bed reactor. Second, experiments on this reactor setup enable a baseline for comparing conventional and fast pyrolysis processes in terms of the effect of heating rate. On the other hand as one of the objectives of this research is production of bio-oil and as mentioned in chapter 2, fast pyrolysis process targets this objective specifically, design and fabrication of a fast pyrolysis reactor seems necessary for this investigation by considering the available resources. This also allows performing a comparison between two rigs production as an extra investigation parameter.

In this chapter the design parameters consists of reactor material, heating rate, final reaction temperature and nitrogen velocity of the pyrolysis rigs will be reviewed initially. Then the thermodynamics calculation of the rigs will be presented followed by brief explanation on different designs that were investigated in this research. The chapter will be finalised by a conclusion.

3.2 Design Parameters

The parameters affecting bio-oil yield and quality in pyrolysis processes include reactor design (geometry, material and function), reaction parameters (heating rate, temperature, residence time, system pressure and catalyst), and biomass (type, water content, size and shape) [32]. In designing a new reactor, considerations need to be given to reduce the operating temperature in the bed, increase heating conversion capacity in the bed and condenser, prevent soot formation in the bed by avoiding the recycled heating gas to be overheated beyond $600^{o}C$, minimise abrasion of char in the reactor and collect char separately using innovative separation processes [17]. In addition to the geometry of the reactor, the material of construction, heat transfer, final temperature and N_2 flow rate are the parameters to be considered in the design. Other parameters such as biomass grain size are indirectly related to the reactor design.

3.2.1 Reactor Material

It is mentioned in last chapter that bio-oil is corrosive even at low temperatures with a pH value of approximately 3 and high oxygen and water contents in general thus the material for the reactor, storage, burner and even the diesel engine must be resistant to corrosion. Stainless steel has been the material of choice for pyrolysis reactors for many years [71]. Practical tests such as x-ray photoelectron spectroscopy (XPS) and Auger electron spectroscopy (AES) demonstrated that bio-oil can corrode aluminium, mild steel and nickel based alloys whereas cobalt based alloys, stainless steel, plastics and brass are highly resistant to bio-oil [72]. As an example, Figure 3 - 1 shows the weight loss of three metal bars in contact with bio-oil at $80^{o}C$. High chromium stainless steel was the best for practical applications especially in diesel engines [72]. The strong resistance of stainless steel 316 against corrosion is because after removal of iron atoms,

the chromium species move from the bulk to the surface of the metal to create a layer of chromium oxide, and this resistant layer prevents further corrosion of the alloy, but it slightly increases the total metal weight [72].

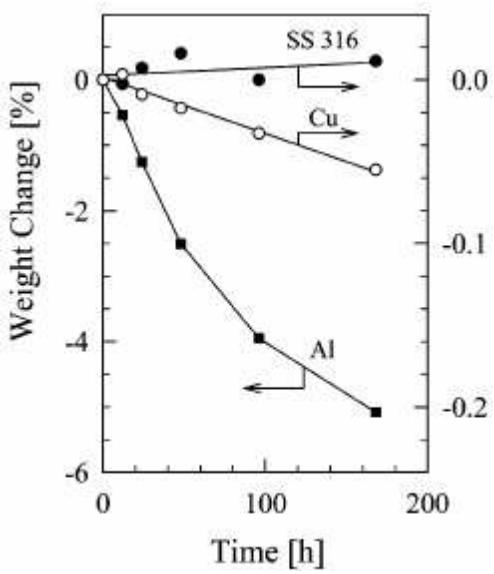

Figure 3 - 1 Weight change (%) of three metal bars in contact with bio-oil at 353 K [72]

As temperatures up to 1073 K will be investigated in this research (will be mentioned in chapter 5, section 5.2.2), among all materials, stainless steel 316 seems to be the best choice based on its resistance to corrosion, high temperature and robust characteristics.

3.2.2 Heating Rate

Heating rate or cooling rate has the same unit as power (Watts) but the result of heating power can be shown as temperature rise rate (for example K/s). Based on that, in this research Heating Rate is being used instead Temperature Rise Rate, although the unit is temperature per unit time.

A high heating rate is desirable to have high bio-oil production. Convection heating instead of generally solid-to-solid conduction in fast pyrolysis can be an alternative method that has been tested [73]. Although the heating rate is less compared to

conduction, higher quality product (bio-oil without solid particles) is produced at the expense of the possibly lower yield [73]. Low reaction temperature and high heating rate as can be observed in Figure 3 - 2 are the main requirements for pyrolysis with high bio-oil yield whereas the same conditions, but with low heating rate can give rise to high char product [44].

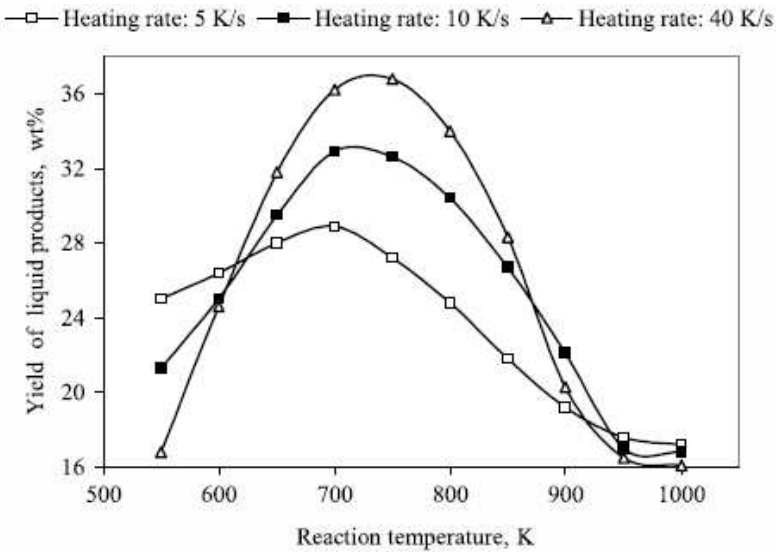

Figure 3 - 2 Effect of heating rate on bio-oil yield from olive cake [44]

To improve fast pyrolysis, heating rate is a direct parameter which is affected by other indirect parameters such as biomass grain size, type of heat transfer and its rate or development [36]. For instance, in any kind of bed or furnace, radiation is always present although often neglected in calculations; the total heating rate can be optimised by either encouraging or discouraging this aspect of heat transfer [36].

Based on the above, apart from investigation on the conventional pyrolysis (slow pyrolysis) rig as base line, a rapid heating fast pyrolysis rig is being designed and used based on availability of resources to match the requirements of the project. The details of both rigs will be described in this chapter.

3.2.3 Final Temperature

A low yield of bio-oil can be observed at lower temperatures. Conversely, very high temperatures result in severe secondary reactions of volatiles which can result in a low yield of bio-oil hence the optimum temperature for gaining both high quality and quantity of bio-oil is vital [4, 40]. A study on the pyrolysis of wood showed that temperature affects the product distribution (Figure 3 - 3) and the optimum temperature for bio-oil production can be reduced with other parameters modification, such as the length of the reactor bed, or increasing the heat transfer surface area. This is found to be helpful in energy saving with the aim of high bio-oil yield [74].

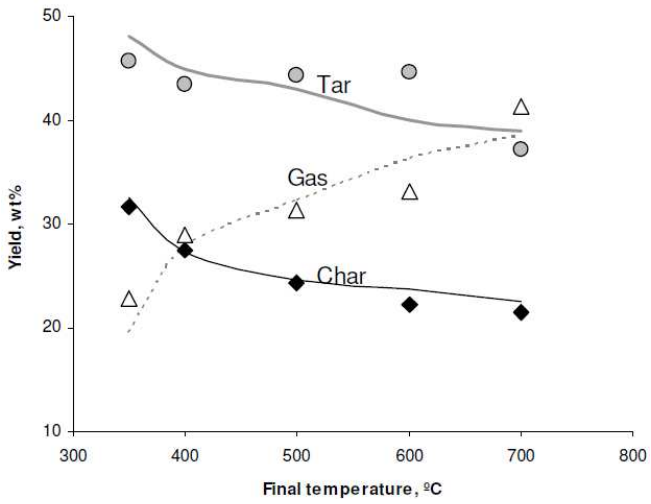

Figure 3 - 3 Comparison between computerised model and experimental results for yield of products in conventional pyrolysis of wood [74]

To prevent further cracking and re-polymerisation in pyrolysis due to excessive heat environment, volatiles should be removed from the bed and cooled down as quickly as possible [36]. Preliminary experiments on biomass pyrolysis in a range of temperatures can provide better judgment of the final temperature choice. TGA analysis on olive waste demonstrated that after the temperature reached 100^oC, the weight loss in biomass was due to vaporisation of absorbed water in the biomass and this continued until 175^oC [36]. The real de-volatilisation occurred between 220^oC and 740^oC

although the main process comprising depolymerisation, decarboxylation and cracking occurred between 200^oC and 400^oC [36].

Although minimum reaction temperature has no effect on the design of the rigs, maximum temperature based on the investigative nature of this research can be up to 1073 K that will dictate the material of choice to be stainless steel.

3.2.4 Nitrogen (N_2) Velocity

By reviewing the available literature on pyrolysis, a range of N_2 flow rates can be observed, but the important point here is that the cross sectional areas of the studied beds are different as well. A simple linear velocity calculation for the reviewed papers has been tabulated in Table 2 - 1 in Chapter 2, and the values shown indicate that the linear velocity range is within 0.87 $\frac{cm}{s}$ to 6.63 $\frac{cm}{s}$.

Based on the investigative nature of this research the full range of the reviewed literature (or even wider range) will be covered based on available resources. It need to be mentioned that the nitrogen can be measured by using volumetric flow meters but to have an understanding of both rigs in similar condition and consistency, the volumetric flow rate is being divided by internal surface area of the bed to have N_2 linear velocity in all the calculations, discussions and conclusions.

3.3 Reactor Design and Fabrication

In considering the reactor design for the current work, not only literature data had to be considered, but the constraints of cost, laboratory space and facilities were also taken into account. As bio-oil is the target of the project, it was decided that a fast pyrolysis system would be the best although conventional pyrolysis is a useful baseline that is

incorporated in this work in order to investigate the effects of heating rate on the final products. As described previously, fast pyrolysis systems require a high heating rate process plus a high cooling rate condenser (quencher). The available laboratory tubular furnaces (Carbolite CTF 12/65/550 and CTF 12/100/900) have a maximum heating rate of $50^{o}C$ per min. Based on Table 2 - 14 in Chapter 2**,** it is impossible to use common laboratory furnaces for fast pyrolysis which should have a heating rate of up to $600^{o}C$ per sec. The condenser design calculations are detailed following by design details of rigs. Finally, different reactor configurations that were designed and tested will be presented and discussed followed by a brief commentary on the fabrication process.

3.3.1 Fixed-bed Reactor

A fixed-bed reactor was designed and fabricated as a baseline for comparison as well as to investigate the effects of heating rate as a pyrolysis parameter. Figure 3 - 4 shows the schematic diagram of the pyrolysis process, and the configurations of the fixed-bed reactor and condenser, respectively.

The detachable fixed-bed reactor has an inner diameter of 52.502 mm connected to a shell and tube condenser to quench the released volatiles. By matching the reactor geometry, a Carbolite tubular furnace type CTF 12/65/550 with a maximum heating rate of 50 K/min is used as a heater. The length of the fixed-bed reactor was chosen to be 10 cm. This rig could be used within the temperature range specified in the DoE matrix, but the maximum heating rate is limited to 50 K/min following the maximum heating rate of the furnace. The bed needs to be placed in the furnace connected to the quenching system before the furnace is turned on. Chapter 5 will present and discuss the

pyrolysis experiments carried out on this setup. The detailed drawings of the main parts of this rig is being represented in Appendix B.

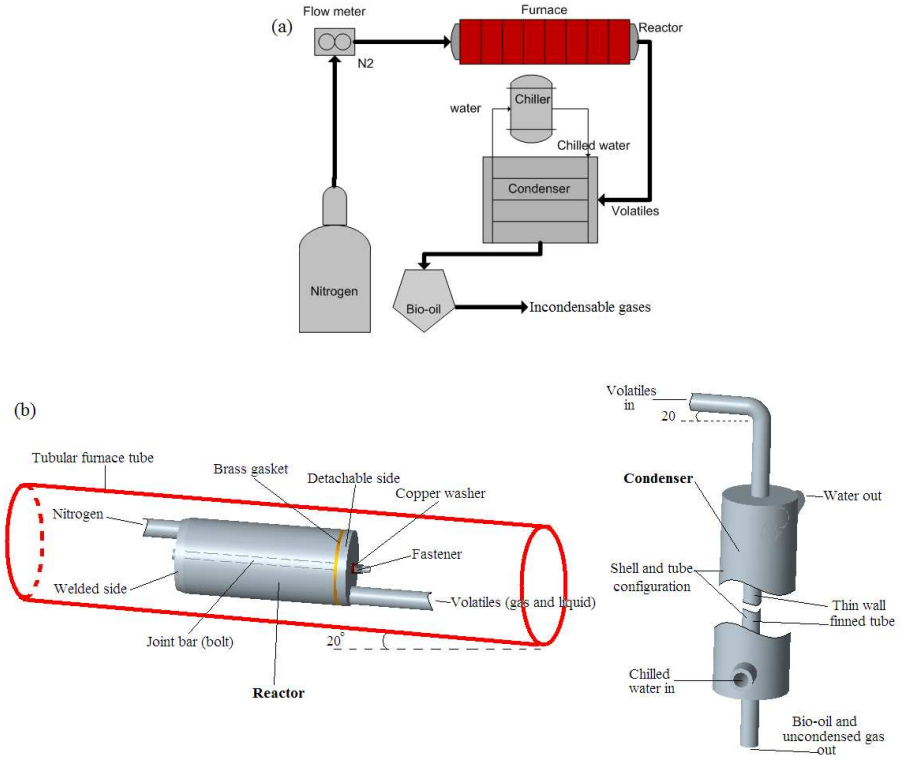

Figure 3 - 4 Pyrolysis rig: (a) schematic diagram of the process (b) rig configurations.

As the available cooling system has less power than tubular furnace, thermodynamics balance seems to be necessary that will be presented here as goal of condenser design. It need to be mentioned that the condenser for both conventional and Rapid Heating rig are the same and in this section the detail thermodynamics calculation of this condenser is presented.

3.3.1.1 Condenser Design

The calculations for the system initiated with boundary conditions and limitations were executed using the thermodynamics approach. The final set of calculations is presented in this section without the trial and error iterations. All the thermodynamics and transport data for the fluids at atmospheric pressure based on the design have been

extracted from "Thermodynamic and Transport Properties of Fluids" by Rogers and Mayhew [78].

The available chiller system to circulate chilled water in the condenser is a Protech refrigerated bath circulator type 632D with full control of water flow rate and temperature. After discussion with the manufacturing company, the maximum cooling capacity of the system at $-10^{o}C$ is 832 W as shown in APPENDIX A, although at higher operating temperatures as chosen for real operations, the power is higher than 832 W. Based on the fact that the UK made Carbolite CTF 12/100/900 and 12/65/550 tubular furnaces (are being used by Rapid Heating fast pyrolysis and conventional pyrolysis rigs respectively) have higher heating capacity of 2 kW as compared to the cooling system with 832 W, the cooling system limits the maximum achievable power for the system.

By considering the design factor of 1.66 for cooling section of the rig (condenser and water cooling bath), the cooling power, $P_{cooling}$ can be estimated as follows, although below calculations is being proved by testing the rigs after calibration and fabrication.

$$P_{cooling} = \frac{\text{Rated cooling power}}{\text{Design factor}} = \frac{832}{1.66} = 499.2 \quad (3.1)$$

Based on the fact that considerable portion of the final bio-oil can be water, hence the thermodynamics behaviour of bio-oil is assumed to be the same as water during condensation process. Additionally, this estimation is the only choice considering that full specifications of water are available whilst thermodynamics data for bio-oil are unknown.

$$\text{For 0.1 kg of cracked bio-oil (water)} \Rightarrow m_{bio-oil} = 0.1 \text{ kg} \quad (3.2)$$

The temperature of bio-oil in gaseous form entering the condenser, T_1, is taken as the upper limit of pyrolysis experiments reviewed from the literature:

$$\Rightarrow T_1 = 900\ ^{o}C = 1173\ K \tag{3.3}$$

To calculate the energy needed to condense the bio-oil (water) from 1173 K down to 300 K (27 ^{o}C) , $E_{cooling}$, the following equation is used whereby the C_p and C_{P_f} values are averaged over the calculated temperatures [78].

$$E_{cooling} = m[C_P(1173 - 373) + h_{fg} + C_{P_f}(373 - 300)] \tag{3.4}$$

$$\overset{(3.2)}{\Longrightarrow} E_{cooling} = 0.1[2.1481 \times 10^3(900) + 2256.7 \times 10^3 + 4.2 \times 10^3(50) \tag{3.5}$$

$$\overset{(3.5)}{\Longrightarrow} E_{cooling} = 4.29 \times 10^5\ J \text{ for 0.1 kg of bio-oil} \tag{3.6}$$

N_2 continuously enters the system at 300 K from the tank and its temperature reaches up to 1173 K. The mass flow rate of N_2, m°, is calculated as follows for a fixed volumetric flow rate of N_2, V° .

$$m^{\circ} = \rho_{N_2} \times V^{\circ} \tag{3.7}$$

By using averaged C_p values for N_2 over the calculated temperatures, the cooling power required for N_2, P_C, is:

$$P_C = m^{\circ} C_P \Delta T = m^{\circ}(1.11985 \times 10^3)(850) = 9.519 \times 10^5 m^{\circ} \tag{3.8}$$

The maximum cooling capacity of the system should be greater than or equal to the combined cooling power required for both bio-oil and N_2. If (t) is the cooling time, the following mathematical statements can be written.

$$\Rightarrow (P_{Cooling})_{Cooling\ system} \geq (P_C)_{nitrogen} + \left(\frac{E_{cooling}}{t}\right)_{Bio-oil} \tag{3.9}$$

$$\xrightarrow{(3.1),\ (3.6)\text{and}\ (3.7)} 499.2 \geq 9.519 \times 10^5 \dot{m} + \frac{4.29\times10^5}{t} \quad (310)$$

$$\Rightarrow \dot{m} \leq 5.244 \times 10^{-4} - \frac{4.51\times10^{-1}}{t} \quad (3.11)$$

This relationship between the cooling time and N_2 mass flow rate is plotted in Figure 3 - 5 for acceptable values of $\dot{m} \geq 0$.

There are two parameters affecting the linear velocity of N_2 ($\dot{x}_{N_2}$), i.e. volumetric flow rate of N_2, $\dot{V}$, and cross sectional area of the bed, A. The maximum N_2 linear velocity from the reviewed papers presented in Table 2 - 1 in Chapter 2 is 6.63 $\frac{cm}{s}$. The chosen bed based on the geometry limitation of the furnace has an internal diameter of 48.70 mm (minimum diameter that is for Rapid Heating rig). By using these values, $\dot{V}$ can be calculated.

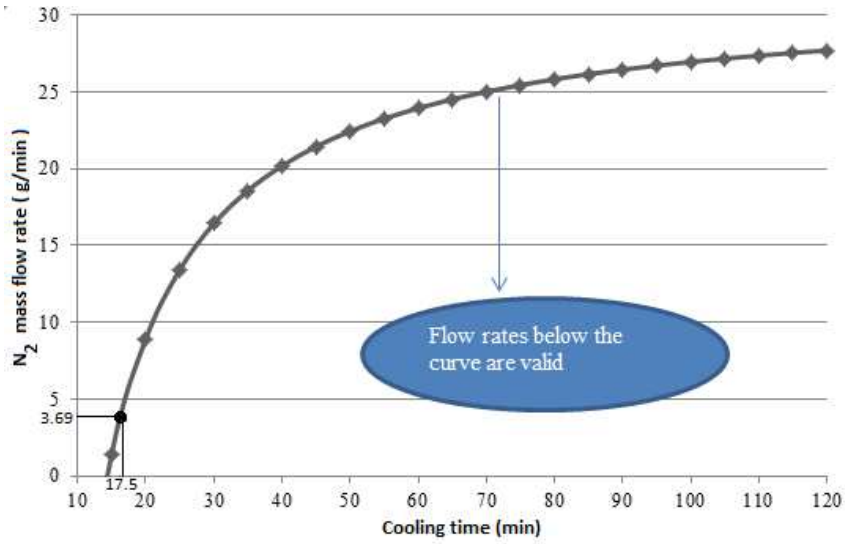

Figure 3 - 5 Plot of Equation 3.11 showing N_2 mass flow rate vs. cooling time

$$\xrightarrow{\text{Cross sectional area of bed}} A = \frac{\pi D^2}{4} = \frac{\pi\times4.87^2}{4} = 13.1344\ cm^2 \quad (3.12)$$

$$\Rightarrow \dot{V} = A \times \dot{x}_{N_2} = 13.1344 \times 6.63 = 87.081\ \frac{cm^3}{s} \quad (3.13)$$

$$\Rightarrow \dot{V} = 5.225 \times 10^{-3} \frac{m^3}{min} \quad (3.14)$$

The maximum mass flow rate is when the density of N_2 is maximum and this occurs at the lowest temperature of the Design of Experiments (DoE).

$$\xrightarrow{\text{At 573 K}} \dot{m} = \rho_{Nitrogen} \times \dot{V} = 0.706 \times 5.225 \times 10^{-3} = 3.689 \times 10^{-3} \frac{kg}{min}$$

$$\Rightarrow \dot{m} = 3.689 \frac{g}{min} \text{ or } \dot{m} = 6.148 \times 10^{-5} \frac{kg}{s} \quad (3.15)$$

Figure 3 - 5 illustrates that the mass flow rate obtained from calculations at the limiting condition is in the valid zone if the cooling time is approximately 17.5 min or higher.

For validation of the inner diameter of bed, the range of obtainable linear velocities of N_2 can be found by using the available cooling system at the minimum, medium and maximum reaction temperatures.

Balancing the net cooling power $\Rightarrow P_{cooling} = (P_C)_{Nitrogen}$

Minimum reaction temperature

$$\xrightarrow{\text{Bed at 573 K (3.7)}} P_{cooling} = \dot{m}(C_P)_{Average\ (573\ K,\ 300\ K)} \Delta T \quad (3.16)$$

$$\Rightarrow 499.2 = \dot{m}\left(\frac{1.04+1.056}{2}\right) \times 10^3{}_P (500 - 300)$$

$$\Rightarrow \dot{m} = 1.592 \times 10^{-3} \frac{kg}{s}$$

$$\xrightarrow{(3.6)\text{and } (3.13)} (\dot{x}_{N_2})_{At\ 573\ K} = \frac{\dot{m}}{A(\rho_{N_2})_{at\ 573\ K}} = \frac{1.592 \times 10^{-3}}{13.1344 \times 10^{-4} \times 0.706} = 171.7 \frac{cm}{s} \quad (3.17)$$

Similarly, the N_2 linear velocity for medium and maximum reaction temperatures based on DoE are given by Equation 3.18.

$$\Rightarrow (\overset{\circ}{x}_{N_2})_{\text{At } 800\text{ K}} = 159.38\ \frac{\text{cm}}{\text{s}} \text{ and } (\overset{\circ}{x}_{N_2})_{\text{At } 1073\text{ K}} = 129.159\ \frac{\text{cm}}{\text{s}} \quad (3.18)$$

Figure 3 - 6 depicts the design coverage range with regard to the N_2 flow rate. The wide range of N_2 linear velocity has been chosen intentionally for the likelihood of further investigation at higher velocities.

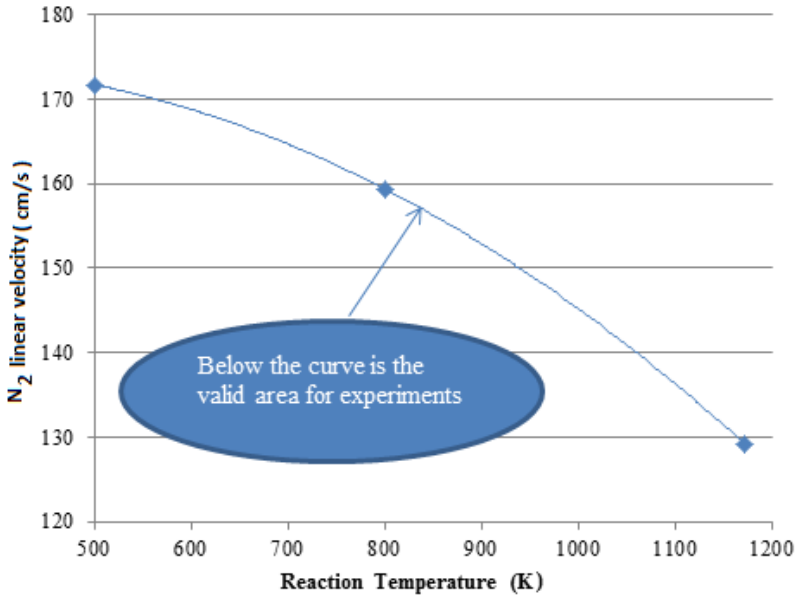

Figure 3 - 6 Maximum achievable N_2 linear velocity over temperature range for the designed reactor.

It need to be considered that the design factor (safety factor) of 1.66 is considered in above calculation. Later by using thermocouples and digital meters, above design is confirmed as a matter of operation and efficiency.

3.3.2 Rapid Heating Reactor

The main idea of this reactor originated from the injection reactor, which will be described in later sections of this chapter. In view of the preliminary tests with different reactor configurations as will be discussed later in this chapter, an alternative approach

utilising a totally mobile reactor was then designed in order to achieve high heating rates with the same furnace. Figure 3 - 7 shows the schematic diagram of this rapid heating reactor.

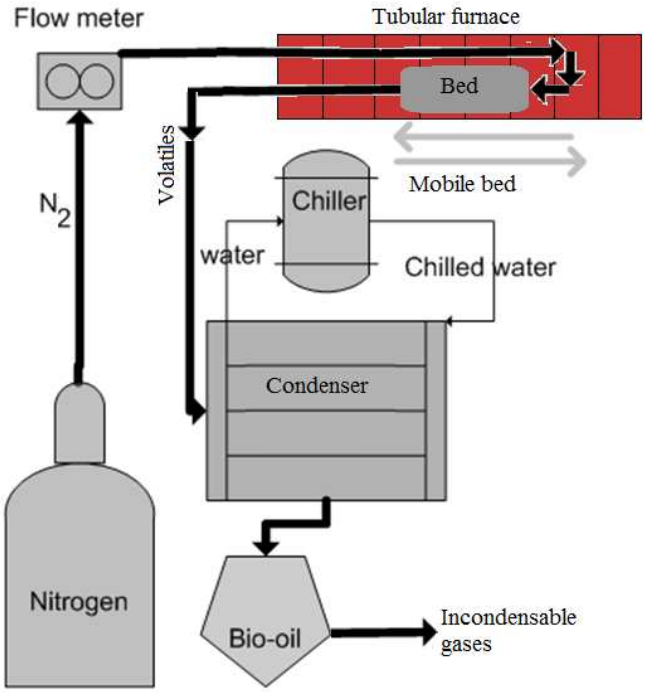

Figure 3 - 7 Rapid heating reactor system

The rapid heating pyrolysis rig was designed in such a way that both inlet and outlet pipes are fixed on one side of the bed as shown in Figure 3 - 7 and Figure 3 - 8 which enables the reactor to be mobile. In order to achieve high heating rate (for rapid heating fast pyrolysis) with maximum 25.67 K/s by using a furnace with a maximum heating rate of 50 K/min, the furnace needs to be turned on without the reactor inside initially. When the temperature of the furnace reaches the reaction temperature, the reactor is placed into the furnace to experience thermal shock with a high heating rate. To prevent leakages from the detachable joints, brass and copper plates were used as gasket and washer, respectively. The unavoidable use of these two metals limited the maximum reaction temperature to 1073 K to prevent any melt down of these sealing materials.

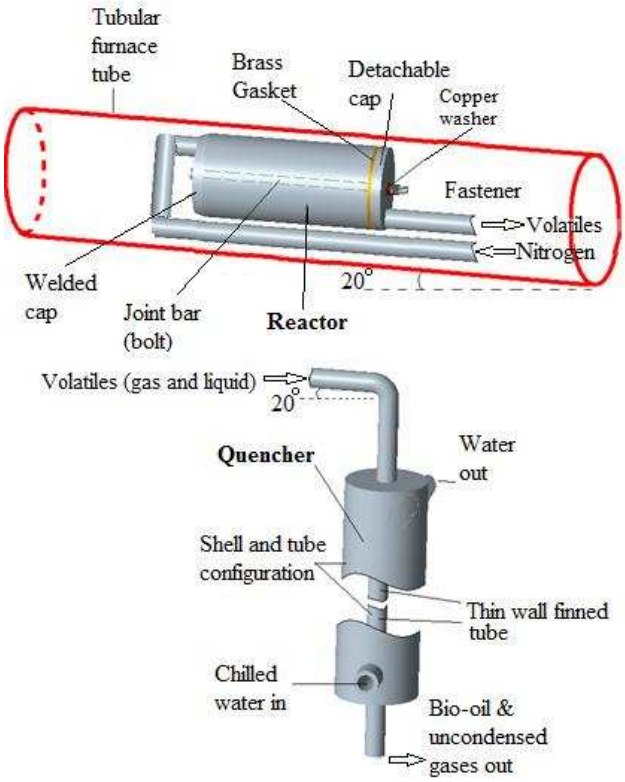

Figure 3 - 8 Parts and joints of rapid heating rig

The detachable rapid heating reactor has an inner diameter of 48.70 mm connected to a shell and tube condenser (its design already mentioned in last section of this chapter under conventional pyrolysis rig design) to quench the released volatiles. By matching the reactor geometry, a Carbolite tubular furnace type CTF 12/100/900 is used as a heater. As discussed before, initial investigations showed that significant uneven heat distribution in the tubular furnace existed. Using reactors equal to or longer than the length of furnace resulted in condensation of volatiles inside the reactor. This phenomenon was the main factor which prevented proper bio-oil collection as the volatiles would condense and cover the inner walls of the reactor only. Therefore, the length of the reactor was chosen to be equal to the maximum heating zone inside the tubular furnace (10 cm) to overcome the condensation problem (Figure 3 - 8). Initial experimental observations also indicated that it was possible under certain conditions

for the biomass to be transformed directly into liquid bio-oil. Both the placement of the reactor outlet tube at minimum height position and inclining the reactor at a 20^{o} angle from the horizontal ensure the collection of this portion of bio-oil. Low-pressure N_2 and gravitational force were used in the whole process to forward both the gas and liquid along the rig. The slanted tube then bends into the vertical shell and tube quencher to allow the gravitational force to drive the bio-oil into the collector at the bottom (Figure 3 - 8). The condenser utilises cooling water in counter-current flow from a refrigerated bath circulator type 632D. The heat transfer area of the condenser was designed such that the outlet gas temperature is below 303 K when the cooling water temperature is fixed at 278 K. The vertical orientation of the condenser also improved the convection heat transfer as gas with higher energy and temperature tends to rise up while cooler gas is forced down via natural convection. The inner tube of the condenser was milled to reduce the wall thickness and to create a finned tube to maximise heat transfer between the water and the gaseous volatiles (Figure 3 - 8).

This rig provided the necessary high heating rates required for fast pyrolysis in addition to covering the whole range of temperatures specified in the DoE matrix. Chapter 5 will discuss in detail the comprehensive pyrolysis tests carried out on this rig.

3.3.3 Fabrication Process

The material (mainly stainless steel) was chosen based on constraints of cost, facilities and manufacturing technology. A reduction in 80% cost of raw materials was achieved by negotiating with different suppliers. The final detailed drawings of the major parts of the designed rigs have been included in APPENDIX B. Although the major fabrication steps have been detailed in APPENDIX C, an important note regarding the sealing of the rig seems necessary to be reported here. Originally, the time allocated for fabrication and troubleshooting was approximately 90 days, but after

carrying out sealing tests using pressurised air (≈ 4 bar), several leakages were detected in the welded zones. This problem caused a further delay of 30 days and after further research, TIG (Tungsten Inert Gas) welding was chosen to cover the leakage spots on the previously MIG (Metal Inert Gas) welded zones. TIG welding has the ability of a higher concentrated arc to create higher temperatures to melt down the stainless steel at the welding spot properly and to cover the leakage spots. Two pieces of coils were sent to an external workshop for welding because the leakages were too complicated to be resolved using the available facilities within the university workshop.

3.4 Other Investigated Reactors

In this section other types of bed will be briefly discussed that was investigated along this research but they have not been used in production of bio-oil. Any of these considered beds could be used with further investigation but that investigation could be out of the scope of this research but they can be areas for further investigation or modification for further study. All the design details for these beds were set in Appendix B. The materials used for these investigations (fabricated beds) mainly was scrap metals available in workshops and the time spent on fabrication and test was the free time in between the main research development.

3.4.1 Fluidised Bed

The ability and range of fluidised bed for pyrolysis process has been discussed in Chapter 2. Despite the ability of this system to facilitate fast pyrolysis targeting bio-oil production, a number of drawbacks exist including more complicated design, generally large footprint and high cost. Considering the allowable budget, it was decided that designing and fabricating a fluidised bed was out of the scope of this research.

3.4.2 Injection Reactor

The second proposal was an injection reactor with a simple design and manageable fabrication. The reactor has been designed based on the fact that the furnace is not able to reach to the target temperature in a short time, but the pyrolysis bed can be left in the furnace without the biomass until steady-state is reached. Once a steady flow of N_2 at the desired temperature and flow rate is achieved, the designed injection system will add the biomass into the system to obtain fast pyrolysis heating rates (Figure 3 - 9). This system was designed, but two problems were faced with this design and based on that after design it was not fabricated and instead Rapid Heating bed was designed and fabricate. Firstly, sealing the system after injection poses the potential risk of explosion based on the probability of mixing high temperature volatiles with air. Secondly, the targeted temperature might not be accurate with the fast introduction of the injector inside the bed with significant difference in temperatures.

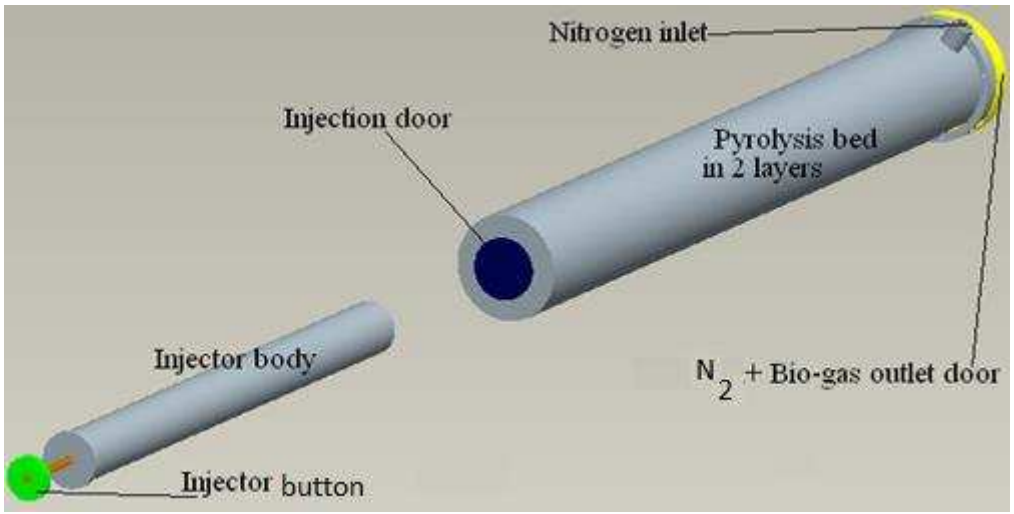

Figure 3 - 9 Injection (spoon) pyrolysis system

3.4.3 Convection Reactor with Single Tube Pre-heater

In this model as shown in Figure 3 - 10**,** the biomass would be placed in a bed outside of the furnace. Instead of heating the bed, the furnace is heating a designed pre-heater (with outer and inner diameters of 60.32 mm and 52.50 mm, respectively) until steady-state conditions marked by a steady flow of N_2 at the desired temperature and flow rate are achieved. The hot N_2 can be channelled into the bed using a high temperature resistant 2-way valve. The short residence time of the biomass in the hot N_2 gas meets the criteria of fast pyrolysis as quenching of the gas occurs immediately after the bed reaction. A condenser was designed as described in Section 3 to complete the process by quenching.

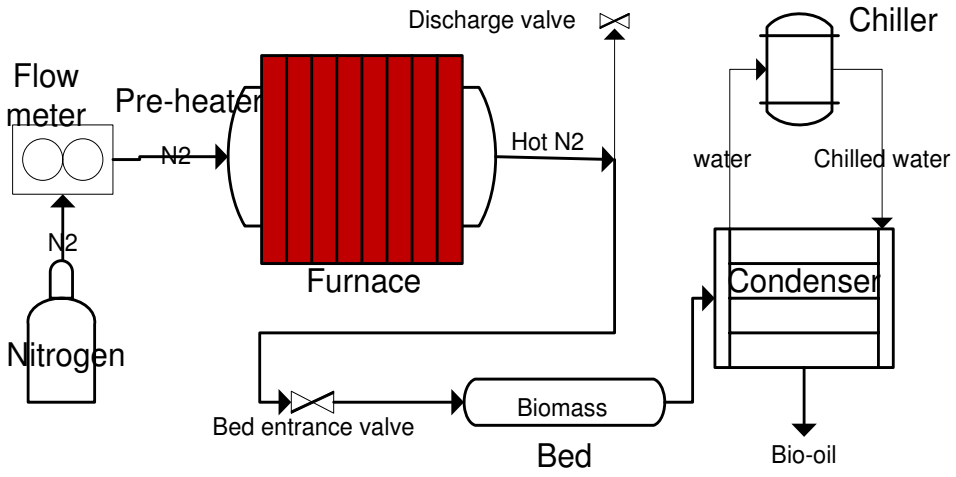

Figure 3 - 10 Schematic operation of convection reactor

Parallel to analytical tests on the Jatropha curcas pressed cake, preliminary tests on the rig were carried out after the pre-heater was fabricated. In the first set of tests, the main problem faced was the low temperature (below 333 K) of output N_2 from the pre-heater section even after setting the temperature of the tubular furnace to maximum (1273 K) and using the maximum experimental N_2 flow of 6.7 cm/s. It was observed that there was almost no correlation between the set furnace temperature and the outlet

N_2 temperature. This unexpected observation resulted in an investigation to clarify and resolve this problem by redesigning the pre-heater.

Heat loss into the surroundings was determined as the most likely reason for the lack of heat transfer into N_2 during operation. This probable source of problem was resolved by using a ceramic fibre insulator which can be used in very high temperature (up to 1573 K) applications. The temperature of N_2 was improved up to 345 K after insulation, but could not reach to the desired temperature for pyrolysis purpose yet.

Subsequently, from temperature tests, it was found that the CTF 12/65/550 tubular furnace has a very limited length (≈ 10 cm) of heating zone. Although the design was focused on using the above furnace, the pre-heater with a longer tube could also be used with CTF 12/100/900 tubular furnace which is longer. The CTF 12/100/900 also had approximately 10 cm of heating zone. Although the manufacturer's catalogue indicated that the heated tube lengths are 550 mm and 900 mm, respectively for the above furnaces, the actual heating length from temperature tests is approximately 100 mm only for both furnaces. This dramatic difference in heating zones directly affected the outlet N_2 temperature from the tubular furnace.

3.4.4 Convection Reactor with Annulus Pre-heater

To increase the heating capacity of pre-heater, one inner pipe (same outer pipe as before and an inner pipe with 42.16 mm outer diameter and 35.06 inner diameter) was designed to be inserted into the original pre-heater to create a double layer pipe (annulus). This effectively meant that the N_2 enters a double layer piping system with increased heating time. It will firstly be heated up in the annulus and subsequently, it will enter into the inner pipe to be further heated. The schematic flow of N_2 in this double tube pre-heater is shown in Figure 3 - 11. After this modification, the

temperature of the N_2 outlet from the double tube pre-heater was raised to 355 K, but was still not sufficiently high for pyrolysis.

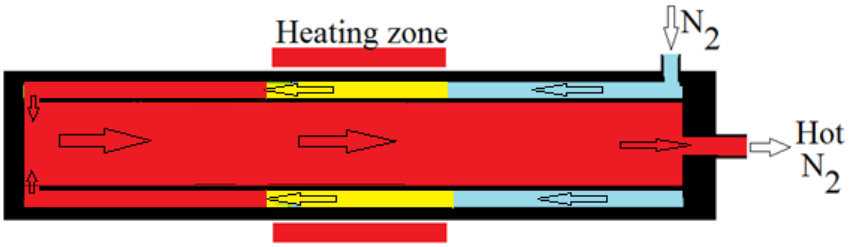

Figure 3 - 11 Annulus pre-heater

3.4.5 Convection Reactor with Finned Pre-heater

After reconsidering the heat transfer within the system, a finned pre-heater was used to improve the heat transfer especially in the limited heating zone. Detachable fins were installed in the heating zone inside the tube with the distance of 3 mm as shown in Figure 3 - 12. As can be observed, N_2 has to pass over the fins in a zigzag (up and down) movement. The increased heating time resulted in an improvement in the outlet N_2 temperature up to 367 K, which was still not high enough.

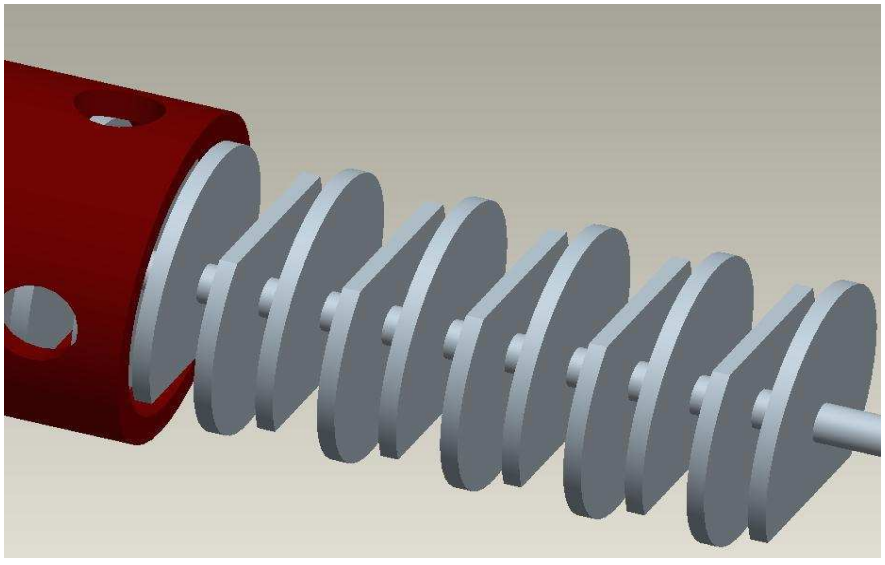

Figure 3 - 12 Detachable fins inside the pre-heater

3.4.6 Convection Reactor with Double Piston Pre-heater

In addition to the preliminary tests described above, the volumetric flow rate / linear velocity of N_2 was tested, and the results obtained demonstrated that this was one of the most effective parameters in determining the outlet gas temperature. Increasing the volumetric flow rate of N_2 up to $25\frac{l}{min}$ for preliminary testing showed that a maximum outlet N_2 temperature of 696 K could be achieved. This could be further increased up to 730 K by adding insulation and detachable fins. Although the temperature reached was sufficiently high for pyrolysis process, the volumetric flow rate / linear velocity of N_2 was now between 10 to 25 times higher than that of the original bed design. To avoid this high operational N_2 velocity and to increase the temperature to cover the whole DoE range, further investigation of correlation between temperature rise and N_2 velocity was carried out. The results of this investigation can be presented mathematically as follows:

At a pre-determined condition (mean point) in the DoE, the linear velocity of N_2 is set to be $2.9\ \frac{\text{cm}}{\text{s}}$.

$$\xrightarrow{\text{in pre-heater with A=13.134 cm}^2} \text{V}^{\text{o}} = 2.285\ \frac{\text{L}}{\text{min}} \tag{3.19}$$

$$m^o = constant \Rightarrow \rho_{in\ pre-heater} \times V^{\circ}_{in\ pre-heater} = \rho_{inlet} \times V^{\circ}_{inlet} \tag{3.20}$$

$$\xrightarrow{3.20\ and\ assumed\ pre-heater\ at\ T=823^{\circ}K} V^{\circ}_{inlet} = 0.836\frac{l}{min} \tag{3.21}$$

For the double tube pre-heater, this volumetric flow rate results in Reynolds numbers within the laminar region.

$$Re_{annulus} = \frac{\rho v(D_o - D_i)}{\mu} = 11.41\ and\ Re_{pipe} = \frac{\rho v D}{\mu} = 22.394 \tag{3.22}$$

The Reynolds numbers cum experimental observations instigated an investigation into the effects of Reynolds number on the convection heat transfer. For turbulent flow inside the pipes, the Dittus-Boelter correlation is commonly used for calculation of the convection heat transfer coefficient [75–77]:

$$\xrightarrow{Dittus-Boelter} \bar{h} = \frac{k}{D_H}(0.023)\, Re_D^{0.8} pr^{0.4} \quad \text{(Turbulent flow)} \tag{3.23}$$

Direct mathematical relationship between the Reynolds number and the convection heat transfer coefficient as shown above was corroborated by tests on the pre-heater pipes. By using the definition of Reynolds number, the diameter of the pipe for the experimental range can be calculated as follows.

$$Re = \frac{\rho v D}{\mu} \xrightarrow{1150\ K} Re = \frac{0.3069\, vD}{4.511\times10^{-5}} \tag{3.24}$$

To avoid laminar flow, the Reynolds number must be a minimum of 4000.

$$\xrightarrow{(3.24)} vD \geq 0.588 \Rightarrow \frac{\dot{m}}{\rho A} D \geq 0.588 \xrightarrow{Pre-heater\ condition} D = 0.11\ mm \tag{3.25}$$

The significant difference between the current pre-heater pipe diameter and the above theoretical diameter explains the low temperatures measured at the pre-heater outlet in experimental tests. To reduce the size of the pre-heater pipe, two pieces of cylindrical steel with a total length of 10 cm were fabricated and drilled with 0.5 mm drill bit (minimum possible based on limitation of drilling system) and placed inside the pre-heater pipe as depicted in Figure 3 - 13. Experimental tests resulted in a final temperature of 375 K at a N_2 velocity of 6.7 cm/s (maximum flow based on DoE) without insulation. Based on the geometry of this design, a higher velocity of N_2 cannot be achieved at low inlet pressure.

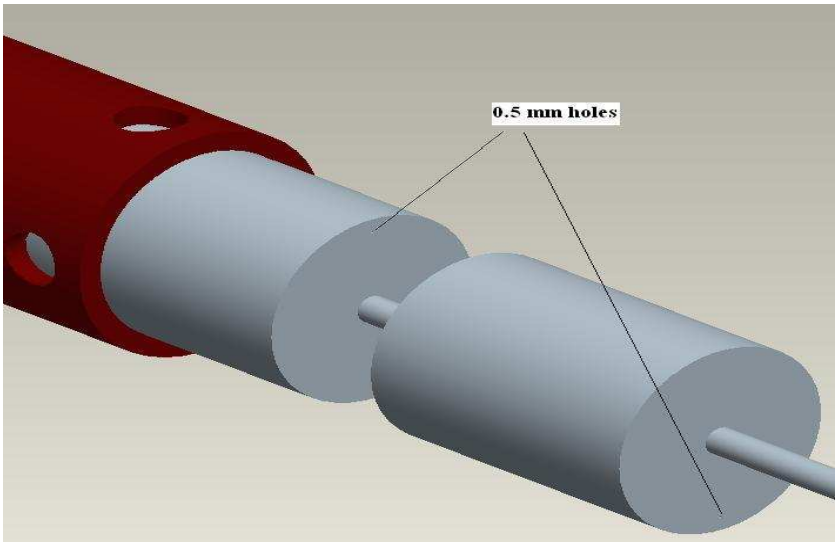

Figure 3 - 13 Double pistons with opposite side holes (for Reynolds number test)

3.4.7 Convection Reactor with Heating Discs Pre-heater

In this configuration, a set of 20 discs were fabricated with thickness of 3 mm and were joint together on a steel bar. The distance between each of them was 0.5 mm, and each of them has a hole with diameter of 0.5 mm as shown in Figure 3 - 14. The discs were installed in the pre-heater pipe in such a way that the consecutive disc holes were not aligned along a straight line as pictured in Figure 3 - 14 to create turbulent flow and increase the convection heat transfer. Theoretically, the Reynolds number is increased with this configuration, and the position of discs aids in creating turbulence flow to improve convection heat transfer. Experimentally, the outlet temperature of N_2 increased up to 475 K at a N_2 velocity of 6.7 cm/s and a furnace temperature of 1273 K. Although minor pyrolysis reaction was observed, the majority of biomass (≈ 80%) in the bed did not change colour after 2 hr, which indicated that full pyrolysis could not be developed based on this temperature.

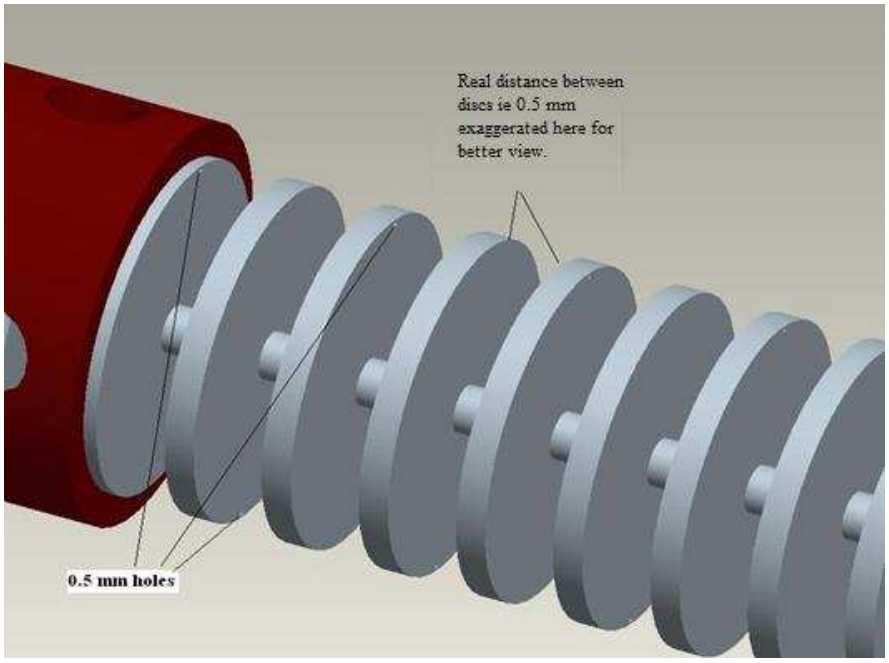

Figure 3 - 14 Heating discs pre-heater

3.4.8 Convection Reactor with Heating Coil Pre-heater

Another pre-heater as can be seen in Figure 3 - 15 was then designed by coiling a stainless steel tube with internal diameter of 0.5 mm. Fabrication of this was carried out by Swagelok in Malaysia.

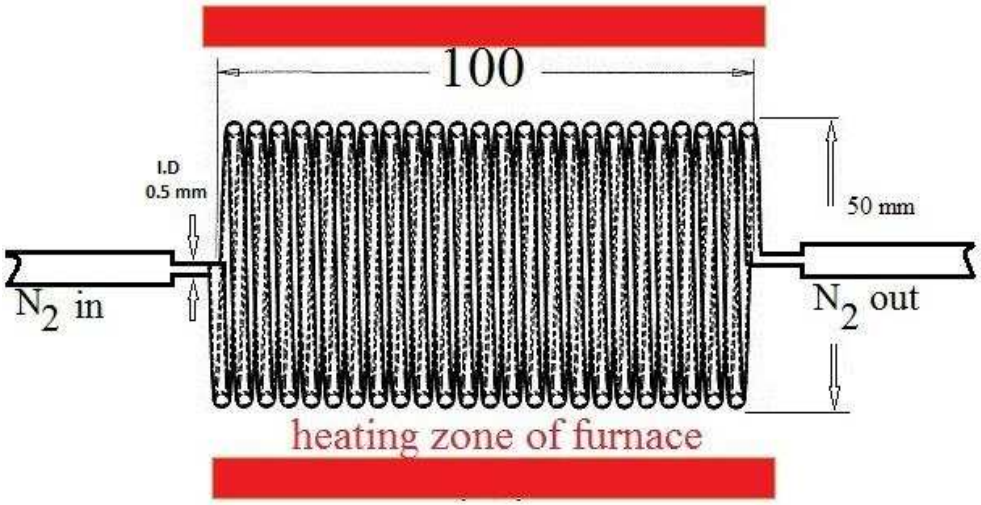

Figure 3 - 15 Heating coil pre-heater

Theoretically, the Reynolds number should keep increasing along the whole length of the compacted coil which is set under the heating zone. The convection heat transfer was significantly increased as evident by the increased N_2 outlet temperature of 667 K at a N_2 velocity of 6.7 cm/s and a furnace temperature of 1273 K. It was observed experimentally that pyrolysis process occurred within the bed, but was not completed. This was attributed to the observation that half the biomass did not changed colour after 2 hr of reaction.

3.5 Concluding Remarks

After experimentally testing with several reactor configurations, two reactor configurations, i.e. fixed-bed and rapid heating were finally chosen as the final rig setups for conventional and fast pyrolysis experiments, respectively. The rapid heating reactor can heat the biomass with a heating rate of 25.67 K/s whereas the fixed-bed has a heating rate of 50 K/min. By using these two rigs, the whole temperature range from 573 K up to 1073 K can be investigated. A condenser capable of quenching the volatiles from the pyrolysis reactors to produce bio-oil has also been designed using a thermodynamics approach and fabricated as part of the test rigs.

CHAPTER 4 JATROPHA CURCAS PRESSED CAKE PHYSICOCHEMICAL CHARACTERISATION

4.1 Introduction

Based on the fact that the source of biomass for this research is Jatropha curcas pressed cake, it seems essential to look into its characteristics before attempting to produce bio-oil from it. Apart from indicating the kind of preparation or treatment is needed before pyrolysis, this investigation can indicate how different the sample used in this research is from other Jatropha curcas pressed cake samples as well as confirming its viability to be used in this research. It also can show the differences between this source and other type of biomass resources that are covered in Chapter 2.

The chapter will cover the source of biomass following by describing the methods that are being used for these preliminary tests on samples before pyrolysis. Later the results from different tests were analysed and the chapter will be concluded at the end.

4.2 Feedstock

Jatropha curcas pressed cake was obtained from Bionas Group (Malaysia) to be used as the pyrolysis feedstock for this research. This company is using Jatropha curcas oil by milling (pressing) its seed to produce biodiesel and other bio-fuels products. The pressed cake is the waste product of the milling process.

4.2 Methodology

After delivery of the pressed cake to The University of Nottingham Malaysia Campus, it was oven dried tested at 377 K for a minimum of 24 hr based on ASTM D4442-03 method B and simultaneously, the moisture content of the sample was determined by taking the average of triplicate mass measurements using BS 1016-102:2000 method [79–80]. Basically for all tests that are being mentioned in this chapter minimum of three tests were conducted. After making sure that the difference between three test results (maximum number and minimum number) is below 5%, they are averaged and demonstrated. The gross calorific value of the biomass was measured by using a Parr 6100 calorimetric bomb based on ASTM D2015-96 method [81].

The biomass was prepared for other tests including pyrolysis tests by grinding into powder form in a 2-step process. Firstly, the pressed cake was converted into granules using a Retsch SM100 Comfort grinder machine. Secondly, the granules were ground and sieved using a sieve size of 0.2 mm in a Retsch ZM200 centrifuge grinder.

TGA by using a Mettler-Toledo TGA/DSC 1 unit was carried out on the Jatropha curcas pressed cake to determine its moisture, volatiles, fixed carbon and ash contents [82].

A Thermo Conductivity Detector Infra-Red (TCD-IR) was used to analyse the organic elements, i.e. carbon, hydrogen, nitrogen and oxygen (C-H-N-O) of the Jatropha curcas waste. For the analysis of inorganic elements, Inductively Coupled Plasma Mass Spectrometry (ICP-MS) Thermo-Fisher Scientific X-Series^{II} equipped with Collision Cell Technology with Energy Discrimination (CCTED) was used. The milled Jatropha curcas waste was digested in duplicates and analysed in duplicates. The

elemental content is expressed as a percentage of the mass of the sample analysed. All elements below 0.01% are excluded, and silicon content was not analysed.

For the rest of detectable inorganic elements not measured by the ICP-MS, the results of an Energy Dispersive X-ray Spectroscopy (EDX) Oxford Instrument Analytical model X-Max Silicon Drift Detector 20 mm^2 were used. Figure 4 - 1 and Figure 4 - 2 show the photograph and interpreted spectrum, respectively from the EDX unit.

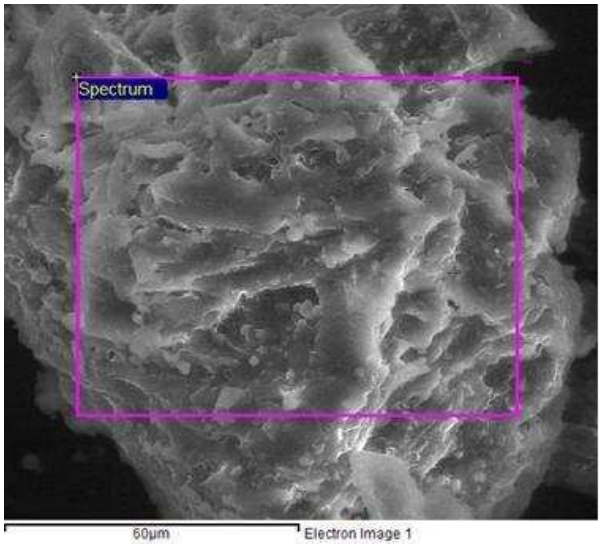

Figure 4 - 1 Photograph taken from Jatropha curcas powder by EDX unit

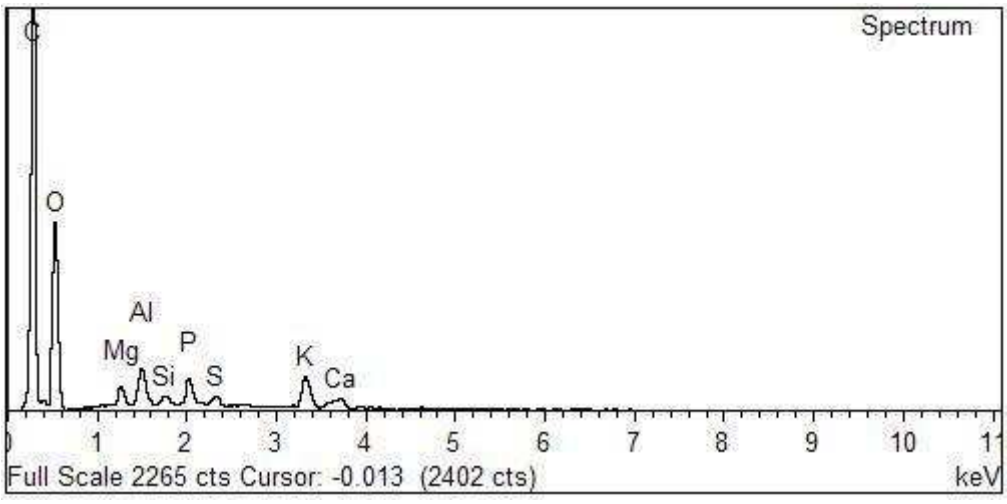

Figure 4 - 2 EDX spectrum for Jatropha curcas pressed cake

Cross-Polarization/Magic Angle Spinning (CP/MAS) solid-state ^{13}C Nuclear Magnetic Resonance (NMR) was used to determine the fraction of organic compounds in the biomass. It is a powerful technique that can measure the aromaticity level of solid fuels. Solid-state ^{13}C NMR shows the placement of carbon. Based on the molecule that the carbon-13 is attached to, to bring it into a resonance condition under special radio frequency, a special magnetic field needs to be applied. This means that the carbon molecule construction can be interpreted directly from the results of ^{13}C NMR spectra. The ^{13}C CP-MAS spectrum of Jatropha curcas waste displays signals related to the intensities of the carbons that construct lignin, hemicellulose and cellulose (Figure 4 - 3).

Except for TGA, calorimetric bomb and EDX, all the other analytical tests as described above were carried out at the University of Nottingham, United Kingdom Campus laboratories.

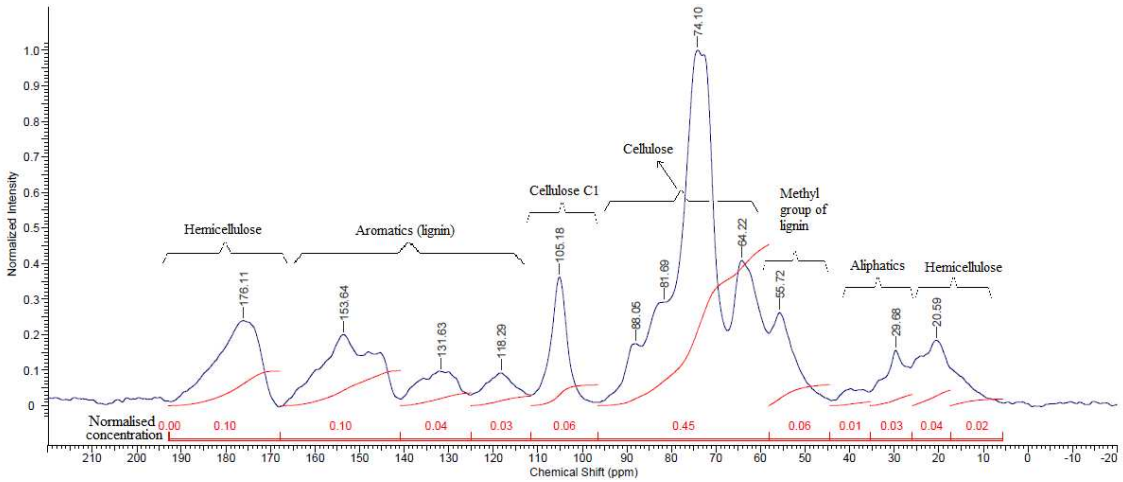

Figure 4 - 3 ^{13}C CP-MAS spectrum of Jatropha curcas waste signals and their intensities

4.3 Results and Discussion

4.3.1 Moisture Content

Table 4 - 1 tabulates the results of the physicochemical tests on the Jatropha curcas pressed cake while the TGA results are shown in Figure 4 - 4. As shown in both Figure 4 - 4 and Table 4 - 1, the moisture content of Jatropha curcas waste from the oven drying method matches with the TGA with less than 0.1 wt% difference. Thus, this confirms the accuracy of both results. Having less than 4 wt% moisture can reduce the energy consumption and cost of bio-oil production by omitting the drying process as drying is only suggested for pyrolysis process for above 10 wt% moisture content [17]. A moisture content of below 4 wt% is relatively low considering that under Malaysian climate conditions, the average humidity is approximately 80% [83].

Table 4 - 1 Physicochemical properties of Jatropha curcas pressed cake

Physicochemical property		Unit	Value	Method
Moisture content		wt%	3.40	Oven Drying
Gross calorific value		MJ/Kg	19.11	Bomb Calorimeter
Moisture content		wt%	3.31	Thermo-Gravimetric Analysis
Volatiles content			70.98	
Fixed carbon content			19.72	
Ash content			5.99	
Carbon	(C)	wt%	45.75	Thermo Conductivity Detector Infra-Red
Oxygen	(O)		38.20	
Hydrogen	(H)		6.24	
Nitrogen	(N)		3.56	
Potassium	(K)	wt%	1.87	Inductively Coupled Plasma Mass Spectrometry
Magnesium	(Mg)		0.79	
Calcium	(Ca)		0.52	
Iron	(Fe)		0.10	
Sodium	(Na)		0.05	
Aluminium	(Al)		0.02	
Phosphorus	(P)	wt%	0.75	Energy Dispersive X-ray Spectroscopy
Sulphur	(S)		0.22	
Silicon	(Si)		0.09	
Undetectable elements		wt%	1.84	By calculation
Cellulose		Carbon wt%	48.92	^{13}C Nuclear Magnetic Resonance
Lignin			25.00	
Hemicellulose			13.04	
Cellulose C1			6.52	
Aliphatic			6.52	

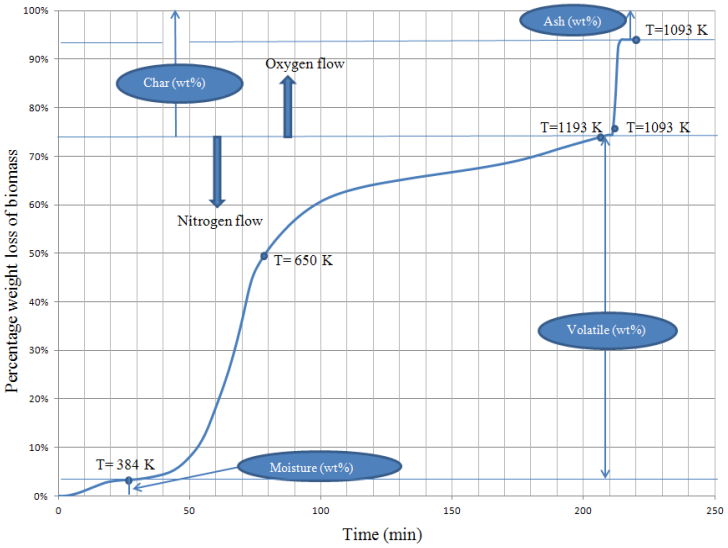

Figure 4 - 4 Thermo-gravimetric analysis (TGA) of Jatropha curcas pressed cake

4.3.2 Gross Calorific Value

The Jatropha curcas pressed cake has a typical biomass average gross calorific value of 19.11 MJ/kg (Table 4 - 1) [17]. The gross calorific value is important in determining the viability of bio-oil production through energy balance analysis as discussed in Chapter 5.

4.3.3 Volatiles, Fixed Carbon and Ash Contents

Figure 4 - 4 shows that the Jatropha curcas pressed cake has a maximum volatile content of 70.98 wt%, which is indicative of the potential bio-oil content. The same figure shows that more than 60 wt% of the total volatiles is cracked under temperatures as low as 650 K. This indicates that this waste has the potential to be used as a source of fuel economically (low cost and/or energy).

As a result from Figure 4 - 4 which is also shown in Table 4 - 1, the Jatropha curcas waste has only 19.72 wt% fixed carbon content or combustible char which again indicates its potential as a source of liquid biofuel.

Ash comprises below 6 wt% of the Jatropha curcas waste (Table 4 - 1). Although it is not directly related to this research, this value shows the potential of the waste to be used as a solid fuel. In some countries such as UK whereby coal is a major source of energy production, this solid waste can be a competitive coal co-firing fuel. The low ash content reduces the challenges in using this waste as a solid co-firing fuel.

4.3.4 Carbon, Hydrogen, Nitrogen and Oxygen Contents

The average carbon content of 11 different types of wood biomass sources has been reported as 50.20 wt% [84]. The carbon content of the Jatropha curcas waste is 45.75 wt%, which is close to this average (Table 4 - 1). Although a higher amount of initial carbon can be indicative of higher energy content since carbon is involved in combustion, other elements of the original biomass and final bio-oil also play important roles in determining their physicochemical characteristics.

Based on Table 4 - 1, the Jatropha curcas waste has an almost equal amount of hydrogen as the average amount of other 11 different biomass sources [84] which is indicative of its potential as a bio-oil source.

Although nitrogen is not directly involved in combustion, its content needs to be investigated as it is linked to NO_x pollution. Table 4 - 1 shows that the nitrogen content of Jatropha curcas waste is approximately 5 wt% more than the average of 11 different biomass types [84]. Chapter 7 further investigates the nitrogen content in the produced bio-oil.

One of the challenges faced in practical bio-oil applications is its high oxygen content. The Jatropha curcas waste contains 38.20 wt% of oxygen (Table 4 - 1), but the average oxygen content of 11 different biomass sources as reported by Ragland et al. [84] is 43.50 wt%. This is generally an advantage as compared to other biomass

resources even though the chemical bonding of oxygen in the biomass needs to be investigated.

4.3.5 Inorganic Elements

From Table 4 - 1, it can be seen that with the exception of potassium with less than 2 wt%, all other inorganic elements have less than 1 wt% each in the Jatropha curcas waste. Although the amount of sulphur is only 0.22 wt%, it is important to focus on this element amongst all inorganic elements because of its health implications when released as SO_x emissions, for example ASTM D7544-10 [85]. Chapter 7 deals with this aspect in detail for the produced bio-oil.

4.3.6 Organic Compounds

The total celluloses and lignin are the portions of organic compounds within the biomass that are involved in the formation of light and heavy oils during pyrolysis. Based on Table 4 - 1, above 80 wt% of Jatropha curcas waste have the potential to be transformed into light and heavy oils, which are the key components of bio-oil.

4.4 Concluding Remarks

Physicochemical characterisation of Jatropha curcas pressed cake has been carried out. The results obtained shows that the waste has comparably lower moisture and oxygen contents, and similar gross calorific value, volatiles, fixed carbon, ash, carbon and hydrogen contents as compared to reported averages of 11 different biomass sources. This biomass also contains a low amount of inorganic elements (below 2 wt%), but over 80 wt% of combined celluloses and lignin. Although the results for nitrogen and sulphur contents are slightly higher as compared to the reported average, they will be investigated by physicochemical characterisation of bio-oil discussed later on in Chapter 7. The findings of the characterisation study indicate that the Jatropha curcas

pressed cake is a potential source of bio-oil production and for this sample except grinding no other preparation or treatments prior to pyrolysis is needed.

CHAPTER 5 PARAMETRIC INVESTIGATION OF CONVENTIONAL FIXED-BED PYROLYSIS AND RAPID HEATING FAST PYROLYSIS

5.1 Introduction

Conventional and fast pyrolysis processes in two designed fixed-bed and rapid heating reactors to produce bio-oil has been investigated. This chapter discusses the parametric investigation of conventional and rapid heating fast pyrolysis in the fixed-bed reactors. Design of Experiment (DoE) was performed in order to study the effects of reaction temperature, N_2 linear velocity and heating rate on bio-oil yield, calorific value, water content and acidity. Additionally, insights into the underlying processes involved during conventional pyrolysis were elucidated by a combination of TGA and DSC. An energy balance was also carried out to further analyse the overall pyrolysis process.

5.2 Methodology

5.2.1 Biomass feedstock and pyrolysis rigs

The biomass feedstock used in the pyrolysis experiments was Jatropha curcas pressed cake and its pre-treatment prior to pyrolysis has been described in Chapter 4, which is mentioned to be the two steps grinding only. A fixed-bed and a rapid heating pyrolysis rigs were used for conventional and fast pyrolysis processes, respectively. The details of both rigs have been reported in Chapter 3.

5.2.2 Design of Experiment (DoE)

The DoE followed a full factorial matrix as listed in Table 5 - 1. The biomass was pyrolysed over a temperature range of 573 K to 1073 K, and a N_2 linear velocity range of $7.8x10^{-5}$ m/s to $6.7x10^{-2}$ m/s to produce bio-oil. As the real temperature inside the bed and temperature setting on the furnace showed difference at each testing point (maximum of 24 K for 1073 K test point, which means the furnace should be set at 1097 to make sure the bed temperature is at 1073) in preliminary tests, the real temperature inside the bed is considered instead of temperature setting on furnace in this research for discussions and all calculations. Preliminary tests also showed that at temperatures below 573 K, no tangible reactions were occurring in the reactors hence this limited the minimum reaction temperature. The N_2 velocity was initially set to three different values with a minimum velocity of $0.7x10^{-2}$ m/s (and increment of 3 cm/s), but after observing that low N_2 velocity positively impacted the bio-oil yield, the tested range was expanded to five values with the minimum velocity of $7.8x10^{-5}$ m/s (dividing the minimum achievable volumetric rate by surface area of the bed) chosen based on the flow meter limitation of measurement, which is minimum of 10 cm^3/min. The heating rate for conventional pyrolysis process was fixed to a constant of 50 K/min, which corresponded to the maximum possible setting on the furnace. The heating rate for rapid heating fast pyrolysis process was measured during preliminary tests and has an average value of 25.67 K/s. In this study, the biomass grain size was fixed to be < 0.2 mm in conjunction with commonly used medium particle size in the literature [1, 4, 29] as well as based on the available matching sieve size. For consistency, 50±1 g samples were used in all test runs and the tests were repeated three times. The holding time for the completion of each test as indicated by no visible outlet gas and/or bio-oil droplets in the collector depended on the pyrolysis conditions. The minimum holding time recorded

to be 30 min and the maximum was 90 min. For the purpose of consistency, 90 min were set for all the experiments, even though completion of the reactions and bio-oil production were much shorter in some experiments. For all test runs, the masses of the collected bio-oil and the remaining char were measured to determine their yields and to calculate the gas yield by difference.

Table 5 - 1 DoE for pyrolysis of Jatropha Curcas waste for bio-oil production

Pyrolysis parameters	Unit	Min	Max	Increment	Numbers of run
Reaction Temperature	K	573	1073	125	5
N_2 linear velocity	cm/s	0.0078	6.7	0.6922 and 3	5
Biomass grain size	mm	0.2		-	1
Condenser temperature	K	278		-	1
Heating time	min	90		-	1
Heating rate (2 rigs)	K/min	50	1540.2	-	2
Repeatability					3
Total number of experimental runs					150

5.2.3 Analytical tests

After measuring the mass of each bio-oil sample, they were tested (minimum of 2 times up to the maximum number of tests that show consistent and repeatable results with less than 5% difference) for three important bio-oil specifications of Gross Calorific Value (GCV), water content and acidity (pH).

5.2.3.1 Gross Calorific Value

The gross calorific value of the bio-oil products were tested according to the ASTM D240 method using a Parr 6100 calorimetric bomb unit [86]. Based on the fact that bio-oil contains considerable water content and that this prevents proper ignition in the calorimetric bomb unit, cotton was used to prevent any misfire in the process [28, 29]. The bio-oil and cotton were individually weighed before each test to determine the calorific value of pure bio-oil.

5.2.3.2 Water content

The ASTM E203-08 method was used in the measurement of water content using a Mettler Toledo V20 Karl Fischer titrator unit. Based on preliminary testing results, methanol could not be used as a solvent in the Karl Fischer titration because of its reaction with ketones producing water as a result [28–29, 87]. To prevent this reaction, the Combisolvent Keto (Merck) was used instead of methanol. Accordingly, the CombiTitrant 5 Keto (Merck) was also used to give accurate water content results.

Dissolving each bio-oil sample taken for water content testing in the Combisolvent Keto (9:1 weight ratio of bio-oil to solvent) enables consistent results to be achieved from the Karl Fischer titration unit. This is because without making up the above mentioned solution, injecting very little amount of bio-oil (approximately 0.25 g based on Karl Fischer unit instruction) cannot represent the water concentration in the whole bio-oil sample and this causes inconsistent results.

5.2.3.3 Acidity

The ASTM E70-07 method was adhered to when measuring the pH of the bio-oil samples by using a Metrohm 785 DMP Titrino Auto Titrator unit [88]. To ensure repeatable results, the samples were continuously stirred to obtain homogeneous samples while the pH readings were recorded.

5.2.3.4 Thermo-Gravimetric Analysis (TGA) and Differential Scanning Calorimeter (DSC)

Although mass measurements and analytical tests of the bio-oil products allow the effects of pyrolysis parameters on bio-oil quantity and quality to be investigated, fundamental knowledge of the heat and mass transfers occurring inside the reactor is

limited. Both TGA and DSC analyses enable a better understanding of the mechanisms that are taking place inside the pyrolysis reactor.

Each experimental test point in the conventional pyrolysis process was also tested by using a Mettler-Toledo TGA/DSC 1 unit to simulate the heat and mass transfer characteristics of the actual experiment. This was accomplished by downsizing the actual experimental geometry into the size of the TGA/DSC unit. The geometry of the TGA/DSC unit was measured and the actual experiments on conventional pyrolysis rig were simulated using the TGA/DSC unit such that the N_2 linear velocity was the same as the actual experiments.

5.3 Result and Discussion

5.3.1 Bio-oil yield

Figure 5 - 1 and Figure 5 - 2 show how the N_2 velocity and reaction temperature affect the bio-oil yield as well as the three key specifications (water content, GCV and acidity) of the bio-oil product in conventional and fast pyrolysis processes, respectively. Since each test point was repeated thrice (for bio-oil yield) and the key specifications were analysed at least twice, the average of six measurements are plotted in Figure 5 - 1((b), (c) and (d)) and Figure 5 - 2((b), (c) and (d)).

The error bars shown indicate the maximum and minimum values for each test point. In Figure 5 - 1(a) and Figure 5 - 2(a), it is clearly seen that the bio-oil yield obtained from the both pyrolysis processes increases when the velocity of N_2 flowing through the bed reduces. The phenomenon is likely to be caused by the unnecessary cooling effect of extra N_2 in bed at higher linear velocities. The N_2 flowing through the bed should

only be enough to ensure that no O_2 is available in the bed for reactions to occur with the heated biomass.

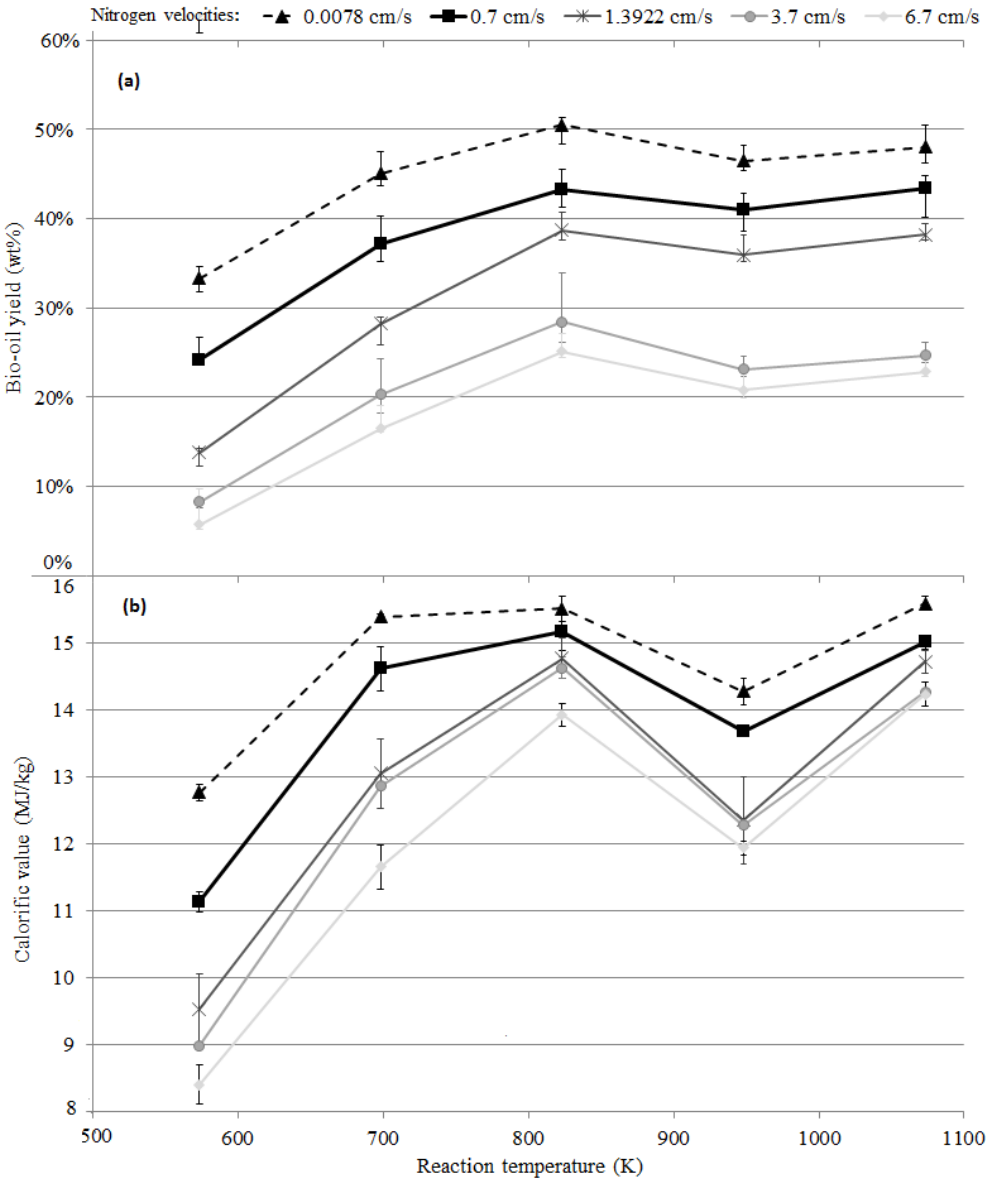

Figure 5 - 1 Effect of temperature and N_2 velocity on bio-oil (a) yield, (b) and calorific value from conventional pyrolysis

The unnecessary cooling in the bed due to the extra N_2 prevents uniform heating of the biomass and consequently, limits the necessary cracking of the biomass. This delay in cracking and bonding prolongs the duration of the pyrolysis process as observed during the experiments which is unfavourable from the aspect of energy consumption.

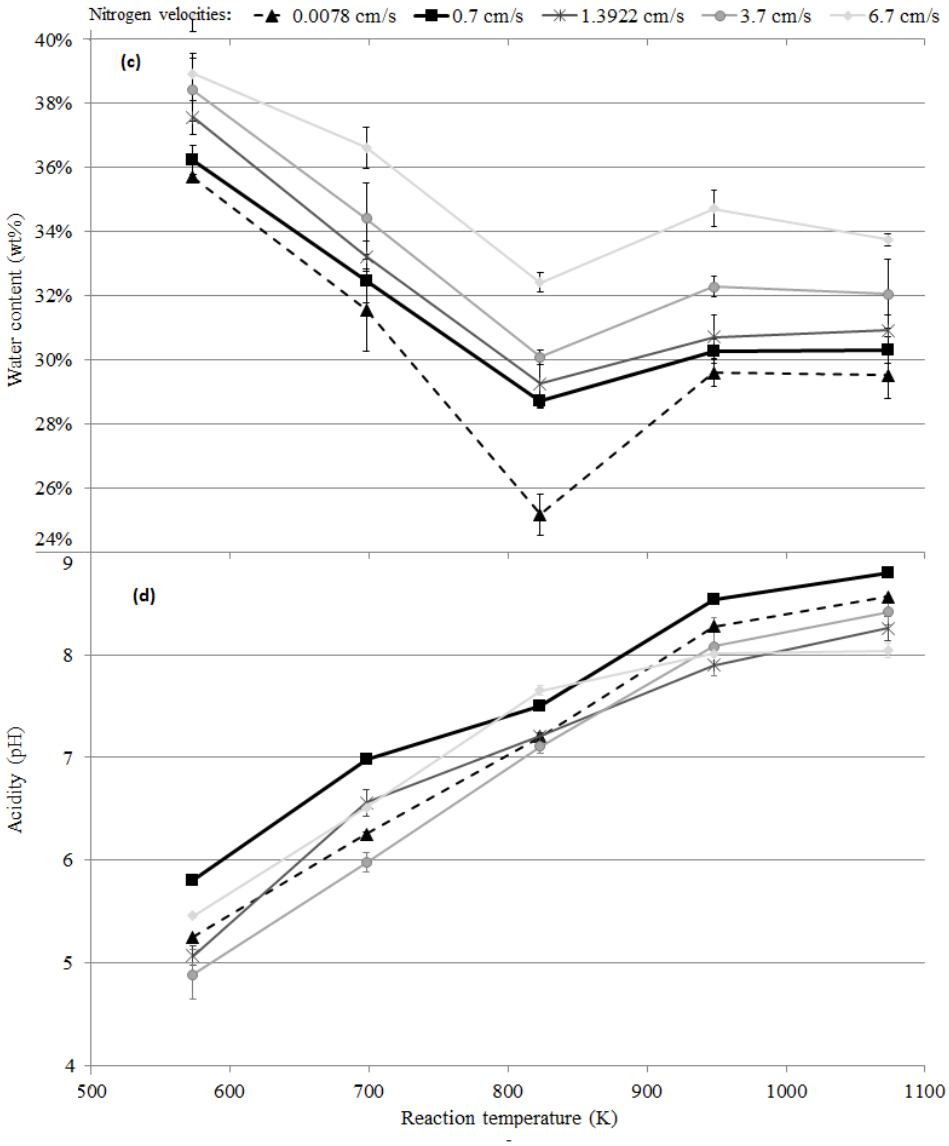

Figure 5 - 1 Effect of temperature and N_2 velocity on bio-oil (c) water content and (d) acidity from conventional pyrolysis

Figure 5 - 1(a) also shows that for a fixed N_2 flow rate and hence velocity in fixed-bed reactor, when the reaction temperature increases, the bio-oil yield increases to a maximum amount at approximately 823 K. Above this temperature, a slight decrease is experienced followed by a final increase. The slow heating rate of the furnace, i.e. 50 K/min implies that the biomass experiences a longer residence time from 573 up till 823

K. This means that by having a higher heating rate, the final reaction temperature for maximum bio-oil yield can be reduced.

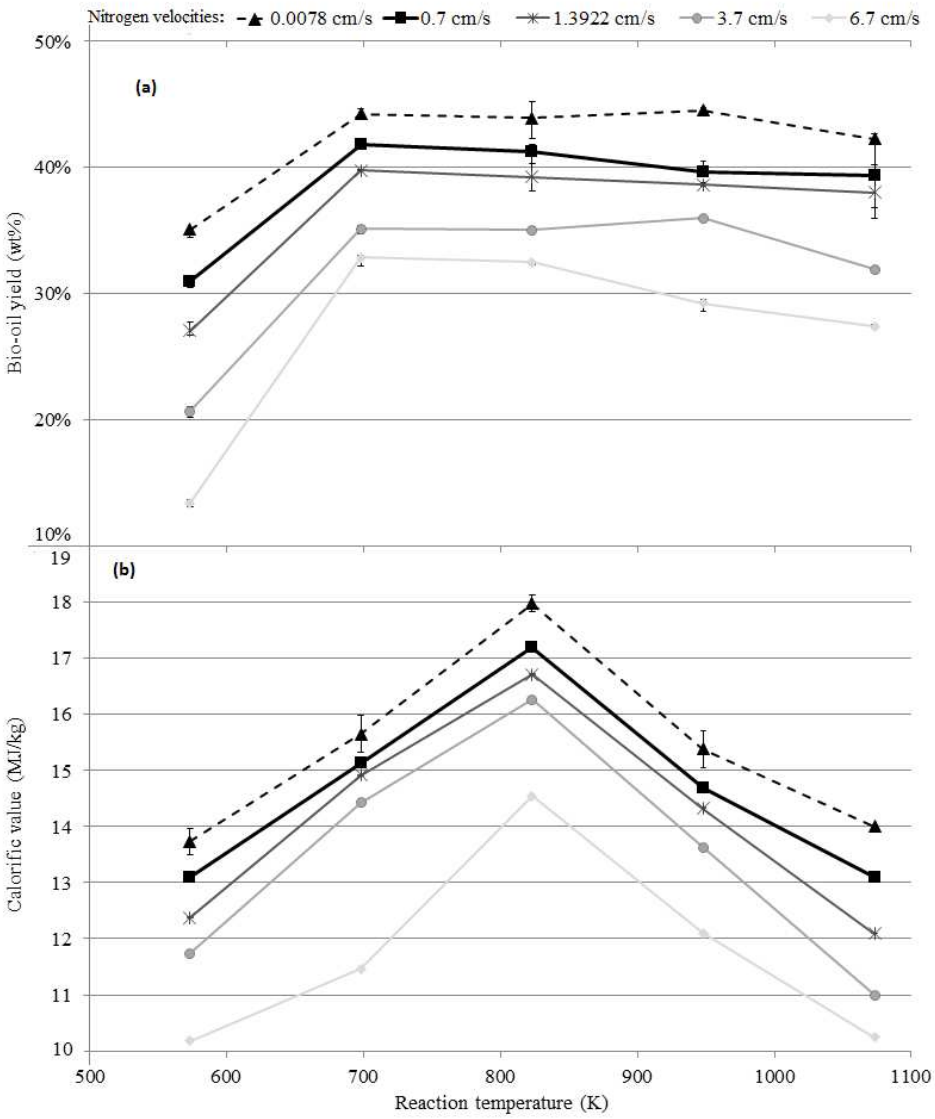

Figure 5 - 2 Effect of temperature and N_2 velocity on bio-oil (a) yield and (b) calorific value from fast pyrolysis

This is proven by Figure 5 - 2(a) which illustrates that in the rapid heating reactor, the maximum yield occurs at approximately 700 K which is noticeably lower than in the conventional pyrolysis reactor. Due to the slow heating rate of the furnace in conventional pyrolysis, the total temperature range from 573 to 823 K is being experienced by the biomass and not only the 823 K point. The generally higher amount

of bio-oil yield in the conventional pyrolysis as compared to the fast pyrolysis can be attributed to the higher percentage of water content (Figure 5 - 1(c) and Figure 5 - 2(c)), which is a drawback in terms of bio-oil quality.

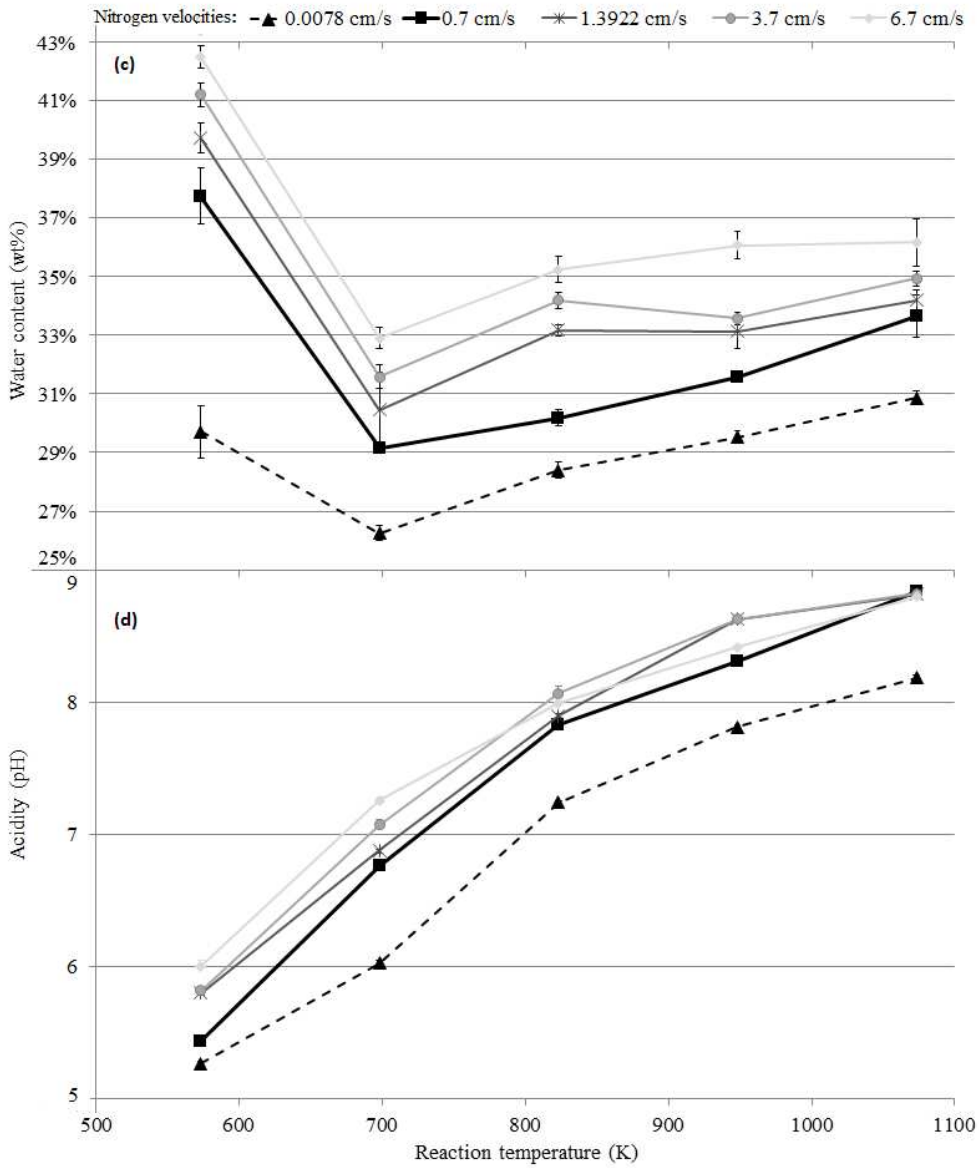

Figure 5 - 2 Effect of temperature and N_2 velocity on bio-oil (c) water content and (d) acidity from fast pyrolysis

Figure 5 - 3 and Figure 5 - 4 show the yield of bio-oil and its two by-products of char and gas at the minimum N_2 velocity of 0.0078 cm/s, which corresponds to maximum bio-oil yield seen in Figure 5 - 1(a) and Figure 5 - 2(a), respectively.

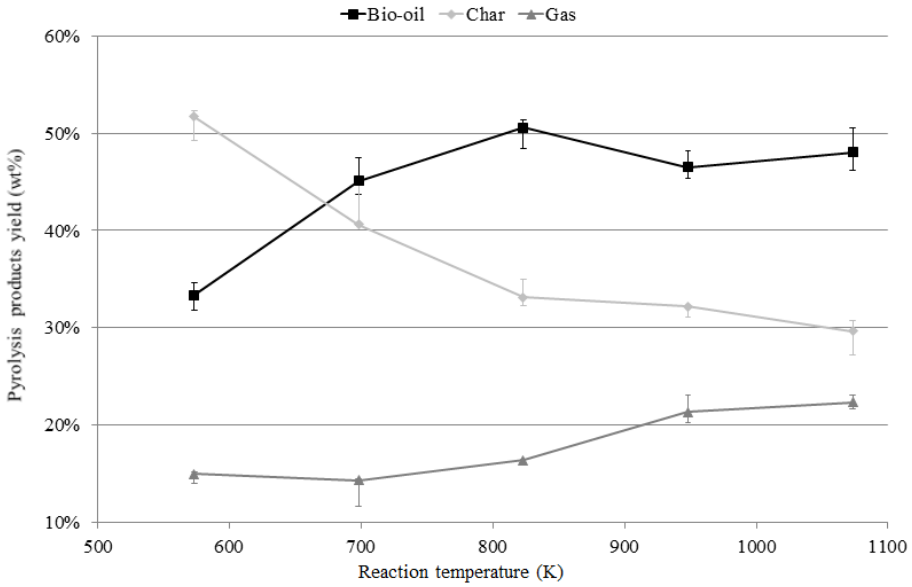

Figure 5 - 3 Conventional pyrolysis products against reaction temperature for a N_2 velocity of 0.0078 cm/s

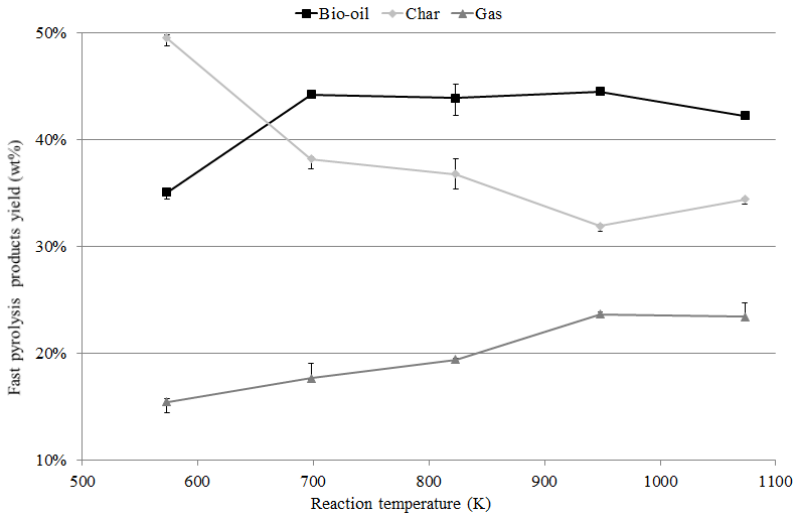

Figure 5 - 4 Fast pyrolysis products against reaction temperature for a N_2 velocity of 0.0078 cm/s

At temperatures below 573 K, no noticeable bio-oil product was observed because the heat was sufficient to crack the hemicellulose only, and produce mainly carbon monoxide (CO) and CO_2 gases [19]. As temperature increases, the cellulose breaks down first. Then, at higher temperatures, the lignin starts to crack down into char, water and heavy oil. This justifies the decrease in char production in favour of higher bio-oil product and almost constant amount of gas release shown in Figure 5 - 3 and Figure 5 - 4. They also show that beyond 823 K, further gasification occurs, and fine

and light gases such as hydrogen are generated resulting in lower bio-oil production compared to lower temperature [19].

5.3.2 Bio-oil characterisation

5.3.2.1 Gross Calorific Value

The specification for gross calorific value of pyrolysis liquid biofuels to be used in burners based on ASTM D7544-10 is a minimum of 15 MJ/kg [85]. Not only do the unprocessed bio-oil from conventional pyrolysis meets this specification between the temperatures of 670 K and 850 K for lower N_2 linear velocity test points, but a wider range of bio-oils produced from rapid heating fast pyrolysis fulfil the same criteria as shown in Figure 5 - 1(b) and Figure 5 - 2(b).

The chemical compositions of bio-oil samples that are produced at different testing points are different. Consequently, their heats of combustion are not expected to be the same. This can be confirmed if the water content is neglected and only the gross calorific value of the combustible portion of bio-oil is considered. Although water extraction was carried out in this project and will be discussed in Chapter 7, the theoretical calculation of GCV of bio-oil considering no water is omitted here because the practicality of it is still questionable by many scientists for biomass sources. Nonetheless, the water content has a direct effect on gross calorific value. Figure 5 - 1(b and c) and Figure 5 - 2(b and c) show that the gross calorific value and water content curves are horizontally symmetrical, which shows that the major factor affecting the calorific value is the water content of bio-oil. For rapid heating fast pyrolysis, this effect is not so prominent and is likely being dominated by the chemical composition of the produced bio-oil itself which is dependent on the reaction temperature.

5.3.2.2 Water content

Figure 5 - 1(c) and Figure 5 - 2(c) depict that the percentage of water content in the produced bio-oil samples starts with a maximum amount at the lowest pyrolysis temperature and decreases till a minimum point. Then, it keeps increasing up to a limited maximum point depends on the N_2 velocity. The major difference between conventional pyrolysis and rapid heating pyrolysis is that this minimum will be shifted to lower temperature in fast pyrolysis. The horizontally symmetrical shapes between Figure 5 - 1(b) and Figure 5 - 1(c), as well as Figure 5 - 2(b) and Figure 5 - 2(c) suggest that under temperatures, in which cracking and bonding are maximised, more oil and heavy oil in the product is produced and hence less water is measured. Both Figure 5 - 1(c) and Figure 5 - 2(c) also suggest that by increasing the N_2 velocity, unnecessary cooling in the bed which interferes with the cracking process occurs and results in increased water content in the bio-oil. The maximum allowable water content in liquid bio-fuels is limited to 30 wt% [85]. The samples that produced at minimum N_2 linear velocity met this limit for reaction temperatures above 730 K for conventional pyrolysis and within 600 to 1000 K for rapid heating pyrolysis.

5.3.2.3 Acidity of bio-oil

One of the drawbacks of bio-oil is its typical acidic condition [17]. The results of ASTM E70 test method on the Jatropha curcas bio-oil samples indicate that the pH values range from 4.9 to 8.8 at all testing points for both conventional and fast pyrolysis processes as can be seen in Figure 5 - 1(d) and Figure 5 - 2(d), respectively. These results also suggest that the chemical composition of bio-oil is dependent on the reaction temperature since acidity is related to the composition. The figures also demonstrate that pH is not being systematically changed by changing the N_2 linear velocity in the reactors. In Chapter 7, it will be shown that the pH measured for

optimum quantity (yield) and quality bio-oil can be considered as neutral for both processes.

5.3.3 Thermo-Gravimetric Analysis (TGA) and Differential Scanning Calorimeter (DSC)

Figure 5 - 5 illustrates the heat and mass transfer characteristics of the conventional pyrolysis process using the combined results of both TGA and DSC. The analysis was conducted under optimum pyrolysis conditions for best combined quantity (yield) and quality of bio-oil, which are reaction temperature of 800 K and a N_2 linear velocity of 0.0078 cm/s (this optimum condition will be found in the next chapter by using empirical correlations and normalisation).

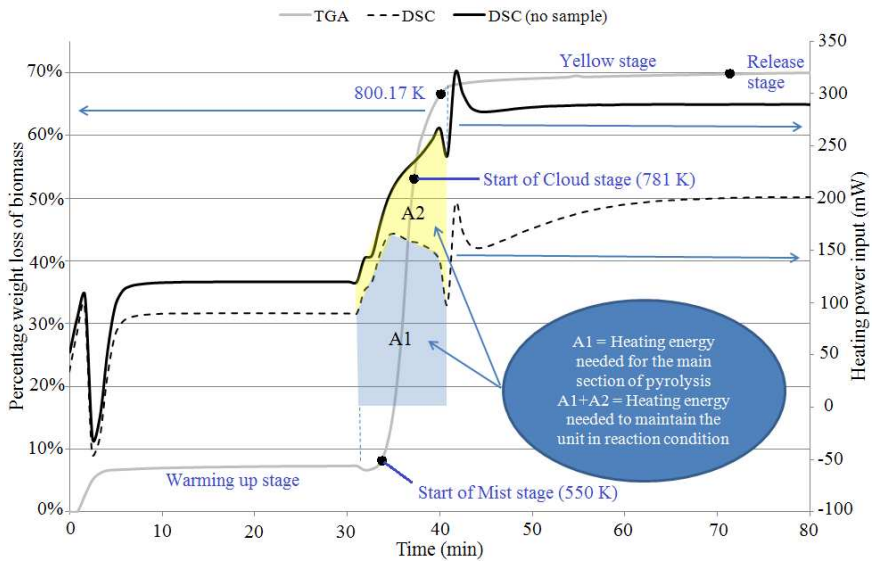

Figure 5 - 5 Heat and mass transfer characteristics during the conventional pyrolysis process at optimum point [89]

In Figure 5 - 5, the weight loss of the biomass in the bed (TGA curve with solid grey line) and the heating power required for the pyrolysis process (DSC curve with dashed black line) are plotted. For the purpose of energy calculations, the heating power curve (DSC curve with solid black line) is also plotted for the period that the unit was run

without any biomass inside. By interpreting the data shown in both Figure 5 - 3 and Figure 5 - 5 in addition to recorded experimental observations, the pyrolysis process can be divided into five stages described by the following:

5.3.3.1 Warming up stage

In this first stage, normally no tangible bio-oil is produced and no visible gas can be observed at the outlet of the condenser. Generally, this stage ranges from 298 K up to approximately 550 K (Figure 5 - 5). The term "warming up" is chosen to describe this stage because energy from the furnace is used to raise the temperature of the bed itself and part of the heat is being used to vaporise the moisture content of the biomass.

5.3.3.2 Mist stage

By increasing the temperature of the system above 550 K (Figure 5 - 5), cracking of biomass starts. Experimentally, a light white mist can be observed at the outlet of the condenser and an odour is emitted as a result of the chemical reactions within the reactor. In this stage, the main portion of bio-oil production occurs in the reactor up to temperatures close to 781 K.

5.3.3.3 Cloud stage

Above 781 K, the mist thickens into a cloudy white outlet (Figure 5 - 5). The odour of the outlet gas increases dramatically. Although the chemical reactions are faster in this temperature region between 781 K and 800 K, the stage only contributes below 10% of bio-oil production.

5.3.3.4 Yellow stage

When the cloud stage reaches a peak point, the outlet gas turns yellowish and finally, a thick yellowish brown colour is observed at the condenser outlet. Before this stage, the temperature reaches 800 K (targeted reaction temperature) in the bed. The yellowish

brown colour of the outlet gas suggests the presence of sulphur based gases although the exact chemical composition requires further investigation which is beyond the scope of this study [89]. In this stage, the outlet gas cannot be trapped in the condenser and the slight weight loss shown by the TGA curve occurs within the bed only. Generally, no noticeable increase in bio-oil production is obtained in the yellow stage.

5.3.3.5 Release stage

Finally, when all the biomass in the reactor is cracked into volatiles and only char remains, the pyrolysis process stops slowly. The outlet gas becomes visibly thinner and its colour changes first to white and then it becomes invisible. The plateau at the end of the TGA curve in Figure 5 - 5 indicates that no more volatiles are being produced. At the end of this stage, there will be no more gas exiting either the reactor or the condenser except N_2 from the N_2 supply tank. The experimental run is then considered as finished.

The TGA curve in Figure 5 - 5 also shows that over 90% of volatiles separation occurs during the highlighted region (A1) hence the area A1 corresponds to the main energy required to break the chemical bonds within the biomass and separate the volatiles with the target of producing bio-oil.

During the experimental runs, a sudden increase in the temperature of the outlet volatiles prior to entering the condenser is observed especially in the Mist and Cloud stages. Although the pyrolysis process is generally considered as an endothermic process, partial exothermic processes are taking place while the main cracking process is proceeding. The results from the TGA/DSC unit confirm this as just after the Mist stage, the DSC curve has a low negative gradient which dramatically dives at the beginning of the Yellow stage before the end of the pyrolysis process.

5.3.4 Energy balance

In the experimental rig used, the energy consumption is higher as compared to typical commercial production lines, but an energy balance for the designed unit can give an indication of the viability of the whole process when it is analysed realistically. This aim can only be achieved with the combination of the TGA/DSC results and the actual test rig results.

By integrating the power curve (P(t)) in Figure 5 - 5 (dashed DSC curve), the thermal energy (E_{th}) required for the pyrolysis process (area A1) can be calculated using Equation (5.1) as follows [89]:

$$\int_{t_1}^{t_2} P(t)dt = \int_{t_1}^{t_2} \frac{dE_{th}}{dt} dt = E_{th} \quad (5.1)$$

This integration can be executed by using two different approaches:

1. By curve fitting first and after finding the curve equation(s), the amount of energy can be determined by carrying out analytical integration. The accuracy of this method depends on the accuracy of the curve fitting method used.

2. By applying trapezoidal rule (or other similar method) in numerical integration, the amount of energy can be calculated by calculating the area A1 in Figure 5 - 5. The accuracy of this method depends on the number of steps that is used to divide the area A1 in Figure 5 - 5.

By using Equation (5.1) Figure 5 - 5 and choosing curve fitting method, the energy (area A1) required for cracking 11.23 mg of sample is calculated to be 43.89 J (equivalent to 3.91 MJ for 1 kg of biomass). The yield of bio-oil at this experimental

point is 50.08%. Therefore, the total energy consumption for the production of 1 kg bio-oil can be determined as follows:

$$E_{th} = 3.91 \times \frac{100}{50.08} = 7.81 \text{ MJ} \quad (5.2)$$

The gross calorific value of bio-oil measured at the same test point is 15.12 MJ/kg. This is 93.60% more than the input heating energy. This is not taking into account the remaining gaseous volatiles and char. The char (at the same testing point), for instance, has a gross calorific value of 24.18 MJ/kg. Both the gas and solid remaining have the potential to be utilised as fuel, but this aspect falls beyond the scope of this study and is worthy of future investigation.

In Figure 5 - 5, the summation of areas A1 and A2 (integration of solid DSC curve) represents the energy that is required to heat up the system until it reaches the targeted reaction temperature and maintain the system at the same temperature for the same length of time needed to crack 11.23 mg of sample. The combined area is 31% bigger compared to area A1 alone, which as explained previously represents the energy required to crack 11.23 mg sample in the TGA/DSC unit. This significant increase indicates that when cracking is initiated within the reactor, the exothermic reactions release a significant amount of heat into the system (especially during the Mist and Cloud stages). This additional heat helps the electrical furnace in further cracking the rest of the biomass, propagating like a chain reaction. The observations also imply that the more biomass there is in the reactor, the less the electrical energy from the furnace is required to crack the biomass. The major electrical energy of furnace is used to heat up the reactor walls itself. Therefore, it can be deduced that operating any pyrolysis unit at its full capacity (maximum possible biomass in reactor) aids in saving energy because the existing exothermic reactions help to develop the biomass cracking process.

5.4 Concluding Remarks

Experimental parametric results from a conventional fixed-bed and rapid heating fast pyrolysis reactors show that both reaction temperature and N_2 linear velocity strongly influence the yield and key specifications of bio-oil produced from Jatropha curcas pressed cake. The calorific value, water content and acidity of bio-oils produced from both rigs under specific range of operation comply with the ASTM D7554-10 bio-fuel standard, which indicate that they can be used in burners without any modifications as long as other specifications match with the ASTM D7554-10 bio-fuel standard. Using the rapid heating fast pyrolysis process may reduce the bio-oil yield, but the quality of bio-oil improves in terms of water content and gross calorific value. Additionally, the maximum yield is obtained with a reduction in reaction temperature of 53 K and a shortened reaction time. This is preferable as less energy is consumed as compared to the conventional pyrolysis. Finally, an energy balance analysis of the conventional pyrolysis reactor confirms the viability of the pyrolysis process with a 93.60% increase in energy by only considering the bio-oil as fuel and neglecting the fuel potentials of the char and gas.

Further analysis on the samples taken from both rigs will be analysed in next chapters by pointing out the optimised condition by using mathematical models in chapter 6 and full physicochemical characterisation in chapter 7.

CHAPTER 6 EMPIRICAL CORRELATIONS DEVELOPMENT AND PROCESS OPTIMISATION

6.1 Introduction

Experimentally testing all the possible parametric points in the majority of research works is almost impossible from the aspects of time and cost. Nevertheless, a better understanding of the effects of input parameters on the output results is afforded by having more comprehensive results. To balance the need between a sensible number of experimental runs and sufficiently comprehensive results, mathematical modelling of the system can be used as long as the model is validated against actual experiments. The full factorial experimental test matrix as described in Chapter 4 was introduced to create a proper baseline for a reliable model to be developed. A reliable method for modelling of experimental results is regression, which is used in this work.

6.1.1 Linear and Nonlinear Regression

The first step in linear and nonlinear regression is to estimate the relationship between all available outputs of the experiment (dependant variables) as a function of each input parameter of the experiment (independent variable). If dependant variables can be assumed to have a linear relationship with independent variables, the model can be defined as a linear regression model. The two independent variables in this research are reaction temperature and N_2 velocity, and four dependant variables are bio-oil yield, gross calorific value, water content and acidity. Later in this chapter, it will be shown

that the acidity of bio-oil can be modelled as a linear function of these two parameters. Hence, the model that is developed in this case is a linear regression model.

Conversely, if the dependant variables are modelled as any other function apart from a linear function of independent variables, the developed model is defined as a nonlinear regression model. One example that will be shown later is the bio-oil yield, which has a nonlinear relationship with reaction temperature and N_2 velocity for both conventional and rapid heating fast pyrolysis processes.

6.2 Empirical Correlations Development

First, by averaging the triplicate test results for bio-oil yield produced by the conventional pyrolysis method, a total number of 25 test points have been used to develop an empirical correlation for bio-oil yield. Different functions such as linear, exponential, logarithmic, power and polynomials were fitted to the experimental data and the Root Mean Square (RMS) of each fitted curves were calculated. The minimum summation of RMS is taken to be the best fitted curve. By looking at Figure 5 - 1(a), the partial correlation between reaction temperature and bio-oil yield can be modelled as a cubic polynomial. In contrast, the partial correlation between N_2 linear velocity in the bed and bio-oil yield can be modelled as a quadratic polynomial. By using nonlinear multiple regression method, the relationship between the independent variables and the bio-oil yield can be modelled [90]. Generalising these partial correlations into a multiple correlation by summation of the two aforementioned polynomials, the following equation can be written:

$$B = c + n_1 N + n_2 N^2 + t_1 T + t_2 T^2 + t_3 T^3 \quad (6.1)$$

In Equation 6.1, B, N and T are the bio-oil yield (wt%), N_2 linear velocity (m/s) and reaction temperature (K/1000), respectively. To find the constant number c and

the other five coefficients, six equations need to be defined and solved simultaneously. As Equation 6.1 is valid over the range of experimental matrix, all test points can be described by it. Likewise, the summation of all the experimental points can be described by Equation 6.2:

$$\sum B_i=c+n_1\sum N_i+n_2\sum N_i^2+t_1\sum T_i+t_2\sum T_i^2+t_3\sum T_i^3 \quad (6.2)$$

By multiplying Equation 6.1 by different powers of N and T or a combination of both, and using the summation in Equation 6.2, the five equations below for instance can be generated:

$$\sum N_i.B_i = c\sum N_i+ n_1\sum N_i^2 + n_2\sum N_i^3 + t_1\sum N_i.T_i + t_2\sum N_i.T_i^2 + t_3\sum N_i.T_i^3 \quad (6.3)$$

$$\sum T_i.N_i.B_i = cT_i.N_i + n_1T_i.N_i^2 + n_2T_i.N_i^3 + t_1T_i^2.N_i + t_2T_i^3.N_i + t_3T_i^4.N_i \quad (6.4)$$

$$\sum T_i.N_i^2.B_i = c\sum T_i.N_i^2 + n_1\sum T_i.N_i^3 + n_2\sum T_i.N_i^4 + t_1\sum T_i^2.N_i^2 + t_2\sum T_i^3.N_i^2 + t_3\sum T_i^4.N_i^2 \quad (6.5)$$

$$\sum T_i^2.N_i^2.B_i = c\sum T_i^2.N_i^2 + n_1\sum T_i^2.N_i^3 + n_2\sum T_i^2.N_i^4 + t_1\sum T_i^3.N_i^2 + t_2\sum T_i^3.N_i^2 + t_3\sum T_i^5.N_i^2 \quad (6.6)$$

$$\sum T_i^3.N_i^2.B_i = c\sum T_i^3.N_i^2 + n_1\sum T_i^3.N_i^3 + n_2\sum T_i^3.N_i^4 + t_1\sum T_i^4.N_i^2 + t_2\sum T_i^5.N_i^2 + t_3\sum T_i^6.N_i^2 \quad (6.7)$$

The constants of Equation 6.1 can be found by solving the above 6 by 6 simultaneous equations (Equations 6.2 to 6.7) to result in Equation 6.8 below:

$$B= -58.3 -9.95N+0.95N^2+176.98T+0.01T^2-68.859T^3 \quad (6.8)$$

Similarly, by using the same method, the quality specifications of bio-oil can be modelled by relating them to the pyrolysis parameters (for acidity only, linear multiple regression method is used instead of nonlinear). The results for gross calorific value (C in MJ/kg), water content (W in wt%) and acidity (P in pH scale) are shown by Equations 6.9 to 6.11, respectively where similarly, for all of them, N is in cm/s and T is in K/1000:

$$C = 1.46 - 0.97N + 0.09N^2 + 20.11\,T - 0.002T^2 - 5.48T^3 \quad (6.9)$$

$$W = 73.57 + 0.68\,N - 96.86\,T + 52.27\,T^2 \quad (6.10)$$

$$P = 1.97 - 0.03\,N + 6.36\,T \quad (6.11)$$

Likewise, for the rapid heating fast pyrolysis process, the same methodology is used to develop the following empirical correlations shown in Equations 6.12 to 6.15.

$$B = -62.83 - 2.11N + 245.94\,T - 139.91T^2 \quad (6.12)$$

$$C = -21.73 - 1.21N + 0.30N^2 - 0.03N^3 + 94.82T - 57.87\,T^2 \quad (6.13)$$

$$W = 69.97 + 2.53N - 0.24N^2 - 72.59T - 0.001T^2 + 31.18T^3 \quad (6.14)$$

$$P = -4.76 + 0.37N - 0.04N^2 + 19.38T + 0.001T^2 - 6.53T^3 \quad (6.15)$$

6.3 Validation of Empirical Correlations

To validate the above models, first, the results from the proposed correlations were compared to the experimental results and over the tested experimental range; the maximum error is below 5%. The second validation step was to choose four previously untested points for pyrolysis testing (in between the original test points) and compare the test results with the modelling results to ensure that the error is below 5% for all of them. Also the optimum condition that will be found in section 6.2.1 through normalisation was used for validation to represent the fifth testing point. Table 6 - 1 and Table 6 - 2 summarises the validation results for both conventional and fast pyrolysis, respectively which are all below 5% error. Based on the fact that the models are developed from a full factorial testing set (DoE) and validated experimentally, they can be used to predict the bio-oil yield, gross calorific value,

water content and acidity of any point as long as the parameters are within the test matrix range.

Table 6 - 1 Validation of empirical correlations for conventional pyrolysis

	Reaction temperature	N_2 linear velocity	Bio-oil yield	Gross calorific value	Water content	Acidity
Unit	K	cm/s	wt%	MJ/kg	wt%	pH
Validating Points			Experimental result (Empirical result)			
1	636	0.351	33.69 (33.18)	12.77 (12.51)	32.34 (33.34)	6.01 (6.00)
2	761	5.1948	19.58 (19.89)	12.17 (11.78)	35.26 (33.64)	6.52 (6.67)
3	886	1.0452	41.57 (41.24)	14.14 (14.55)	28.64 (29.49)	7.58 (7.57)
4	1011	2.5428	31.31 (30.28)	14.43 (14.25)	29.28 (30.79)	8.74 (8.33)
Optimum point	800	0.0078	50.08 (47.95)	15.12 (14.74)	28.34 (29.54)	6.77 (7.05)

Table 6 - 2 Validation of empirical correlations for fast pyrolysis

	Reaction temperature	N_2 linear velocity	Bio-oil yield	Gross calorific value	Water content	Acidity
Unit	K	cm/s	wt%	MJ/kg	wt%	pH
Validating Points			Experimental result (Empirical result)			
1	636	0.351	34.85 (36.26)	14.38 (14.78)	31.56 (32.68)	5.81 (6.01)
2	761	5.1948	33.59 (32.35)	13.97 (14.52)	34.65 (35.13)	8.02 (7.95)
3	886	1.0452	41.72 (43.04)	15.42 (15.88)	30.41 (29.72)	8.37 (8.21)
4	1011	2.5428	36.27 (37.44)	12.87 (13.35)	32.53 (33.69)	9.02 (8.77)
Optimum point	747	0.0078	40.93 (42.81)	16.92 (16.80)	28.02 (28.76)	7.01 (7.00)

6.3.1 Optimisation

Although the experimental results can directly give the optimum experimental point for each individual specification of bio-oil, from a practical viewpoint, it would be necessary to determine the optimum point for the best combined yield and quality

specifications. The optimum point is not necessarily one of the experimental points and is found by using the developed empirical correlations.

Normalisation is used to combine the effects of pyrolysis parameters on bio-oil yield and quality specifications. B_1, C_1, W_1 and P_1 (P_1 is pH closest to 7) are the optimum bio-oil yield, gross calorific value, water content and pH of bio-oil, respectively whereas B_2, C_2, W_2 and P_2 (P_2 is pH furthest from 7) are their worst counterparts. Four dimensionless numbers (b, c, w and p) are defined for the four specifications of interest:

$$b = \frac{B - B_2}{B_1 - B_2} \quad \Longrightarrow \quad 0 \leq b \leq 1 \tag{6.16}$$

$$c = \frac{C - C_2}{C_1 - C_2} \quad \Longrightarrow \quad 0 \leq c \leq 1 \tag{6.17}$$

$$w = 1 - \frac{W - W_1}{W_2 - W_1} \quad \Longrightarrow \quad 0 \leq w \leq 1 \tag{6.18}$$

$$p = 1 - \frac{|P-7| - |P_1-7|}{|P_2-7| - |P_1-7|} \quad \Longrightarrow \quad 0 \leq p \leq 1 \tag{6.19}$$

For each specification, the empirical correlations are used to generate a comprehensive data set by setting the resolutions of the N_2 flow meter and tubular furnace thermometer as the increments within the iteration loops. A computer programme is written using Matlab software for this purpose. By iterating for each point, dimensionless numbers can be found for each individual bio-oil specification. 0 represents the worst point while 1 represents the optimum point for each individual specification. The average (index number i) of all four numbers is a number between 0 and 1:

$$i = \frac{b + c + w + p}{4} \quad \Longrightarrow \quad 0 \leq i \leq 1 \tag{6.20}$$

The maximum amount of this number (closest to one) represents the optimum point considering all four combined specifications. Experimental pyrolysis tests were finally carried out under the respective optimum conditions for both the conventional and fast pyrolysis processes. A comparison of both the experimental and modelling results as listed in Table 6 - 1 and Table 6 - 2 shows that the error is below 5% at optimum conditions too. This, in addition to the validation described before, demonstrates the validity of the developed empirical correlations as well as the proposed optimisation process.

The validated model shows that for conventional pyrolysis, the optimum combined quantity and quality of bio-oil occurs at a reaction temperature of 800 K and a N_2 linear velocity of 0.0078 cm/s. The experimental results shows that at this point, 50.08 wt% of Jatropha curcas pressed cake is converted to bio-oil with a gross calorific value of 15.12 MJ/kg, water content of 28.34 wt% and pH of 6.77. Conversely, at optimum conditions for rapid heating fast pyrolysis (reaction temperature of 747 K and N_2 linear velocity of 0.0078 cm/s), 40.93 wt% of biomass is converted into bio-oil with a gross calorific value of 16.92 MJ/kg, water content of 28.02 wt% and pH of 7.01. It should be noted that under optimum pyrolysis conditions, both produced bio-oils comply with the ASTM D7554-10 burner bio-fuel standard in terms of gross calorific value and water content. In addition, their pH values are approximately neutral, which is an advantage from the point of view of practical applications.

6.4 Concluding Remarks

Empirical correlations have been developed using linear and nonlinear multiple regression method to describe the relationships between the bio-oil yield and key specifications to the pyrolysis parameters. Validation of the correlations was carried out against actual experimental test data with less than 5% error. By using these developed empirical correlations, the optimum pyrolysis conditions for both conventional and rapid heating fast pyrolysis have been determined. At optimum conventional pyrolysis conditions (reaction temperature of 800 K and N_2 linear velocity of 0.0078 cm/s), 50.08 wt% of the waste was cracked down into bio-oil, which has 28.34 wt% water content, a gross calorific value of 15.12 MJ/kg and a pH of 6.77. In contrast, at optimum conditions for rapid heating fast pyrolysis (reaction temperature of 747 K and N_2 linear velocity of 0.0078 cm/s), 40.93 wt% of biomass was converted into bio-oil with a gross calorific value of 16.92 MJ/kg, water content of 28.02 wt% and pH of 7.01. Under optimum pyrolysis conditions, both produced bio-oils comply with the ASTM D7554-10 burner bio-fuel standard in terms of gross calorific value and water content. Furthermore, their pH values are approximately neutral, which is an advantage in practical applications.

CHAPTER 7 BIO-OIL PHYSICOCHEMICAL CHARACTERISATION

7.1 Introduction

In view of potential future commercialisation, it is necessary to test the physicochemical properties of bio-oil produced from pyrolysis processes. The results will indicate whether the bio-oil can be used directly as a biofuel or requires upgrading. This chapter reports on the determination of bio-oil physicochemical properties and comparison of these against fuel specifications of available standards. The optimum bio-oil products from both pyrolysis processes were tested and compared against the ASTM D7544-10 standard for burner biofuels [85]. Apart from that, emulsions of both bio-oils in normal diesel were also tested and compared with diesel (EN 590) and biodiesel (ASTM D6751-01) specifications standards [91–92].

7.2 Methodology

Two different approaches were used for bio-oil characterisation. The first was testing the bio-oils against the ASTM D7544-10 standard for burner biofuels. The second was emulsifying 10 wt% of bio-oils with 90 wt% of pure diesel and comparing the final products against the ASTM D6751-01 and EN590 for biodiesel and diesel fuels standard specifications, respectively [85, 91–92].

The optimum conventional pyrolysis conditions for the production of bio-oil from Jatropha curcas waste were determined at a reaction temperature of 800 K and a N_2 linear velocity of 0.0078 cm/s [89]. Meanwhile, for rapid heating fast pyrolysis, the optimum conditions were at a reaction temperature of 747 K and a N_2 linear velocity of

0.0078 cm/s (Chapter 6). Pyrolysis tests were carried out at the two conditions specified above in order to collect sufficient quantity of bio-oil samples for testing against the above mentioned standards. All other experimental conditions remained the same as specified in Chapter 5. The only difference was that 100±1 g (maximum capacity of rig) of Jatropha curcas waste was used in each run to collect more bio-oil product. In general, bio-oil can be considered as immiscible in diesel due to its considerable water content which makes it significantly polar [28–29]. While collecting the bio-oils in large quantities of over 500 g, phase separation could be observed as shown in Figure 7 - 1. This phase separation could not be observed fully in previous testing routines as the amount of samples was considerably low.

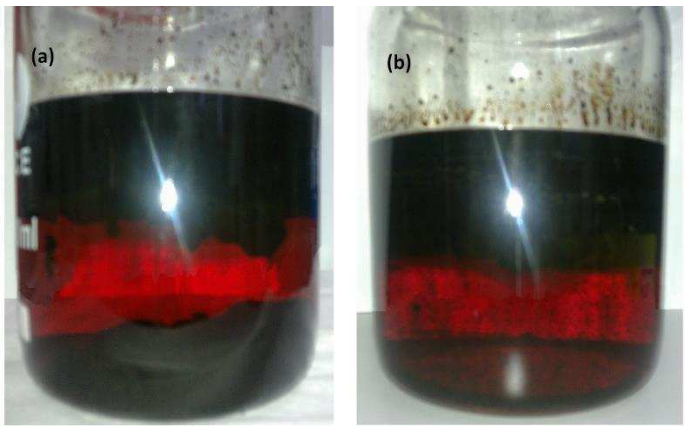

Figure 7 - 1 Phase separation in (a) conventional and (b) fast pyrolysis bio-oil

Conventional pyrolysis bio-oil (Figure 7 - 1 (a)) separated with a boundary of a mixture of two phases, but fast pyrolysis oil (Figure 7 - 1 (b)) separated clearly into two phases with a fine horizontal line. For conventional pyrolysis bio-oil, it took approximately a week to reach equilibrium state in a separatory funnel whereby acceptable separation could be observed. The top layer was opaque while the bottom layer was almost transparent and light brown in colour. For each of the bio-oil samples, the two phases were separated and tested for its gross calorific value, water content and acidity.

Table 7 - 1 Physicochemical characteristics of the separated layers of bio-oils

Specification	Unit	FPB* top layer	SPB** top layer	FPB bottom layer	SPB bottom layer
Layer Amount	wt%	64.31	61.04	35.69	38.96
Calorific Value	MJ/kg	29.30	25.63	4.89	misfire
Water Content	wt%	7.90	12.18	63.93	55.61
Acidity	pH	7.29	8.23	7.78	6.65

*Fast Pyrolysis Bio-oil ** Slow Pyrolysis Bio-oil

The data in Table 7 - 1 indicate that the bottom layers of both bio-oils can be considered as mainly water, and have low value as a fuel. This is inferred from the high water contents and low calorific values. In contrast, the top layers of both bio-oils can be considered as combustible oils. These oil layers (Note: there is no specific name for this phase in the literature and it can be termed as bio-oil, but to prevent confusion with the crude pyrolysis product, it is referred to as dehydrated bio-oil) have higher calorific values than the general bio-oil and lower water contents [28–29]. The findings described above assisted in formulating a fuel which can be emulsified in diesel with more ease and be more stable for a longer time (over 24 hr). 10 wt% of bio-oil was mixed with 90 wt% of commercial diesel fuel taken from a Shell petrol station in Semenyih, Malaysia (pure diesel) for comparison of physicochemical properties between commercial diesel and these emulsions.

In the Karl Fischer titrator, dry methanol is used as a solvent and this was the first indication that the bio-oil can be dissolved in methanol. As alcohol has hydrophilic as well as lipophilic properties, it can be used as a solvent for bio-oil, which has considerable amount of water. During physicochemical characterisation, the Jatropha curcas bio-oil was tested by adding up to 5 wt% of methanol and observations showed that this amount was sufficient to create a homogenous emulsion for Karl Fischer tests with repeatable results for water content.

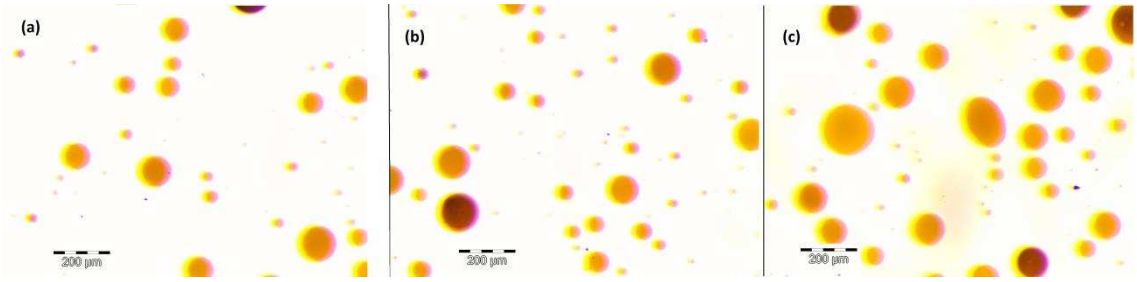

Figure 7 - 2 Microscopic view of emulsion of dehydrated slow pyrolysis bio-oil in diesel after (a) 0, (b) 2.5 and (c) 5 hr

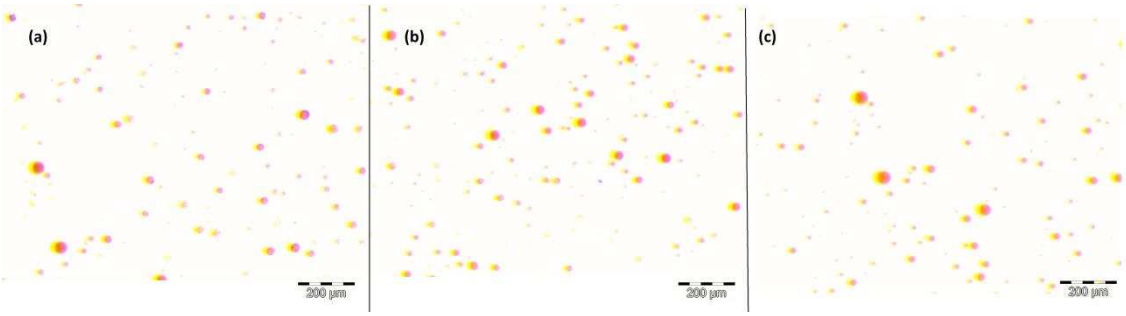

Figure 7 - 3 Microscopic view of emulsion of dehydrated fast pyrolysis bio-oil in diesel after (a) 0, (b) 2.5 and (c) 5 hr

As can be observed in Figure 7 - 2 and Figure 7 - 3, the 10 wt% emulsions of both conventional and fast dehydrated bio-oils (contain 5 wt% of methanol) after 5 hr is consistent with the newly mixed emulsions. The only difference that can be observed is that fast pyrolysis dehydrated bio-oil (FPDB) dispersed and distributed better (with smaller zones) as compared to conventional pyrolysis dehydrated bio-oil (CPDB). Based on the above observations, 5 wt% methanol was added to accumulated FPDB and CPDB before doing comprehensive physicochemical tests. The aim of adding this was to dilute the solidified bio-oil in the mixture as well as to form a homogenous, stable and uniform emulsion. This means that the final product that was compared to diesel

contained 0.5 wt% methanol, 9.5 wt% dehydrated bio-oil and 90 wt% pure diesel for selected tests.

One litre of each of the five products (CPDB, FPDB, CPDB BO10 (emulsion of 9.5 wt% of CPDB and 0.5 wt% methanol in 90 wt% diesel), FPDB BO10 (emulsion of 9.5 wt% FPDB and 5 wt% methanol in 90 wt% diesel) and diesel) were prepared and sealed in air tight opaque bottles covered by aluminium foil to prevent photochemical changes. The samples were sent to SGS laboratory (Petrochemical Inspection (M) Sdn. Bhd.) for external testing of fuel specifications. As a precautionary measure, all samples were kept in the dark and refrigerated above the freezing point of water when tests were not being run. Additionally, all samples were shaken for a minimum of 15 min before any test to ensure that homogenous samples were being tested.

7.3 Results and Discussion

The final combined results of all physicochemical characterisation tests are tabulated and compared to the ASTM D7544-10, ASTM D6751-01 and EN 590 [85, 91–92].

Table 7 - 2 Specifications of dehydrated bio-oils and their emulsions with diesel

Specification	Unit	Method	Reference	FPDB BO10*	CPDB BO10**	FPDB***	CPDB****	Diesel	ASTM D7544-10 (Burner biofuel)	ASTM D6751-01 (Biodiesel)	EN 590 (Diesel)
Gross calorific value	MJ/kg	ASTM D240	[86]	43.8617	43.495	29.2971	25.63	45.48	15 min	Not required	Not required
Water content	wt%	ASTM E203	[87]	0.79	1.22	7.9	12.18	0	30	0.05 max	0.0002 max
Solid content	wt%	ASTM D7579	[93]	0	0	0	0	0	2.5 max	0.05 max	0.000024max
Kinematic viscosity (40°C)	mm^2/s	ASTM D445A	[94]	4.412	4.16	21.65	18.547	2.652	125 max	1.9 min, 6 max	2 min, 4.5 max
Density (20°C)	kg/m^3	ASTM D4052	[95]	842.168	842.959	913.62	905.67	829.6	1100 min, 1300 max	Not required	Not required
Sulphur content	wt%	ASTM D4294	[96]	0.07	0.096	0.149	0.093	0.0615 min, 0.0965 max	0.05 max	0.05 max	0.00035 max
Ash content	wt%	ASTM D482	[97]	0.001	0.001	0.001	0.001	0.001	0.25	Not required	0.01
pH	scale	ASTM E70	[88]	5.22	5.325	7.285	7.775	4.22	report	report	Not required
Flash point	°C	ASTM D93-B	[98]	57	66	70	82	67	45 min	93 min	55 min
Pour point	°C	ASTM D97	[99]	–6	–3	–42	–42	-	–9 max	Not required	Not required
Iodine value	g/100 g	EN 14111	[100]	10.6	10.5	44.066	44.357	-	Not required	Not required	Not required
Cetane number	Rating	ASTM D6890	[100]	52.5	51.7	-	-	65.1	Not required	47 min	51 min
Copper corrosion strip	Rating (50°C, 3hr)	ASTM D130	[100]	1a	1a	1b	1b	1a	Not required	3 max	1 max
Density (15°C)	kg/m^3	ASTM D4052	[95]	845.2	846.1	915	907.3	831.546	Not required	Not required	820 min, 845 max
Carbon	wt%	ASTM D5291	[100]	80.55	80.54	44.1	44	84.6	Not required	Not required	Not required
Hydrogen	wt%	ASTM D5291	[100]	13.17	13.18	11.1	11.2	13.4	Not required	Not required	Not required
Nitrogen	wt%	ASTM D5291	[100]	0.36	0.36	2.7	2.7	0.1	Not required	Not required	Not required
Oxygen	wt%	Calculation	-	5.92	5.92	42.1	42.1	1.9	Not required	Not required	Not required

* Emulsion of 9.5 wt% of Fast Pyrolysis Dehydrated Bio-oil and 0.5 wt% methanol in 90 wt% diesel

** Emulsion of 9.5 wt% of Conventional Pyrolysis Dehydrated Bio-oil and 0.5 wt% methanol in 90 wt% diesel

*** Fast Pyrolysis Dehydrated Bio-oil

**** Conventional Pyrolysis Dehydrated Bio-oil

7.3.1 Water Content

Table 7 - 2 shows that CPDB and FPDB have water contents ranging between 7.9 wt% to 12.18 wt% which is less than half of the maximum allowable water content specified in the burner biofuels standard [85]. Although no water content could be detected by using the ASTM E203 method for the emulsions in diesel, a maximum water content of 1.22 wt% (for CPDB BO10) by calculation can be estimated. These are negligible amounts, but need to be confirmed by further investigation to ensure that no water content is in the emulsions if they are to be used in commercial diesel engines. Catalytic pyrolysis or other secondary processes can be used to reduce (or remove) the water content to meet the requirements of both diesel and biodiesel standards for commercial diesel engines.

7.3.2 Solid Content

Based on the nature of the investigated pyrolysis processes, the flow rates of the gases are too slow to be able to transfer any particles into the collector. The analytical results based on the ASTM D7579 shown in Table 7 - 2 confirm this [93]. For the emulsions of dehydrated bio-oils in diesel, the samples were filtered before sending for external laboratory tests. In short, the dehydrated bio-oils and their emulsions in diesel do not pose any concerns with regard to solid content unless other pyrolysis processes such as fluidised bed are used.

7.3.3 Kinematic Viscosity at 40^{o}C

By having considerable water content, the viscosity of the original bio-oil samples are comparable to diesel and biodiesel, but as the water content has been reduced, the dehydrated bio-oils have a viscosity range from 18.547 cSt to 21.65 cSt as can be seen

in Table 7 - 2 which are considerably higher than the diesel and biodiesel range [94]. The CPDB and FPDB are suitable for combustion in burners in term of viscosity because both are less than 125 cSt. Meanwhile, CPDB BO10 and FPDB BO10 have viscosities of 4.16 cSt and 4.412 cSt, respectively which are acceptable and within the range of both biodiesel and diesel standards.

7.3.4 Density

Due to the different requirements of the different standards, two different testing methods were conducted on the samples. The ASTM D4052 method was used to measure the density at 15 ^{o}C which is required by the EN 590 diesel fuel standard and at 20 ^{o}C which is required by biofuel for burners in the ASTM D7544-10 [85, 95]. It needs to be stated that no density requirement is specified in the ASTM D6751-01 for biodiesel fuel [92].

7.3.4.1 Density at 15^{o}C

The standard requirement for commercial diesel fuels (Table 7 - 2) is set to a range between 820 kg/m^3 to 845 kg/m^3 [91]. The CPDB BO10 and FPDB BO10 have densities of 845.2 kg/m^3 and 846.1 kg/m^3, respectively. Although the densities are higher than the standard requirement, the values are considered to be borderline values. One simple solution would be to reduce the percentage of dehydrated bio-oil mixed in diesel to reduce the density to below the maximum limit.

7.3.4.2 Density at 20^{o}C

Any biofuel that is being used in burners need to have a density within 1100 to 1300 kg/m^3 [85]. Both CPDB and FPDB have densities of 905.67 kg/m^3 and 913.62 kg/m^3, respectively. The low densities can be attributed to the fact that significant amount of water has been removed from the samples. Lower densities imply that for a fixed fuel

volumetric flow rate into a burner, less energy is supplied per unit time, which is not a very severe consequence. This situation can be easily addressed by mixing the dehydrated bio-oil with heavy oil for combustion in burners.

7.3.5 Sulphur Content

As shown in Table 7 - 2 for CPDB and FPDB, the sulphur contents are 0.149 and 0.093 wt%, respectively whereas the maximum allowable for burner biofuels is 0.05 wt% [85]. As sulphur content is directly linked to environment, health and safety, it needs to be reduced or removed by secondary processes such as adsorption process of sulphur removal by using sorbent materials, or by mixing Jatropha curcas bio-oil with other burner fuels with lower sulphur content [101].

Similarly, CPDB BO10 and FPDB BO10 have sulphur contents of 0.07 wt% and 0.096 wt%, respectively whereas the maximum allowable sulphur contents for biodiesel and diesel are 0.05 wt% and 0.00035 wt%, respectively. Again, just as for the dehydrated bio-oils, secondary processes are suggested to reduce or remove the sulphur. It needs to be noted here that the diesel used has between 0.0615 wt% to 0.0965 wt% of sulphur which is already way above the diesel standard. This can be expected since there is no legal requirement in Malaysia for local fuel stations to supply ultra-low sulphur diesel. Consequently, this affected the sulphur results for the dehydrated bio-oil in diesel emulsions.

7.3.6 Ash Content

The maximum allowable ash contents for diesel and burner biofuel are 0.01 wt% and 0.25 wt%, respectively [97]. For all the samples, ash contents of not more than 0.001 wt% were detected which means that they adhere to the standards (Table 7 - 2).

7.3.7 Acidity

Although no limits for acidity is specified in any of the standards in Table 7 - 2, to justify the compatibility of the fuels with the tank, pump, fuel delivery and injection system, and combustion chamber for different applications, the acidity of all samples were measured [88]. The diesel fuel itself has a minimum pH of 4.22 while a maximum pH of 7.78 was recorded for CPDB. The pH of the latter is very close to that of pure water. As all other samples have pHs within the above range, it can be concluded that all of them can be used safely with confidence that they are compatible with current combustion systems.

7.3.8 Flash Point

The minimum flash points stipulated in standards for diesel, biodiesel and burner biofuel in Table 7 - 2 are 55 ^{o}C, 130 ^{o}C and 45 ^{o}C, respectively [98]. CPDB and FPDB have flash points of 82 ^{o}C and 70 ^{o}C, respectively while CPDB BO10 and FPDB BO10 have flash points of 66 ^{o}C and 57 ^{o}C, respectively. These measured values show that both dehydrated bio-oils can be safely used in burners and both emulsions can be safely used as a diesel replacement. Although the limit specified in the standard for biodiesels does not allow the use of emulsions as a biodiesel replacement, emulsions of bio-oil in biodiesel with the right proportions will be able to meet the flash point requirement.

7.3.9 Pour Point

The only pour point standard listed in Table 7 - 2 is for burner biofuels with a maximum temperature of –9 ^{o}C [99]. Both dehydrated bio-oils have pour points below the temperature of –42^{o}C hence this means that they can be safely used in burners. Since there are no pour point requirements for diesel or biodiesel, the measured pour points of

CPDB and FPDB (–6 ^{o}C and –3 ^{o}C, respectively) are not as important as other physicochemical properties.

7.3.10 Iodine Value

As can be seen in Table 7 - 2, the iodine value is not of concern in any of the standards. Nonetheless, this property indicates the stability of a fuel especially against oxidation. Furthermore, in the European standard for diesel fuels (ASTM D1959), a maximum amount of 120 g iodine adsorbed in 100 g of fuel is stipulated [91]. Hence, this property was measured for both dehydrated and emulsion samples. In all cases, the iodine values do not exceed 50 g/100 g of fuel which adhere to the ASTM D1959 standard.

7.3.11 Cetane Number

To be able to use a fuel on diesel engine, cetane number is the most important specification as it directly affects the quality of combustion and consequently, the engine performance [91–92, 100]. The cetane number needs to be a minimum rating of 47 as reported in Table 7 - 2. The diesel sample tested has a cetane number rating above this value at 65.1. Although CPDB BO10 and FPDB BO10 have reduced cetane number ratings of 51.7 and 52.5, respectively, both values are well above the allowable minimum rating. Thus, it can be concluded that both emulsions can be run on diesel engines without problems in the combustion or engine performance.

7.3.12 Copper Corrosion Strip

The copper corrosion strip test was performed on all samples to evaluate the potential of the fuel in corroding tank containers or piping systems [91–92, 100]. Previously, in the acidity test, it was clear that none of the samples are as acidic as diesel fuel thus they are unlikely to pose corrosion problems in fuel storage, delivery and combustion

systems. The results of the copper corrosion tests that were performed at 50^{o}C for 3 hr corroborate the acidity test results. Table 7 - 2 shows that both CPDB and FPDB are rated as 1b while CPDB BO10, FPDB BO10 and diesel are rated as 1a. Comparing to both diesel and biodiesel standards, the samples can be used in diesel engine applications without any corrosion concerns. For burner biofuels, no limitation is specified in the ASTM D7544-10 standard [85].

7.3.13 Elemental Analysis

Although there are no limitations in fuel standards regarding elemental composition, elemental analysis was carried out for all samples according to the ASTM D5291 for carbon, hydrogen and nitrogen determination. The amount of oxygen was determined by calculation [100].

7.3.13.1 Carbon Content

As can be observed in Table 7 - 2, the carbon content in the dehydrated bio-oils are almost half that of diesel. This is the major reason behind the lower calorific value as compared to diesel since carbon is the major element involved in combustion. The emulsions of dehydrated bio-oils in diesel have approximately 5 wt% less carbon content on average than diesel. The difference can be considered insignificant.

7.3.13.2 Hydrogen Content

The average hydrogen content in dehydrated bio-oils is approximately 11 wt% whereas for diesel, this is approximately 13 wt%. The difference of only 2 wt% is not significant.

7.3.13.3 Nitrogen Content

The nitrogen content in diesel is as low as 0.1 wt% whereas this rises up to 2.7 wt% for both dehydrated bio-oils. The higher amount of nitrogen in fuel can possibly lead to

increased NO_x emissions. However, this can only be elucidated by comprehensive emission tests, which are beyond the scope of this study. Both emulsions have the same nitrogen content of 0.36 wt% which is still comparable to diesel.

7.3.13.4 Oxygen Content

Apart from carbon, the other major difference between diesel and dehydrated bio-oils is the oxygen content. Table 7 - 2 records 1.9 wt% carbon for diesel and 42.1 wt% for both dehydrated bio-oils. In terms of combustion, oxygen is necessary to enable complete combustion and reduce carbon monoxide formation. Nevertheless, the drawback of a high oxygen content is the lack of fuel stability because of chemical oxidation between oxygen and other compounds. To prevent fuel instability, stabilising agents as well as proper storage in the dark at low temperatures are suggested.

7.4 Concluding Remarks

CPDB and FPDB produced under optimum conditions for conventional and fast pyrolysis respectively were tested against ASTM D7544-10 standard for burner biofuels. Additionally, CPDB BO10 and FPDB BO10 were also tested against ASTM D6751-01 and EN 590 standards for biodiesel and diesel fuels, respectively. The results indicate that both CPDB and FPDB can be used in burners by reducing their sulphur contents. For CPDB BO10 and FPDB BO10, the water contents need to be reduced prior to usage in diesel engines. Lastly, both CPDB BO10 and FPDB BO10 can be used as a diesel fuel replacement, but not as a biodiesel replacement due to the flash points being below the minimum limit. By addressing the key issues above, all the produced fuels can be used in their targeted applications as burner biofuels, or alternative diesel and biodiesel replacements.

CHAPTER 8 CONCLUSIONS

This research study has investigated the production and physicochemical characterisation of bio-oil via pyrolysis of Jatropha curcas waste. The key findings are presented firstly in this chapter followed by several recommendations for future work.

8.1 Key Findings

Two reactors were designed and fabricated from stainless steel to carry out pyrolysis processes on Jatropha curcas waste for the purpose of bio-oil production. The first is a conventional fixed-bed pyrolysis rig with a heating rate of 50 K/min and the second is a rapid heating fast pyrolysis rig with a heating rate of 25.67 K/s. DoE was accomplished for parametric investigation of conventional and fast pyrolysis processes. The physicochemical tests were performed on Jatropha curcas waste. The results obtained showed that the waste has comparably lower moisture and oxygen contents, and similar gross calorific value, volatiles, fixed carbon, ash, carbon and hydrogen contents as compared to reported averages of 11 different biomass sources. This biomass also contains a low amount of inorganic elements (below 2 wt%), but over 80 wt% of combined celluloses and lignin, which indicate its viability for bio-oil production. The Jatropha curcas waste was pyrolysed over a range of temperatures from 573 K up to 1073 K and a range of N_2 linear velocity from 7.8×10^{-5} m/s up to 6.7×10^{-2} m/s. Both reaction temperature and N_2 linear velocity strongly influence the yield and key specifications of bio-oil for both processes. The calorific value, water content and acidity of bio-oils produced from both rigs under specific range of operation comply with the ASTM D7554-10 bio-fuel standard, which indicate that they can be used in burners without any modifications as long as other specifications match with the ASTM D7554-10 bio-fuel standard. Using the rapid heating fast pyrolysis process may reduce

the bio-oil yield, but the quality of bio-oil improves in terms of water content and gross calorific value. Additionally, the maximum yield is obtained with a reduction in reaction temperature of 53 K and a shortened reaction time which is preferable as less energy is consumed compared to the conventional pyrolysis. An energy balance analysis of the conventional pyrolysis reactor confirms the viability of the pyrolysis process with a 93.60% increase in energy by only considering the bio-oil as fuel and neglecting the fuel potentials of the char and gas.

Empirical correlations between the input pyrolysis parameters and the output bio-oil yield cum specifications for both conventional and fast pyrolysis were developed using linear and nonlinear regression method. Validation of the correlations was carried out against actual experimental test data with less than 5% error. By using these developed empirical correlations and performing normalisation method, the optimum pyrolysis conditions for both conventional and rapid heating fast pyrolysis have been determined. At optimum conventional pyrolysis conditions (reaction temperature of 800 K and N_2 linear velocity of 0.0078 cm/s), 50.08 wt% of the waste was cracked down into bio-oil, which has 28.34 wt% water content, a gross calorific value of 15.12 MJ/kg and a pH of 6.77. In contrast, at optimum conditions for rapid heating fast pyrolysis (reaction temperature of 747 K and nitrogen linear velocity of 0.0078 cm/s), 40.93 wt% of biomass was converted into bio-oil with a gross calorific value of 16.92 MJ/kg, water content of 28.02 wt% and pH of 7.01. Under optimum pyrolysis conditions, both produced bio-oils have approximately neutral pH values and comply with the ASTM D7554-10 burner bio-fuel standard in terms of gross calorific value and water content.

CPDB and FPDB produced under optimum conditions for conventional and fast pyrolysis respectively were tested against ASTM D7544-10 standard for burner biofuels. Additionally, CPDB BO10 and FPDB BO10 were also tested against ASTM

D6751-01 and EN 590 standards for biodiesel and diesel fuels, respectively. The results indicate that both CPDB and FPDB can be used in burners by reducing their sulphur contents. For CPDB BO10 and FPDB BO10, the water contents need to be reduced prior to usage in diesel engines. Lastly, both CPDB BO10 and FPDB BO10 can be used as a diesel fuel replacement, but not as a biodiesel replacement due to the flash points being below the minimum limit. By addressing the key issues above, all the produced fuels can be used in their targeted applications as burner biofuels, or alternative diesel and biodiesel replacements.

8.2 Recommendations for Future Work

The following section briefly discusses recommendations for future work.

8.2.1 Catalytic Pyrolysis

Catalytic pyrolysis is defined as using catalysts during pyrolysis to improve the quality of the bio-oil. Catalysts such as zeolites normally crack the heavy volatiles molecules into lighter and smaller chains that can reduce viscosity, oxygen, water and sulphur content of the bio-oil [102–104]. To improve the current bio-oils' sulphur content, catalytic pyrolysis can be investigated as an in situ process which potentially prevents the need for secondary bio-oil upgrading processes.

8.2.2 Co-Pyrolysis

Other waste products such as plastic wastes can be investigated as a co-feedstock with Jatropha curcas waste for pyrolysis. By using plastic wastes, this aids in reducing plastic disposal to the environment. There is evidence from the literature that co-pyrolysis of plastics and Jatropha curcas waste produce better quality bio-oil [105].

8.2.3 Fluidised Bed Reactor

Due to cost constraint, fluidised bed pyrolysis reactor was not designed and fabricated. For further investigation of the production of bio-oil from Jatropha curcas waste with higher quality, using this type of pyrolysis system is suggested as an extension to the current research.

REFERENCES

1. Ayhan Demirbas "Progress and Recent Trends in Biofuels." Progress in Energy and Combustion Science 33 1–18, 2007.

2. J. A. L. Sastre, J.S.J. Alonso, C. R-A. Garcia, E. J. L. Romero-Avila and C. R. Alonso "A study of the Decrease in Fossil CO2 Emissions of Energy Generation by Using Vegetable Oils as Combustible." Building and Environment 38 129–133, 2003.

3. International Energy Agency [online] Available at: www.iea.org [Acceced 30 July 2013]

4. Zhongyang Luo, Shurong Wang, Yanfen Liao, Jinsong Zhou, Yueling Gu and Kefa Cen "Research on biomass fast pyrolysis for liquid fuel" Biomass and Bioenergy 26, pp 455 – 462, 2004.

5. The World Bank, World Development Indicator, [online] Available at: www.google.com/publicdata [Accessed 14 November 2010].

6. World population [online] Available at: http://www.un.org [Accessed 30 July 2013]

7. Hasan Ferdi Gercel "The production and evaluation of bio-oils from the pyrolysis of sunflower-oil cake" Biomass and Bioenergy 23, pp 307 – 314, 2002.

8. Galina Dobele, Igors Urbanovich, Aleksandr Volpert, Valdis Kampars and Eriks Samulis "Fast pyrolysis - Effect of wood drying on the yield and properties of bio-oil" Bioresources 2 (4), pp 699–706, 2007.

9. Hyeon Su Heo, Hyun Ju Park, Young-Kwon Park, Changkook Ryu, Dong Jin Suh, Young-Woong Suh, Jin-Heong Yim and Seung-Soo Kim "Bio-oil production from fast pyrolysis of waste furniture sawdust in a fluidized bed" Bioresource Technology 101, pp S91–S96, 2010.

10. Lin Li and Hongxun Zhang "Production and Characterization of Pyrolysis Oil from Herbaceous Biomass (Achnatherum Splendens)" Energy source 27, pp 319–326, 2005.

11. Ayse E. Putun, Esin Apaydın, Ersan Putun "Rice straw as a bio-oil source via pyrolysis and steam pyrolysis" Energy 29, pp 2171–2180, 2004.

12. Viboon Sricharoenchaikul, Duangduen Atong "Thermal decomposition study on Jatropha curcas L. waste using TGA and fixed bed reactor" Journal of Analytical and Applied Pyrolysis 85, pp 155–162, 2009.

13. Ayse Eren Putun "Biomass to Bio-oil via Fast Pyrolysis of Cotton Straw and Stalk" Energy Sources 24, pp 275–285, 2002.

14. Ayhan Demirbas "Progress and recent trends in biodiesel fuels" Energy Conversion and Management 50, pp 14–34, 2009.

15. Ala Khodier, Paul Kilgallon, Nigel Legrave, Nigel Simms, John Oakey and Tony Bridgwater "Pilot-Scale Combustion of Fast-Pyrolysis Bio-oil: Ash Deposition and Gaseous Emissions" Environmental Progress & Sustainable Energy Vol.28 No.3, DOI 10.1002/ep, pp 397–403, 2009.

16. M. R. F. Zonooz, B. Ali, K. Sopian and O. Saadatian "Review of Current National Energy Policies in Malaysia" 3rd International Conference on Business and Economic Research Proceeding, 898, 2012.

17. Dinesh Mohan, Charles U. Pittman, Jr. and Philip H. Steele "Pyrolysis of Wood/Biomass for Bio-oil: A Critical Review" Energy & Fuels 20 (3), pp 848–889, 2006.

18. M. BALAT and M. F. DEMIRBAS "Bio-oil from Pyrolysis of Black Alder Wood" Energy Sources, Part A, 31, pp 1719–1727, 2009.

19. Ayse E. Putun, Basak Burcu Uzun, Esin Apaydin, Ersan Putun "Bio-oil from olive oil industry wastes: Pyrolysis of olive residue under different conditions" Fuel Processing Technology 87, pp 25 – 32, 2005.

20. Jefferson S. de Oliveira, Polyanna M. Leite, Lincoln B. de Souza, Vinicius M. Mello, Eid C. Silva, Joel C. Rubim, Simoni M.P. Meneghetti and Paulo A.Z. Suarez "Characteristics and composition of Jatropha gossypiifolia and Jatropha curcas L. oils and application for biodiesel production" Biomass and Bioenergy 33, pp 449–453, 2009.

21. Bionas company Malaysia [online] Available at: http://bionas.com.my/bionasmalaysia1.html. [Accessed: 1 October 2010].

22. R.N. Singh, D.K. Vyas, N.S.L. Srivastava and Madhuri Narra "SPRERI experience on holistic approach to utilize all parts of Jatropha curcas fruit for energy" Renewable Energy 33, pp 1868–1873, 2008.

23. A. K. Agarwal "Biofuels (Alcohols and Biodiesel) Applications as Fuels for Internal Combustion Engines" Progress in Energy and Combustion Science 33, 233–271, 2007.

24. Kritana Prueksakorna and Shabbirh Gheewala "Full Chain Energy Analysis of Biodiesel from Jatropha curcas L. in Thailand" Environmental Science and Technology 42, pp 3388–3393, 2008.

25. D.K. Vyas and R.N. Singh "Feasibility study of Jatropha seed husk as an open core gasifier feedstock" Renewable Energy 32, pp 512–517, 2007.

26. R. Manurung, D.A.Z. Wever, J. Wildschut, R.H. Venderbosch, H. Hidayat, J.E.G. van Dam, E.J. Leijenhorst and A.A. Broekhuis, H.J. Heeres "Valorisation of Jatropha curcas L. plant parts: Nut shell conversion to fast pyrolysis oil" Food and Bioproducts Processing 87, pp 187–196, 2009.

27. A. Raja S, R. Kennedy Z, Pillai BC, L. R. Lee C "Flash pyrolysis of Jatropha oil cake in electrically heated fluidized bed reactor" Energy 35, 2819–23, 2010.

28. A. Oasmaa D.C. Elliott and S. Muller "Quality Control in Fast Pyrolysis Bio-oil Production and Use" Environmental Progress & Sustainable Energy Vol.28, No.3 DOI 10.1002/ep, pp 404–409, 2009.

29. A. Oasmaa and C. Peacocke "Properties and fuel use of biomass-derived fast pyrolysis liquids, a guide" VTT Journal. Publication number 731, 2010.

30. J. D. Adjaye and N. N. Bakhshi "Production of hydrocarbons by catalytic upgrading of a fast pyrolysis bio-oil. Part I: Conversion over various catalysts" Fuel Processing Technology 45, pp 161–183, 1995.

31. Nurgul Ozbay, Ayse E. Putun and Ersan Putun "Bio-oil production from rapid pyrolysis of cottonseed cake: product yields and compositions" International Journal of Energy Research 30, pp 501–510, 2006.

32. Nader Mahinpey, Pulikesi Murugan, Thilakavathi Mani and Renata Raina "Analysis of Bio-oil, Biogas, and Biochar from Pressurized Pyrolysis of Wheat Straw Using a Tubular Reactor" Energy & Fuels 23, pp 2736–2742, 2009.

33. Kyung-Hae Lee, Bo-Seung Kang, Young-Kwon Park and Joo-Sik Kim "Influence of Reaction Temperature, Pretreatment, and a Char Removal System on the Production of Bio-oil from Rice Straw by Fast Pyrolysis, Using a Fluidized Bed" Energy & Fuels 19, pp 2179–2184, 2005.

34. F. Ates, E. Putun and A. E. Putun "Fast pyrolysis of sesame stalk: yields and structural analysis of bio-oil" Journal of Analytical and Applied Pyrolysis 71, pp 779–790, 2004.

35. H. F. Gercel and O. Gercel "Bio-oil Production from an Oilseed By-product: Fixed-bed Pyrolysis of Olive Cake" Energy Sources Part A, 29, pp 695–704, 2007.

36. Basak Burcu Uzun, Ayse Eren Putun and Ersan Putun "Rapid Pyrolysis of Olive Residue. 1. Effect of Heat and Mass Transfer Limitations on Product Yields and Bio-oil Compositions" Energy & Fuels 21, pp 1768–1776, 2007.

37. Akwasi A. Boateng, Charles A. Mullen, Neil Goldberg and Kevin B. Hicks "Production of Bio-oil from Alfalfa Stems by Fluidized-Bed Fast Pyrolysis" Ind. Eng. Chem. Res. 47, pp 4115–4122, 2008.

38. A.E. Putun, A. Ozcan and E. Putun "Pyrolysis of hazelnut shells in a fixed-bed tubular reactor: yields and structural analysis of bio-oil" Journal of Analytical and Applied Pyrolysis 52, pp 33–49, 1999.

39. M. Asadullah, M.A. Rahman, M.M. Ali, M.S. Rahman, M.A. Motin, M.B. Sultan, M.R. Alam "Production of bio-oil from fixed bed pyrolysis of bagasse" Fuel 86, pp 2514–2520, 2007.

40. E. Salehi, J. Abedi and T. Harding "Bio-oil from Sawdust: Pyrolysis of Sawdust in a Fixed-Bed System" Energy & Fuels 23, pp 3767–3772, 2007.

41. J. D. Adjaye, N. N. Bakhshi "Production of hydrocarbons by catalytic upgrading of a fast pyrolysis bio-oil. Part II: Comparative catalyst performance and reaction pathways" Fuel Processing Technology 45, pp 185–202, 1995.

42. Ayse E. Putun, Esin Apaydin and Ersan Putun "Bio-oil production from pyrolysis and steam pyrolysis of soybean-cake: product yields and composition" Energy 27, pp 703–713, 2002.

43. Alan Shihadeh and Simone Hochgreb "Impact of Biomass Pyrolysis Oil Process Conditions on Ignition Delay in Compression Ignition Engines" Energy and Fuels 16, pp 552–561, 2002.

44. A. Demirbas "Producing Bio-oil from Olive Cake by Fast Pyrolysis" Energy Sources, Part A, pp 30:38–44, 2008.

45. A. Demirbas "New Biorenewable Fuels from Vegetable Oils" Energy Sources, Part A, 32, pp 628–636, 2010.

46. Fang Xu, Yu Xu, Hao Yin, Xifeng Zhu and Qingxiang Guo "Analysis of Bio-oil Obtained by Biomass Fast Pyrolysis Using Low-Energy Electron-Impact Mass Spectrometry" Energy & Fuels 23, pp 1775–1777, 2009.

47. Michio Ikura, Maria Stanciulescu and Ed Hogan "Emulsification of pyrolysis derived bio-oil in diesel fuel" Biomass and Bioenergy 24, pp 221–232, 2003.

48. Et.G.M. Gubitz, M. Mittelbach, M. Trabi "Exploitation of the tropical oil seed plant Jatropha curcas L." Bioresource Technology 67, pp 73–82, 1999.

49. E. Putun, M. Kockar, F. Gercel, S. Brown, J. Andresen, C. McRae and C.E. Snape "Assessment of the effect of hydrogen pressure on biomass pyrolysis: A study of Euphorbia Rigida, Sunflower oil, industrial waste and pure Cellulose" Renewable Energy 5 Part II, pp 816–818, 1994.

50. H. P. S. Makkar, K. Becker, F. Sporer, and M. Wink "Studies on Nutritive Potential and Toxic Constituents of Different Provenances of Jatropha curcas" Journal of Agricultural and Food Chemistry 45, pp 3152–3157, 1997.

51. S. Jindal, Bhagwati P. Nandwana, and Narendra S. Rathore "Comparative Evaluation of Combustion, Performance, and Emissions of Jatropha Methyl Ester and Karanj Methyl Ester in a Direct Injection Diesel Engine" Energy and fuels 2009.

52. Zhengguo Li, Bin-Lelin, Xiafeng Zhao, Masayuki sagisaka, and Ryosuke Shibazaki "System Approach for Evaluating the Potential Yield and Plantation of Jatropha curcas L. on a Global Scale" Environmental Science and Technology 2010.

53. Emil Akbar, Zahira Yaakob, Siti Kartom Kamarudin, Manal Ismail and Jumat Salimon "Characteristic and Composition of Jatropha Curcas Oil Seed from Malaysia and its Potential as Biodiesel Feedstock" European Journal of Scientific Research ISSN 1450-216X Vol.29 No.3, pp 396–403, 2009.

54. Cesar A. S. da Silva, Guilherme Sanaiotti, Marcelo Lanza, Antonio J. A. Meirelles and Eduardo A. C. Batista "Liquid-Liquid Equilibrium Data for Systems Containing Jatropha curcas Oil + Oleic Acid + Anhydrous Ethanol + Water at (288 to 318) K" Journal of Chemical Engineering, 2009.

55. Hui Zhou, Houfang Lu and Bin Liang "Solubility of Multicomponent Systems in the Biodiesel Production by Transesterification of Jatropha curcas L. Oil with Methanol" Journal of Chemical Engineering 51, pp 1130–1135, 2006.

56. Keith Openshaw "A review of Jatropha curcas: an oil plant of unfulfilled promise" Biomass and Bioenergy 19, pp 1–15, 2000.

57. S. Morris Kupchan, C. W. Sigel, M. J. Matz, J. A. Saenz Renauld, R. C. Haltiwanger and R. F. Bryan "Jatrophone, a Novel Macrocyclic Diterpenoid Tumor Inhibitor from Jatropha gossypiifolia1,2" Journal of the American Chemical Society 92:14, pp 4476–4477, 1970.

58. M. K. Figueiredo, G. A. Romeiro1, R. V. S. Silva1, P. A. Pinto, R. N. Damasceno, L. A. d'Avila, and A. P. Franco " Pyrolysis Oil from the Fruit and Cake of Jatropha curcas Produced Using a Low Temperature Conversion (LTC) Process: Analysis of a Pyrolysis Oil-Diesel Blend" Energy and Power Engineering 3, 332–338, 2011.

59. C. H. Biradar, K. A. Subramanian and M. G. Dastidar "Production and Fuel Quality Upgradation of Bio-oil from Jatropha curcas De-oiled Seed cake" Fuel 119, 81–89, 2014.

60. Charles A. Mullen and Akwasi A. Boateng "Chemical Composition of Bio-oils Produced by Fast Pyrolysis of Two Energy Crops" Energy & Fuels 22, 2104–2109, 2008.

61. Robert C. Brown "The Role of Thermochemical Technologies in Advanced Biorefineries" North Central Region Feedstock Workshop Sioux Falls SD, August 15, 2006.

62. P.L. Spath, J.M. Lane and M.K. Mann "Technoeconomic analysis of options for producing hydrogen from biomass" National Renewable Energy Laboratory, 1617 Cole Blvd., Golden, Colorado, USA 80401.

63. Charles A. Mullen, Akwasi A. Boateng, Kevin B. Hicks, Neil M. Goldberg and Robert A. Moreau "Analysis and Comparison of Bio-oil Produced by Fast Pyrolysis from Three Barley Biomass/Byproduct Streams" Energy & Fuels 24, pp 699–706, 2010.

64. M. Asadullah, M. Anisur Rahman, M. Mohsin Ali, M. Abdul Motin, M. Borhanus Sultan, M. Robiul Alam, M. Sahedur Rahman "Jute stick pyrolysis for bio-oil production in fluidized bed reactor" Bioresource Technology 99, pp 44–50, 2008.

65. Jacques Lédé and Olivier Authier "Temperature and Heating Rate of Solid Particles undergoing a Thermal Decomposition. Which Criteria for Characterizing Fast Pyrolysis?" Journal of Analytical and Applied Pyrolysis 2014.

66. Shuai Zhou, Brennan Pecha, Michiel van Kuppevelt, Armando G. McDonald and Manuel Garcia-Perez "Slow and Fast Pyrolysis of Douglas-fir Lignin: Importance of Liquid-intermediate Formation on the Distribution of Products" Biomass and Bioenergy 66, 398–409, 2014.

67. A.E. Putun, 0. M. Kockar, S. Yorgun, H.F. Gercel, J. Andresen, C.E. Snape and E. Putun "Fixed-bed pyrolysis and hydropyrolysis of sunflower bagasse: Product yields and compositions" Fuel Processing Technology 46, pp 49–62, 1996.

68. Akwasi A. Boateng, Daren E. Daugaard, Neil M. Goldberg and Kevin B. Hicks "Bench-Scale Fluidized-Bed Pyrolysis of Switchgrass for Bio-oil Production" Ind. Eng. Chem. Res. 46, 1891–1897, 2007.

69. Charles A. Mullen, Akwasi A. Boateng, Neil M. Goldberg, Isabel M. Lima, David A. Laird and Kevin B. Hicks "Bio-oil and bio-char production from corn cobs and Stover by fast pyrolysis" Biomass and bioenergy 34, pp 67–74, 2010.

70. Kaushlendra Singh, E. W. Tollner, Sudhagar Mani, L. Mark Risse, K. C. Das and John Worley "Transforming Solid Wastes Into High Quality Bioenergy Products: Entropy Analysis" In 16th North American Waste-to-Energy Conference, Philadelphia Pennsylvania USA, NAWTEC16-1924, May 19–21, 2008.

71. Michael A. Karnofski and Richard Rsinone "Pyrolysis Method" Weyerhaeuser Company Longview, Washington 98632, 1978.

72. Hans Darmstadt, Manuel Garcia-Perez, Alain Adnot, Abdelkader Chaala, Detlef Kretschmer and Christian Roy "Corrosion of Metals by Bio-oil Obtained by Vacuum Pyrolysis of Softwood Bark Residues. An X-ray Photoelectron Spectroscopy and Auger Electron Spectroscopy Study" Energy & Fuels 18, pp 1291–1301, 2004.

73. Mauviel Guillain, Kies Fairouz, Sans Rene Mar, Ferrer Monique and Lede Jacques "Attrition-free pyrolysis to produce bio-oil and char" Bioresource Technology 100, pp 6069–6075, 2009.

74. Yao Bin Yang, Changkook Ryu, David Poole, Paul Gilbert, Adela Khor, Vida Sharifi, Jim Swithenbank "Mathematical Modelling of Biomass Pyrolysis and Gasification in Lab-scale Packed-bed Systems" SUPERGEN - Work package 3 ; Mathematical modeling workshop, SUWIC Sheffield University, 14 March 2006.

75. Frank P. Incropera and David P. DeWitt "Introduction to Heat Transfer" 4th edition, New York, Wiley, 2001.

76. Adrian Bejan "Convection Heat Transfer" 3rd edition, Wiley New Jersey, 2004.

77. J. P. Holman "Heat Transfer" 9th edition (International Edition), Mc Graw-Hill, 2002.

78. G. F. C. Rogers and Y. R. Mayhew "Thermodynamic and Transport Properties of Fluids" 5th edition, Oxford, 1995.

79. American Standards for Testing and Materials "Standard Test Methods for Direct Moisture Content Measurement of Wood and Wood-Base Materials", ASTM D4442 03, 2003.

80. British Standards "Methods for Analysis and Testing of Coal and Coke" BS 1016–102:2000, 2000.

81. American Standards for Testing and Materials "Standard Test Methods for Gross Calorific Value of Coal and Coke by the Adiabatic Bomb Calorimeter" ASTM D2015-96, 1996.
82. A. Sluiter, B. Hames, D. Hyman, C. Payne, R. Ruiz, C. Scarlata, J. Sluiter, D. Templeton, and J. Wolfe "Determination of total solids in biomass and total dissolved solids in liquid process samples. National Renewable Energy Laboratory" NREL/TP-510-4262, 2008.
83. Malaysian Meteorology Department. Meteorology Metadata station page. [http://www.met.gov.my]. [Accessed 04 July 2012]
84. K. W. Ragland, D. J. Aerts, and A. J. Baker "Properties of Wood for Combustion Analysis" Bioresource Technology 37, 161–168, 1991.
85. American Standards for Testing and Materials "Standard Specification for Pyrolysis Liquid Biofuel" ASTM D7544-10, 2010.
86. American Standards for Testing and Materials "Standard Test Method for Calorific value of Liquid Hydrocabon Fuels by Bomb Calorimeter" ASTM D240-09, 2009.
87. American Standards for Testing and Materials "Standard Test Method for Water Using Volumetric Karl Fischer Titration" ASTM E203-08, 2008.
88. American Standards for Testing and Materials "Standard Test Method for pH of Aqueous Solution with the Glass Electrode" ASTM E70-07, 2007.
89. S. A. Jourabchi, S. Gan and H. K. Ng "Pyrolysis of Jatropha curcas Pressed Cake for Bio-oil Production in a Fixed-Bed System" Energy Conversion and Management 78, 518–526, 2014.
90. M.R. Spiegel and L.J. Stephens "Multiple and partial correlation" Statistics. 3rd edition, Schum's outlines. Mc Graw-Hill; 1999.

91. American Standards for Testing Materials "Standard Specification for Biodiesel Fuel Blend Stock (B100) for Middle Distillate Fuels 2012" [online] Available at: http://www.dieselnet.com/tech/fuel_biodiesel_std.php [Accessed 20 July 2012].
92. The first European diesel fuel specification, 1993 [online] Available at: https://www.dieselnet.com/standards/eu/fuel_automotive.php [Accessed 5 January 2012].
93. American Standards for Testing and Materials "Standard Test Method for Pyrolysis Solid Content in Pyrolysis Liquids by Filtration of Solids in Methanol" ASTM D7579-09, 2009.
94. American Standards for Testing and Materials "Standard Test Method for Kinematic Viscosity of Transparent and Opaque Liquids (and the Calculation of Dynamic Viscosity)" ASTM D445 -03, 2003.
95. American Standards for Testing and Materials "Standard Test Method for Density, Relative Density, and API Gravity of Liquids by Digital Density Meter" ASTM D4052-11, 2011.
96. American Standards for Testing and Materials "Standard Test Method for Sulfur in Petroleum and Petroleum Products by Energy Dispersive X-ray Fluorescence Spectrometry" ASTM D4294-10, 2010.
97. American Standards for Testing and Materials "Standard Test Method for Ash from Petroleum Products" ASTM D482-07, 2007.
98. American Standards for Testing and Materials "Standard Test Method for Flash Point by Pensky-Martens Closed Cup Tester" ASTM D93-07, 2007.
99. American Standards for Testing and Materials "Standard Test Method for Pour Point of Petroleum Products" ASTM D97-12, 2012.

100. SGS Laboratory "Petrochemical Inspection (M) Sdn. Bhd." Standard Test Methods on Fuels and Bio-fuels, [online] Available at: http://www.sgs.my/en/ [Accessed 1 January 2012].

101. I. A. H. Al Zubaidy, F. B. Tarsh, N. N. Darwish, B. S. S. Abdul Majid, A. Al Sharafi and L. Abu Chacra " Adsorption Process of Sulfur Removal from Diesel Oil using Sorbent Materials" Journal of Clean Energy Technology vol. 1 No.1, 2013.

102. T. Dickerson and J. Soria "Catlytic Fast Pyrolysis: A Review" Energies 6, 514–538, 2013.

103. R. Ahmad, N. Hamidin and U. F. M. Ali "Bio-oil Product from Non-Catalytic and Catalytic Pyrolysis of Rice Straw" Australian Journal of Basic and Applied Science, 7(5), 61–65, 2013.

104. T. Dickerson and J. Soria "Catlytic Fast Pyrolysis: A Review" Energies 6, 514–538, 2013.

105. Y. C. Rotliwala and P. A. Parikh "Study on Thermal Co-Pyrolysis of Jatropha Deoiled Cake and Polyolefins" Waste Management & Research 29 1251–1261, 2011.

APPENDICES

APPENDIX A: Refrigeration System Specifications

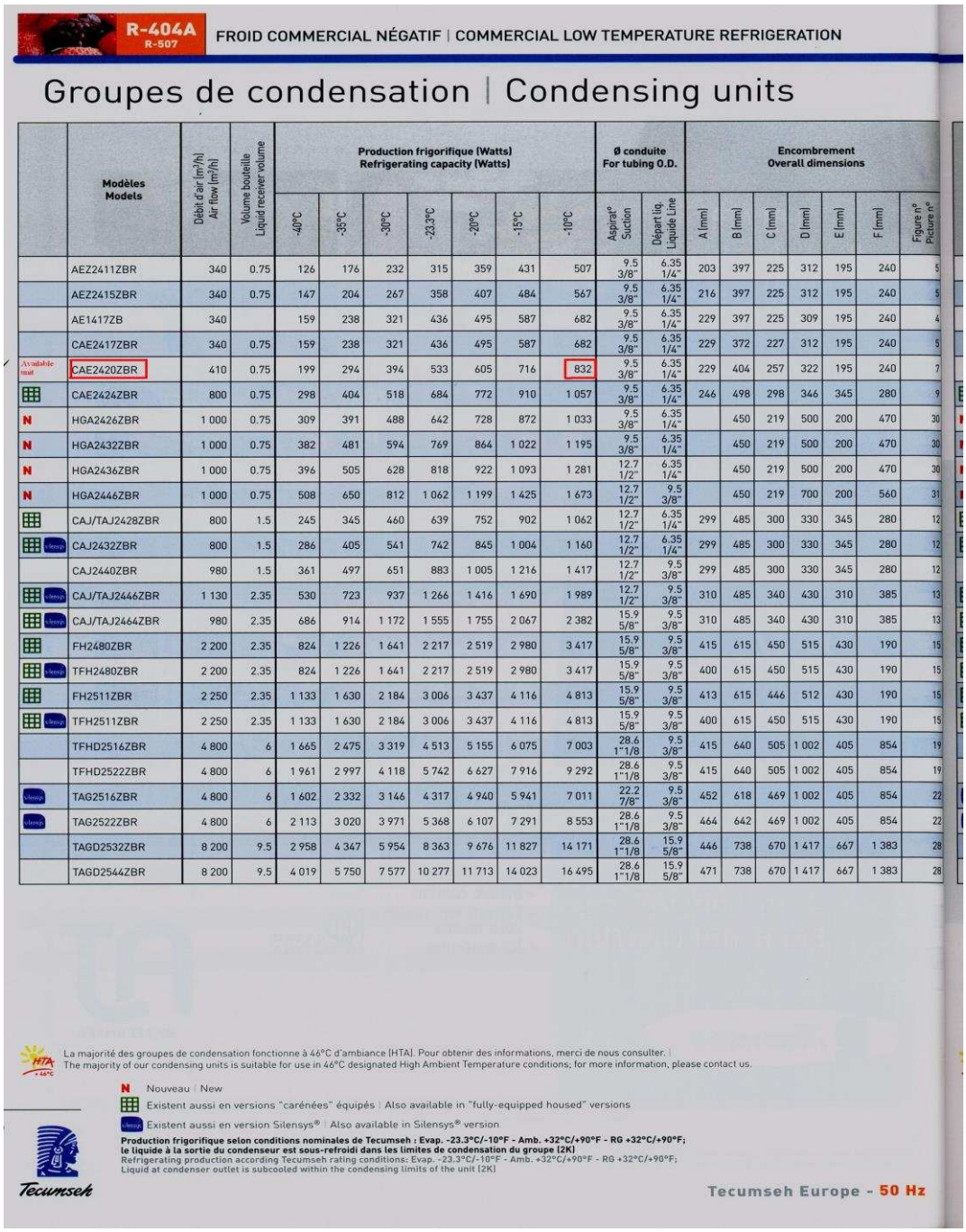

R-404A
R-507

FROID COMMERCIAL NÉGATIF | COMMERCIAL LOW TEMPERATURE REFRIGERATION

Groupes de condensation | Condensing units

	Modèles Models	Débit d'air (m³/h) Air flow (m³/h)	Volume bouteille Liquid receiver volume	Production frigorifique (Watts) Refrigerating capacity (Watts)							Ø conduite For tubing O.D.		Encombrement Overall dimensions						
				-40°C	-35°C	-30°C	-23.3°C	-20°C	-15°C	-10°C	Aspiral° Suction	Départ liq. Liquide Line	A (mm)	B (mm)	C (mm)	D (mm)	E (mm)	F (mm)	Figure n° Picture n°
	AEZ2411ZBR	340	0.75	126	176	232	315	359	431	507	9.5 3/8"	6.35 1/4"	203	397	225	312	195	240	5
	AEZ2415ZBR	340	0.75	147	204	267	358	407	484	567	9.5 3/8"	6.35 1/4"	216	397	225	312	195	240	5
	AE1417ZB	340		159	238	321	436	495	587	682	9.5 3/8"	6.35 1/4"	229	397	225	309	195	240	4
	CAE2417ZBR	340	0.75	159	238	321	436	495	587	682	9.5 3/8"	6.35 1/4"	229	372	227	312	195	240	5
Available mai	CAE2420ZBR	410	0.75	199	294	394	533	605	716	832	9.5 3/8"	6.35 1/4"	229	404	257	322	195	240	7
	CAE2424ZBR	800	0.75	298	404	518	684	772	910	1 057	9.5 3/8"	6.35 1/4"	246	498	298	346	345	280	9
N	HGA2426ZBR	1 000	0.75	309	391	488	642	728	872	1 033	9.5 3/8"	6.35 1/4"		450	219	500	200	470	30
N	HGA2432ZBR	1 000	0.75	382	481	594	769	864	1 022	1 195	9.5 3/8"	6.35 1/4"		450	219	500	200	470	30
N	HGA2436ZBR	1 000	0.75	396	505	628	818	922	1 093	1 281	12.7 1/2"	6.35 1/4"		450	219	500	200	470	30
N	HGA2446ZBR	1 000	0.75	508	650	812	1 062	1 199	1 425	1 673	12.7 1/2"	9.5 3/8"		450	219	700	200	560	31
	CAJ/TAJ2428ZBR	800	1.5	245	345	460	639	752	902	1 062	12.7 1/2"	6.35 1/4"	299	485	300	330	345	280	12
Silensys	CAJ2432ZBR	800	1.5	286	405	541	742	845	1 004	1 160	12.7 1/2"	6.35 1/4"	299	485	300	330	345	280	12
	CAJ2440ZBR	980	1.5	361	497	651	883	1 005	1 216	1 417	12.7 1/2"	9.5 3/8"	299	485	300	330	345	280	12
Silensys	CAJ/TAJ2446ZBR	1 130	2.35	530	723	937	1 266	1 416	1 690	1 989	12.7 1/2"	9.5 3/8"	310	485	340	430	310	385	13
Silensys	CAJ/TAJ2464ZBR	980	2.35	686	914	1 172	1 555	1 755	2 067	2 382	15.9 5/8"	9.5 3/8"	310	485	340	430	310	385	13
	FH2480ZBR	2 200	2.35	824	1 226	1 641	2 217	2 519	2 980	3 417	15.9 5/8"	9.5 3/8"	415	615	450	515	430	190	15
Silensys	TFH2480ZBR	2 200	2.35	824	1 226	1 641	2 217	2 519	2 980	3 417	15.9 5/8"	9.5 3/8"	400	615	450	515	430	190	15
	FH2511ZBR	2 250	2.35	1 133	1 630	2 184	3 006	3 437	4 116	4 813	15.9 5/8"	9.5 3/8"	413	615	446	512	430	190	15
Silensys	TFH2511ZBR	2 250	2.35	1 133	1 630	2 184	3 006	3 437	4 116	4 813	15.9 5/8"	9.5 3/8"	400	615	450	515	430	190	15
	TFHD2516ZBR	4 800	6	1 665	2 475	3 319	4 513	5 155	6 075	7 003	28.6 1"1/8	9.5 3/8"	415	640	505	1 002	405	854	19
	TFHD2522ZBR	4 800	6	1 961	2 997	4 118	5 742	6 627	7 916	9 292	28.6 1"1/8	9.5 3/8"	415	640	505	1 002	405	854	19
Silensys	TAG2516ZBR	4 800	6	1 602	2 332	3 146	4 317	4 940	5 941	7 011	22.2 7/8"	9.5 3/8"	452	618	469	1 002	405	854	22
Silensys	TAG2522ZBR	4 800	6	2 113	3 020	3 971	5 368	6 107	7 291	8 553	28.6 1"1/8	9.5 3/8"	464	642	469	1 002	405	854	22
	TAGD2532ZBR	8 200	9.5	2 958	4 347	5 954	8 363	9 676	11 827	14 171	28.6 1"1/8	15.9 5/8"	446	738	670	1 417	667	1 383	28
	TAGD2544ZBR	8 200	9.5	4 019	5 750	7 577	10 277	11 713	14 023	16 495	28.6 1"1/8	15.9 5/8"	471	738	670	1 417	667	1 383	28

HTA +46°C La majorité des groupes de condensation fonctionne à 46°C d'ambiance (HTA). Pour obtenir des informations, merci de nous consulter. | The majority of our condensing units is suitable for use in 46°C designated High Ambient Temperature conditions; for more information, please contact us.

N Nouveau | New

Existent aussi en versions "carénées" équipés | Also available in "fully-equipped housed" versions

Existent aussi en version Silensys® | Also available in Silensys® version

Production frigorifique selon conditions nominales de Tecumseh : Evap. -23.3°C/-10°F - Amb. +32°C/+90°F - RG +32°C/+90°F; le liquide à la sortie du condenseur est sous-refroidi dans les limites de condensation du groupe (2K)
Refrigerating production according Tecumseh rating conditions: Evap. -23.3°C/-10°F - Amb. +32°C/+90°F - RG +32°C/+90°F; Liquid at condenser outlet is subcooled within the condensing limits of the unit (2K)

Tecumseh

Tecumseh Europe - 50 Hz

APPENDIX B: Designed Reactor Rigs and their Major Parts

Conventional pyrolysis bed (fixed bed reactor)

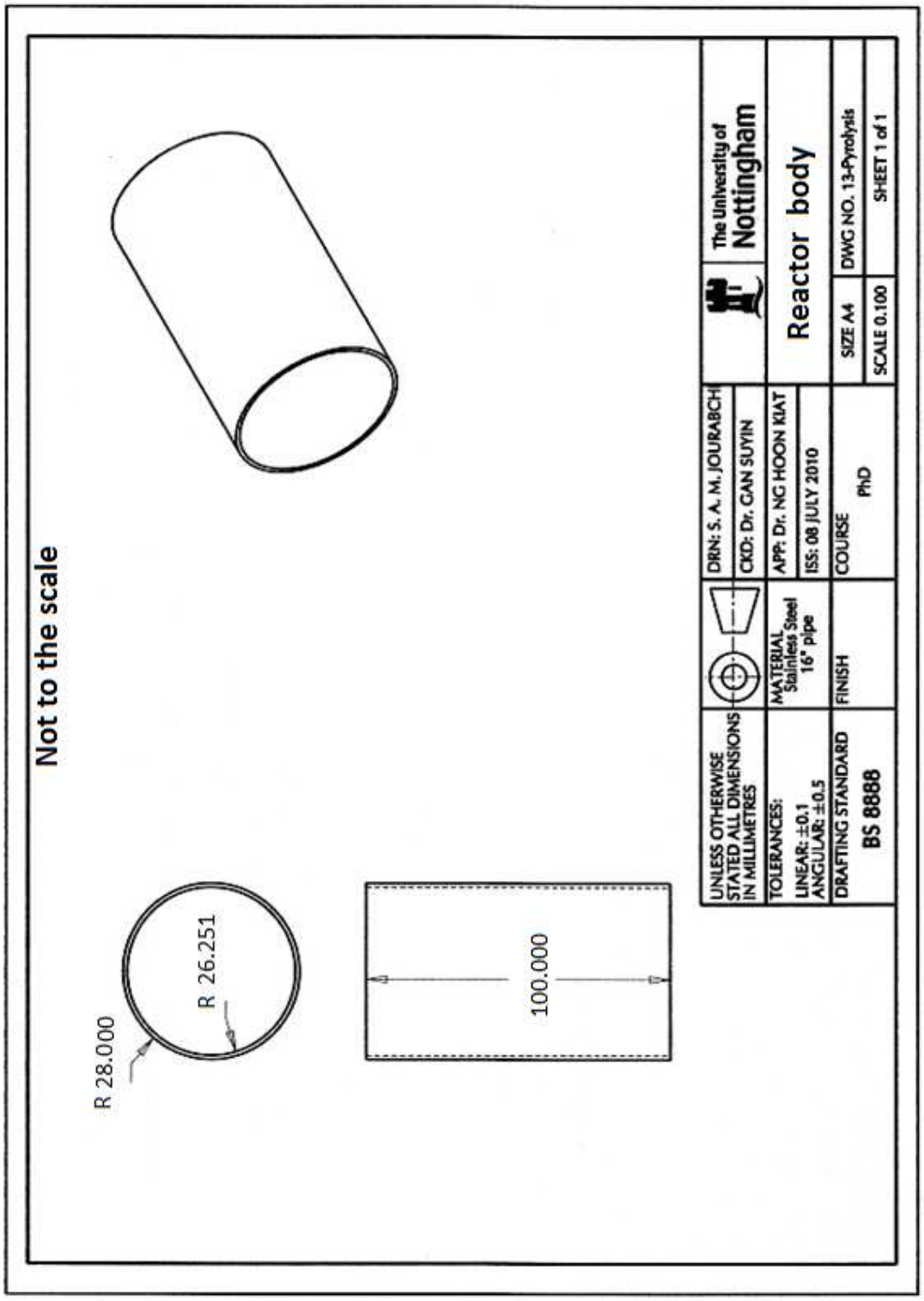

Conventional and fast reactor and also their condenser cap

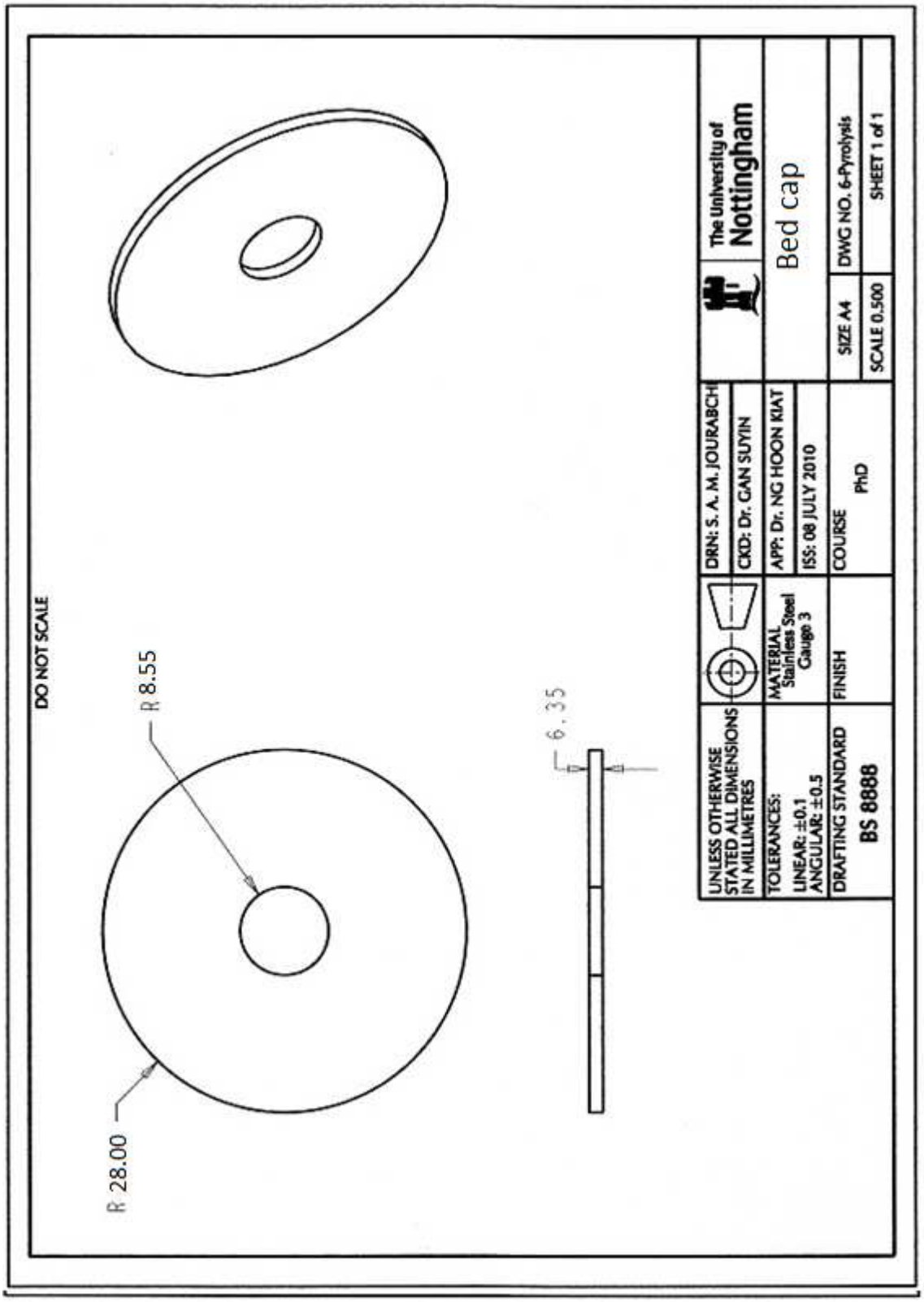

Conventional and fast pyrolysis condenser body

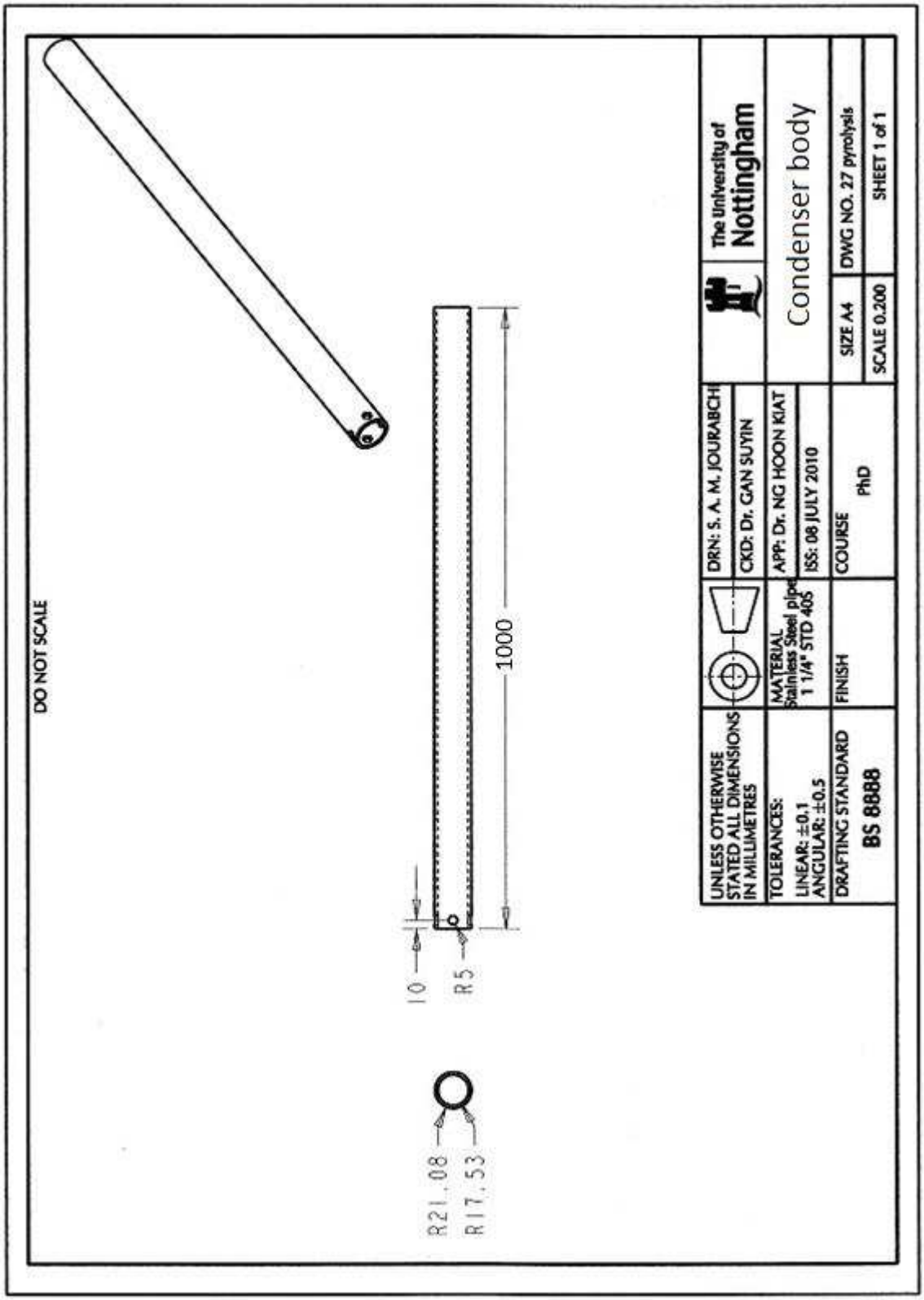

Inlet (nitrogen), outlet (volatiles) and condenser pipe

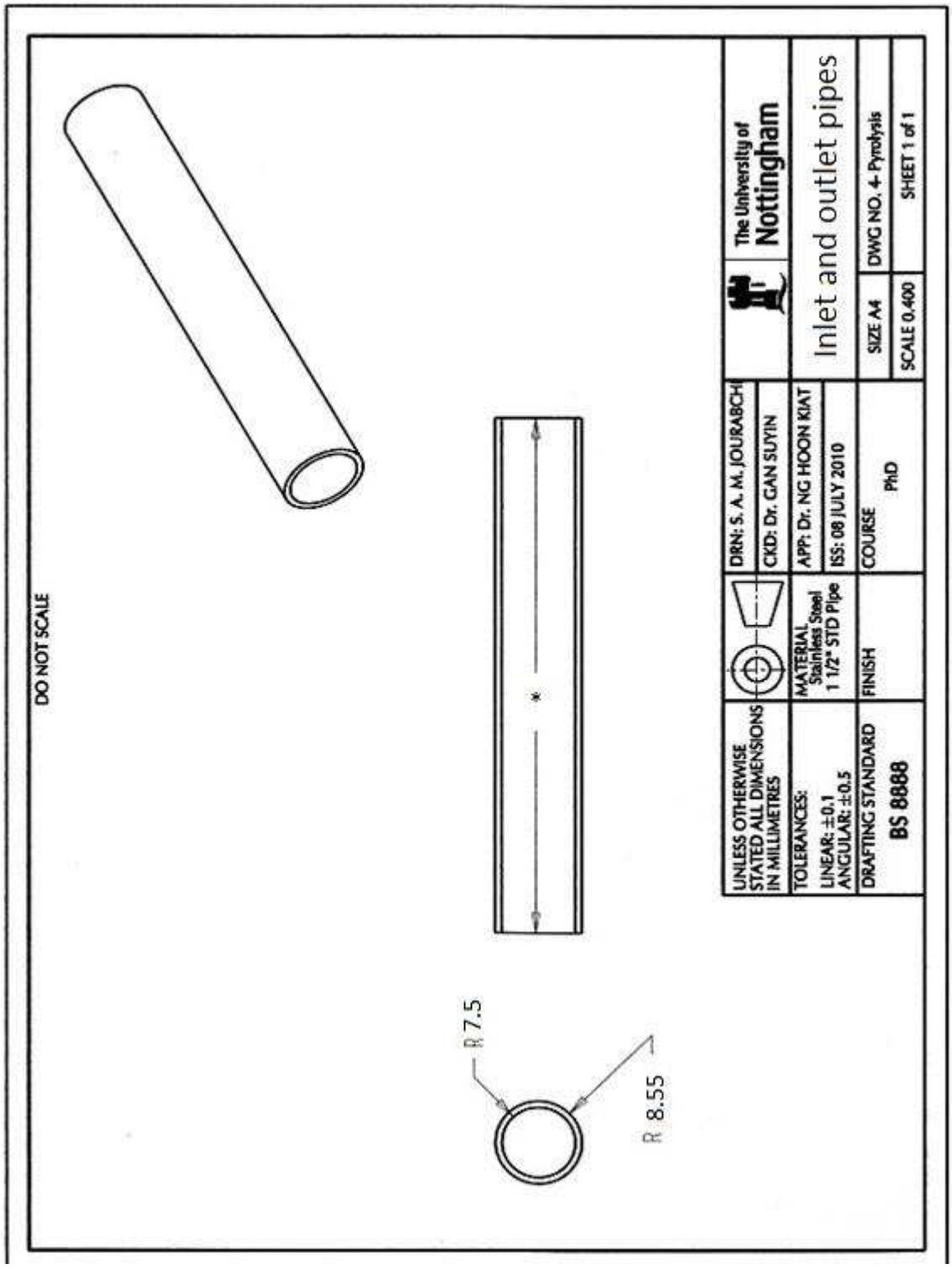

Fast pyrolysis bed (reactor) body

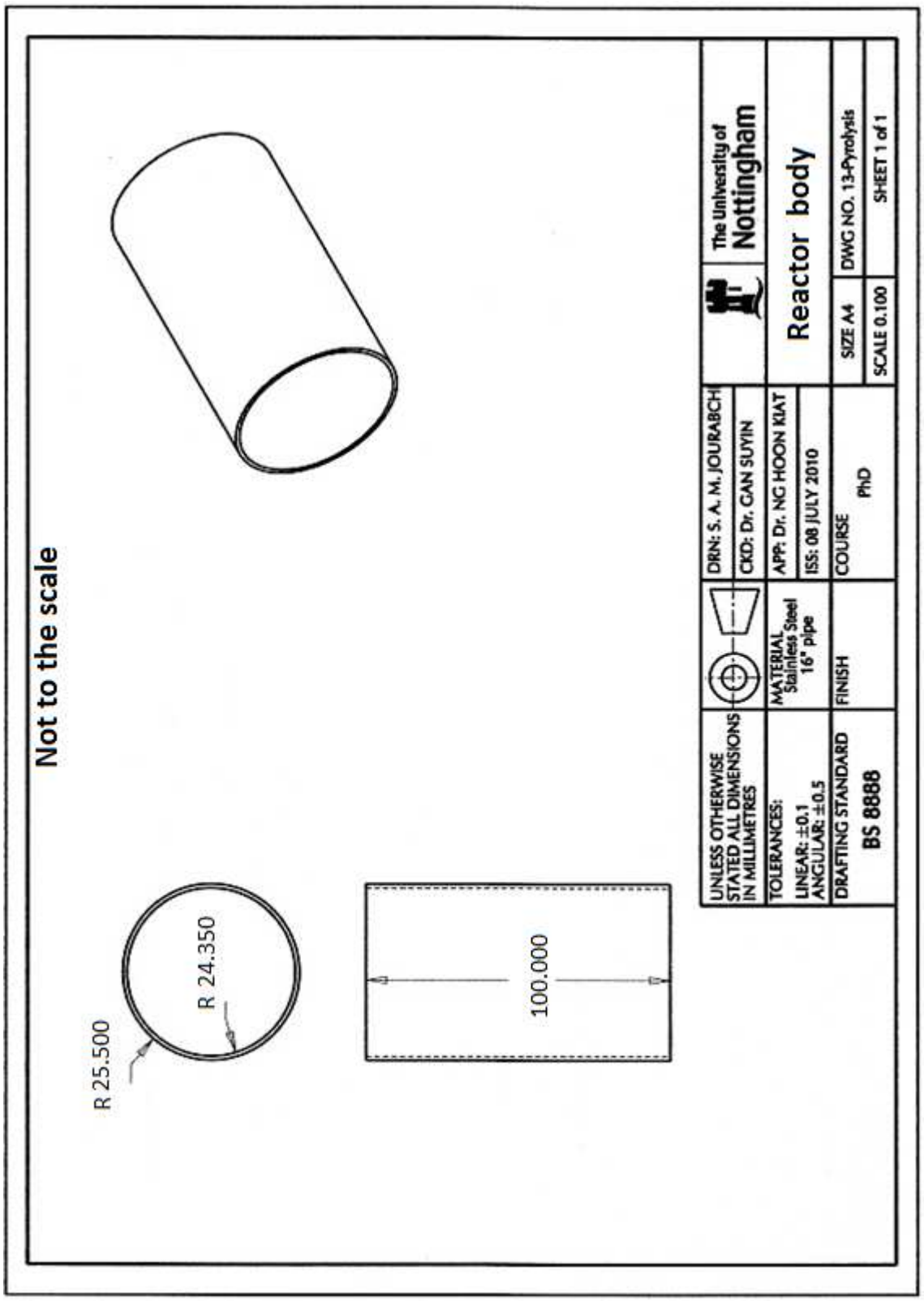

Convection reactor schematic diagram

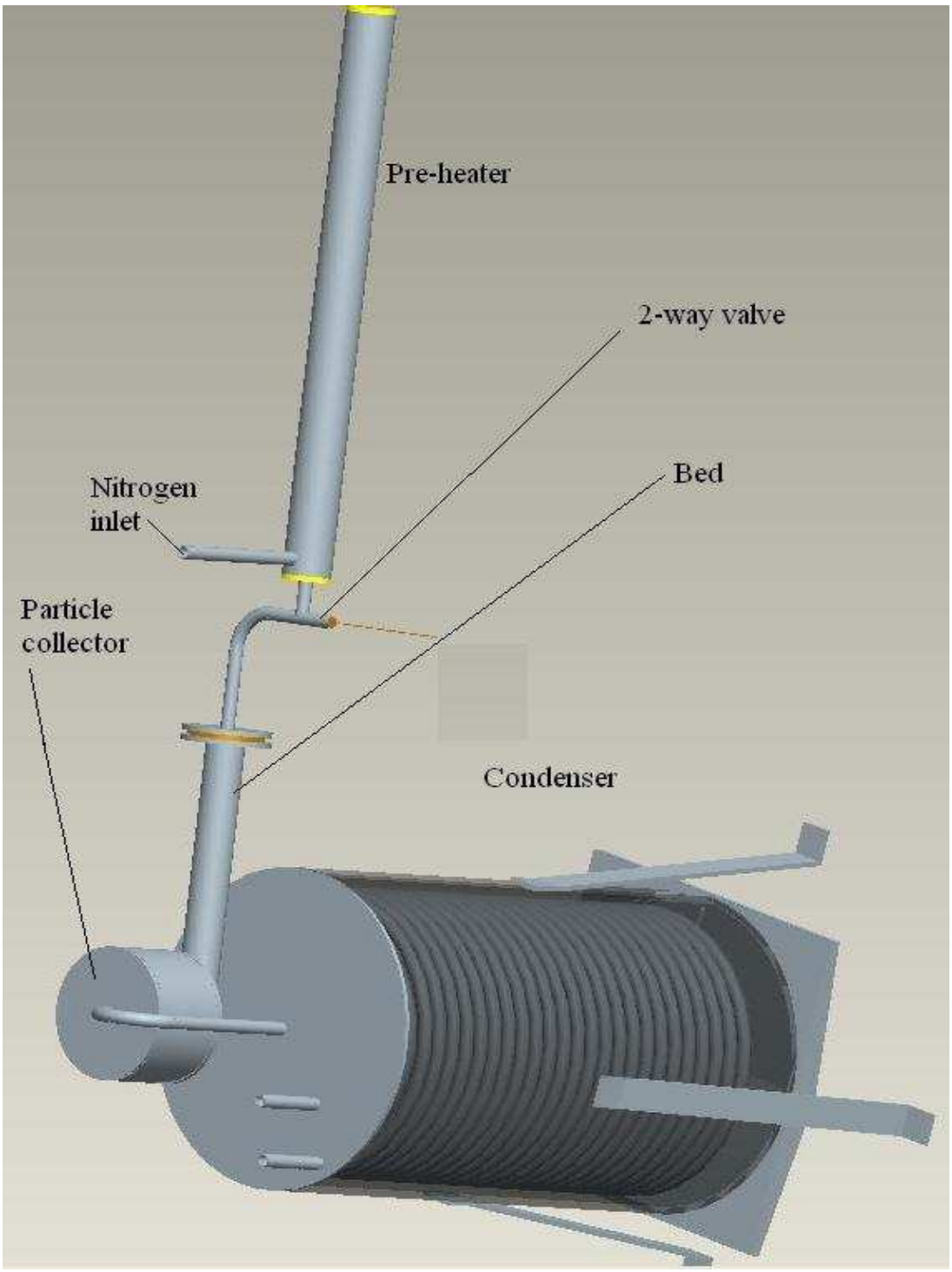

Convection rig condenser major parts

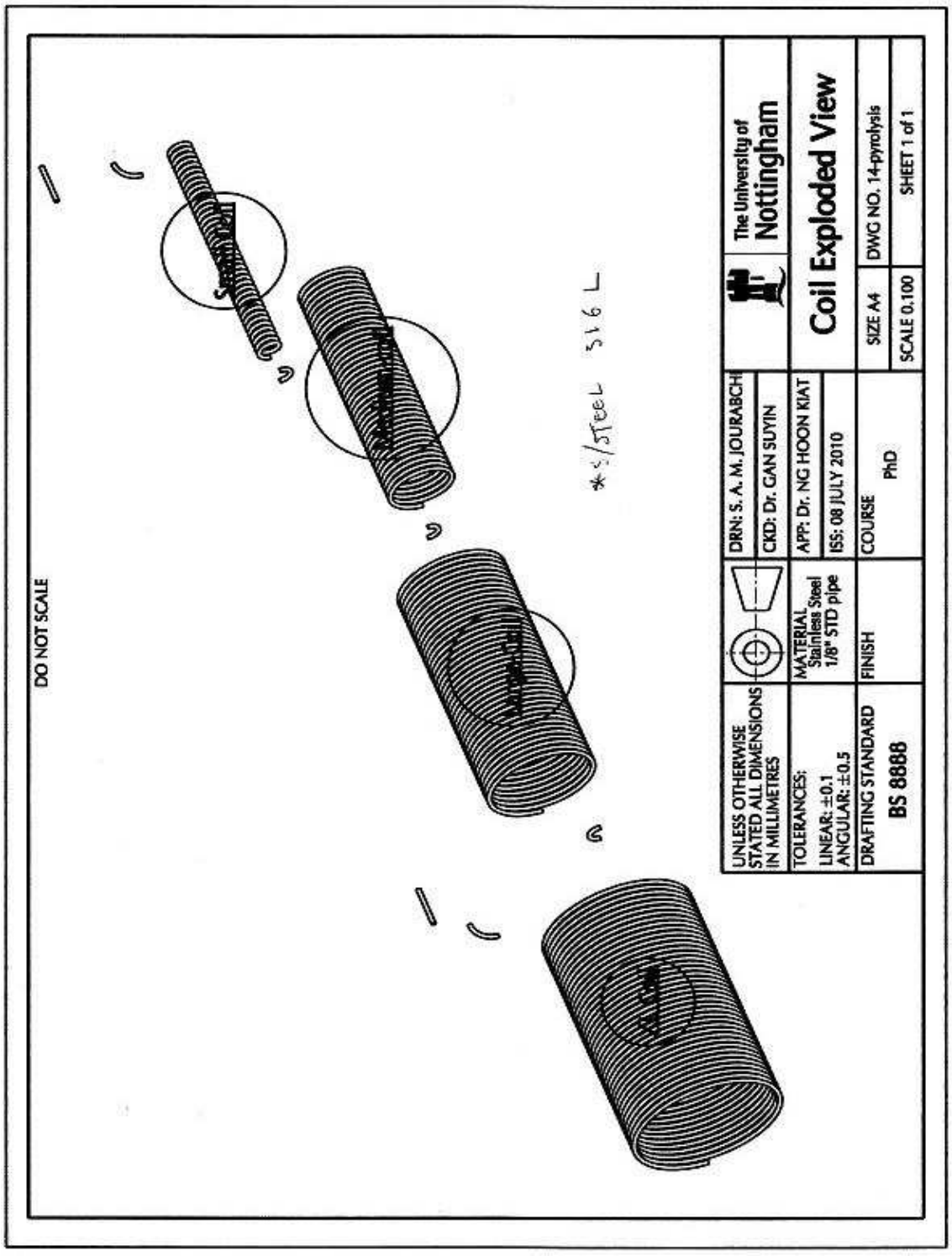

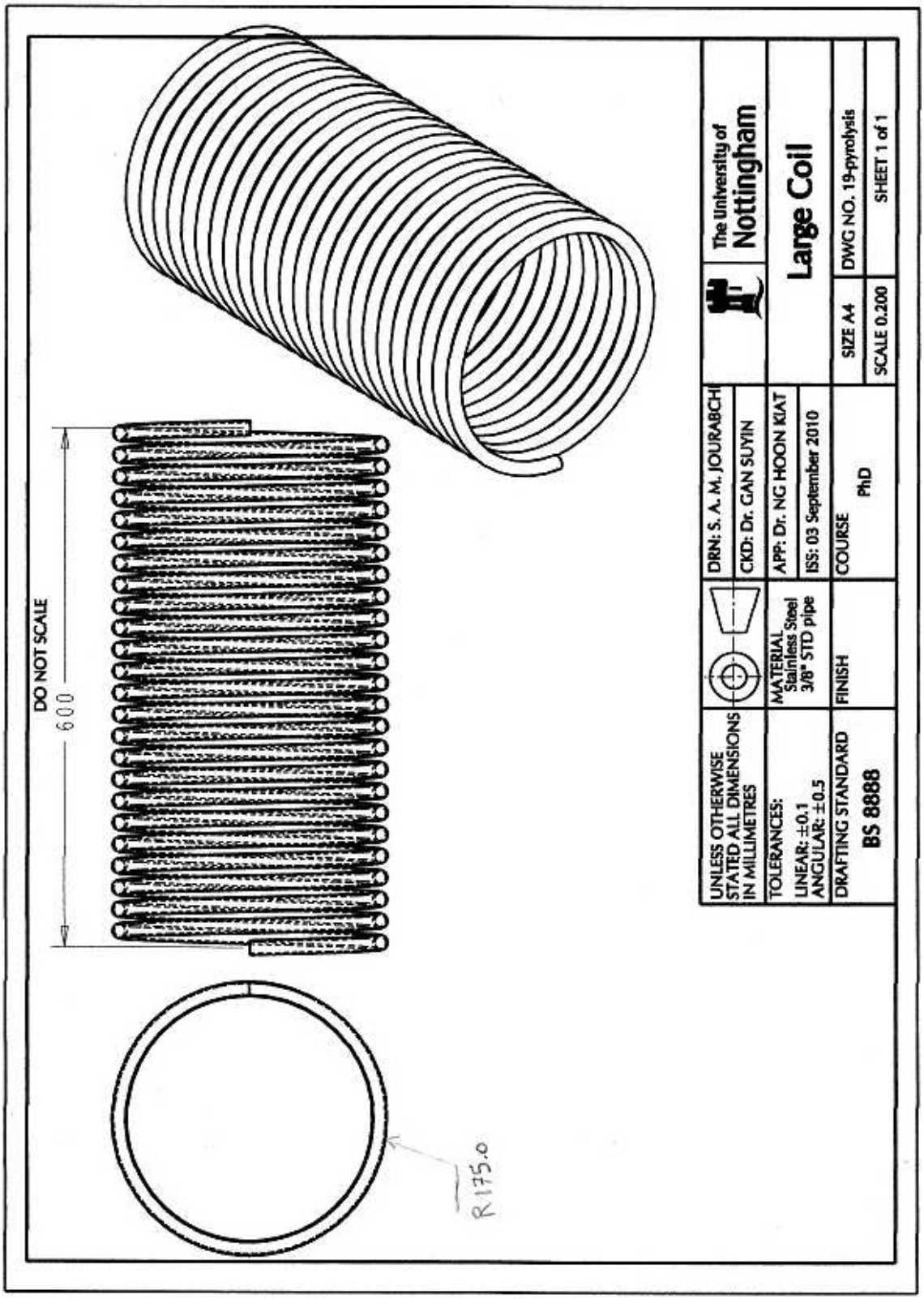
DO NOT SCALE
600
R175.0
UNLESS OTHERWISE STATED ALL DIMENSIONS IN MILLIMETRES
TOLERANCES:
LINEAR: ±0.1
ANGULAR: ±0.5
DRAFTING STANDARD
BS 8888
MATERIAL
Stainless Steel 3/8" STD pipe
FINISH
DRN: S. A. M. JOURABCHI
CKD: Dr. GAN SUYIN
APP: Dr. NG HOON KIAT
ISS: 03 September 2010
COURSE
PhD
The University of Nottingham
Large Coil
SIZE A4
SCALE 0.200
DWG NO. 19-pyrolysis
SHEET 1 of 1

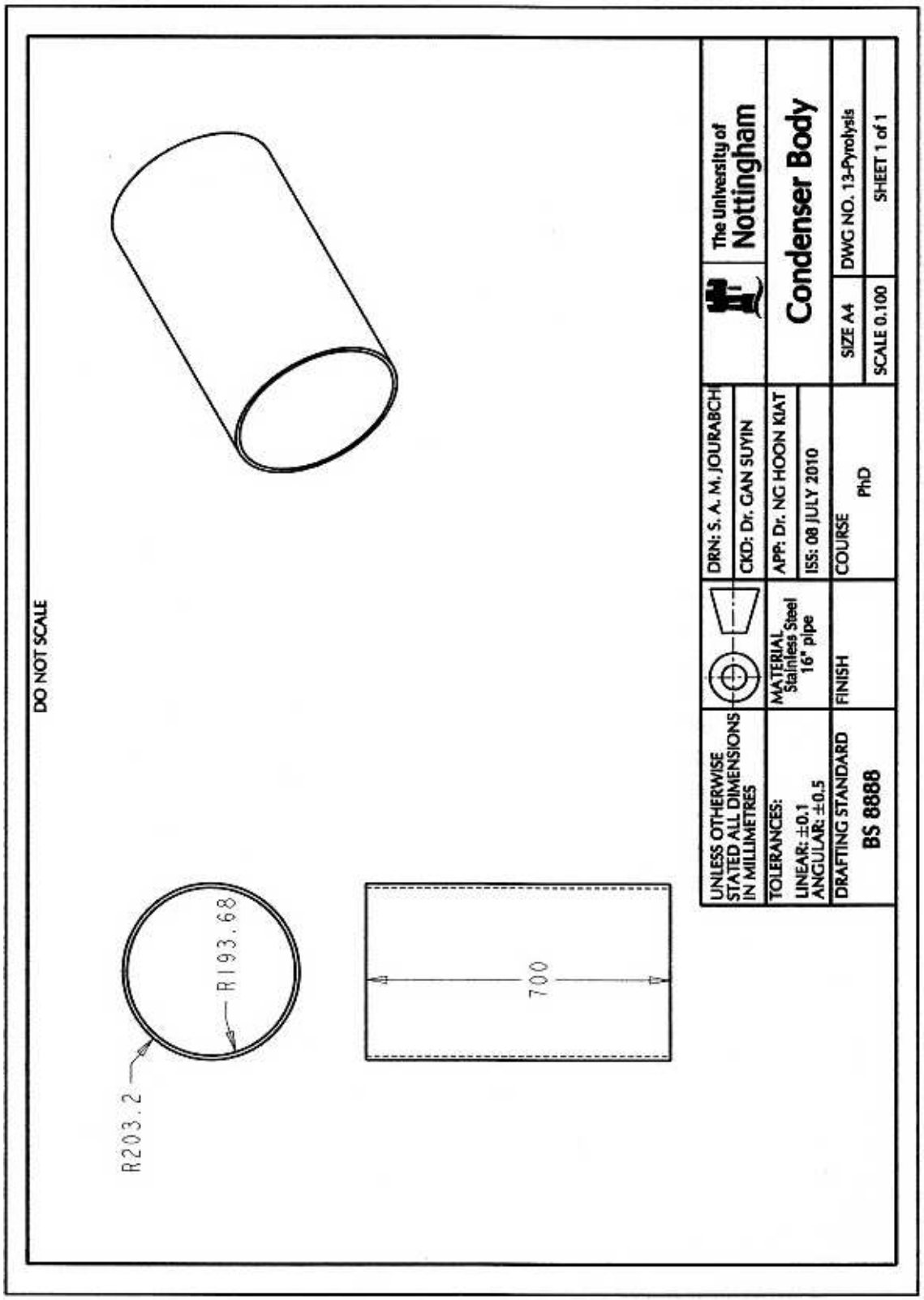
DO NOT SCALE
R203.2
R193.68
700
UNLESS OTHERWISE STATED ALL DIMENSIONS IN MILLIMETRES
TOLERANCES:
UNEAR: ±0.1
ANGULAR: ±0.5
DRAFTING STANDARD
BS 8888
MATERIAL
Stainless Steel 16" pipe
FINISH
DRN: S. A. M. JOURABCHI
CKD: Dr. GAN SUYIN
APP: Dr. NG HOON KIAT
ISS: 08 JULY 2010
COURSE
PhD
The University of Nottingham
Condenser Body
SIZE A4
SCALE 0.100
DWG NO. 13-Pyrolysis
SHEET 1 of 1

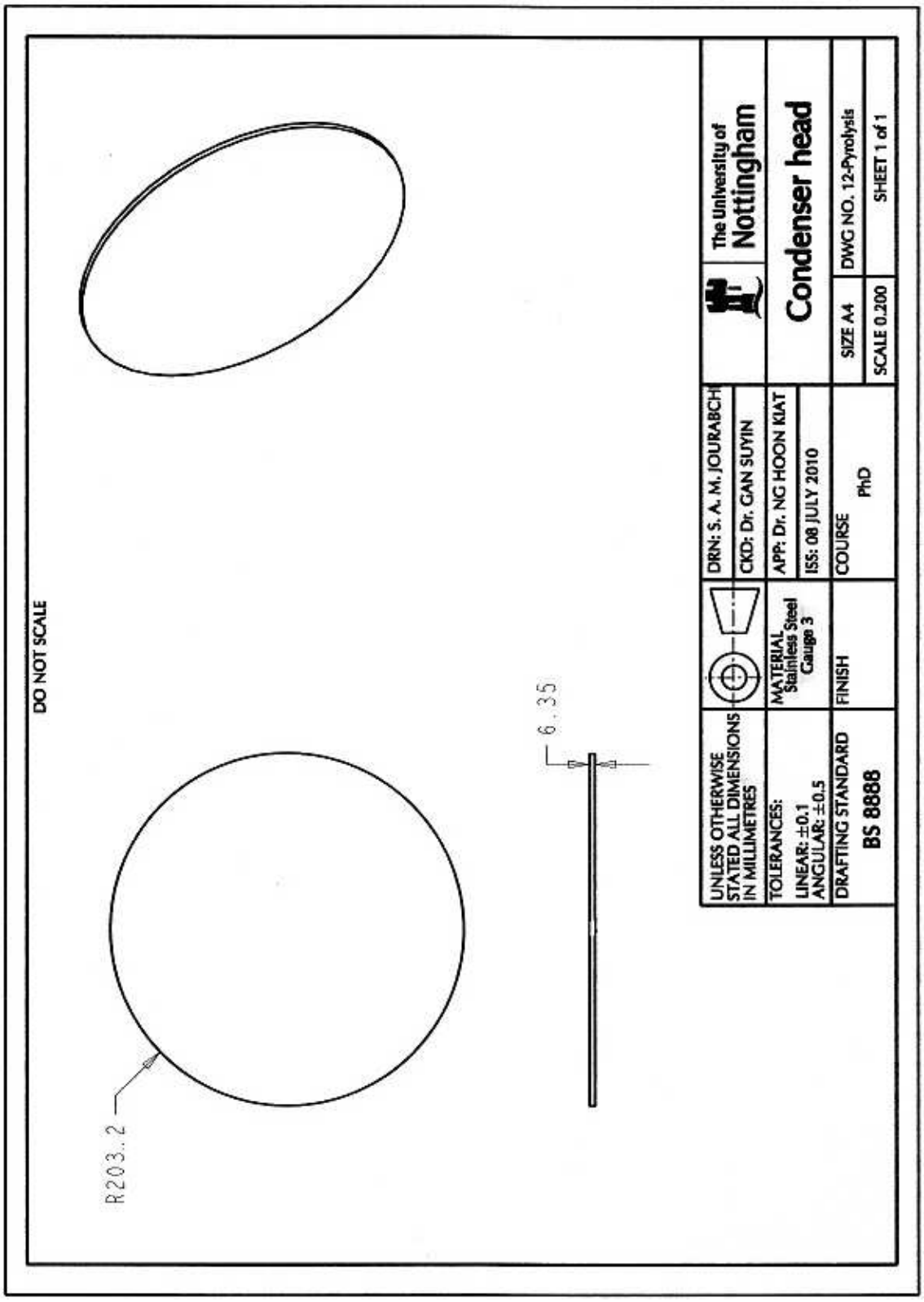
DO NOT SCALE
R203.2
6.35
UNLESS OTHERWISE STATED ALL DIMENSIONS IN MILLIMETRES
TOLERANCES:
LINEAR: ±0.1
ANGULAR: ±0.5
DRAFTING STANDARD
BS 8888
MATERIAL
Stainless Steel Gauge 3
FINISH
DRN: S. A. M. JOURABCHI
CKD: Dr. GAN SUYIN
APP: Dr. NG HOON KIAT
ISS: 08 JULY 2010
COURSE
PhD
The University of Nottingham
Condenser head
SIZE A4
SCALE 0.200
DWG NO. 12-Pyrolysis
SHEET 1 of 1

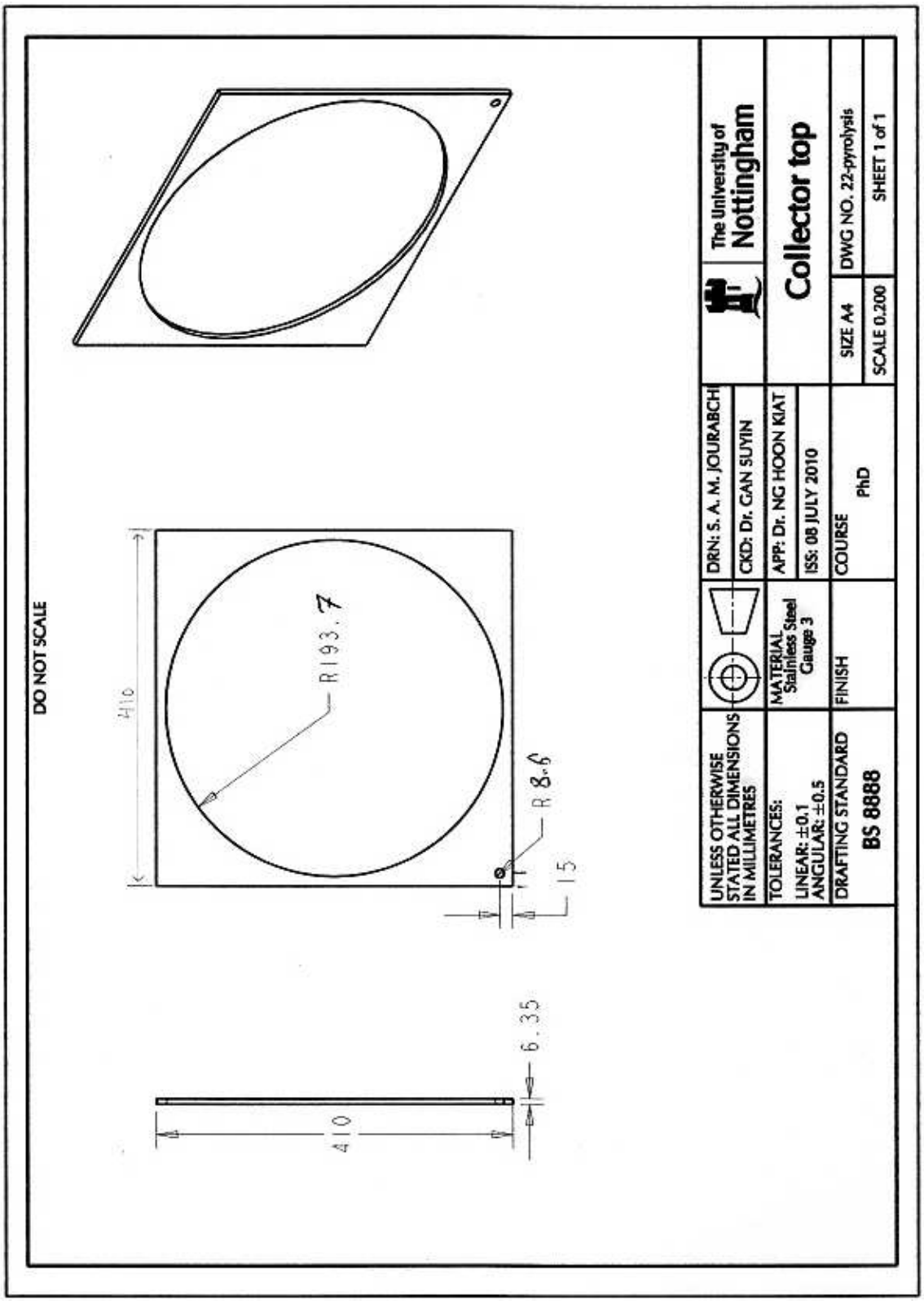
DO NOT SCALE
R193.7
410
R 8.6
15
6.35
UNLESS OTHERWISE STATED ALL DIMENSIONS IN MILLIMETRES
TOLERANCES:
LINEAR: ±0.1
ANGULAR: ±0.5
DRAFTING STANDARD
BS 8888
MATERIAL
Stainless Steel
Gauge 3
FINISH
DRN: S. A. M. JOURABCHI
CKD: Dr. GAN SUYIN
APP: Dr. NG HOON KIAT
ISS: 08 JULY 2010
COURSE
PhD
The University of Nottingham
Collector top
SIZE A4
SCALE 0.200
DWG NO. 22-pyrolysis
SHEET 1 of 1

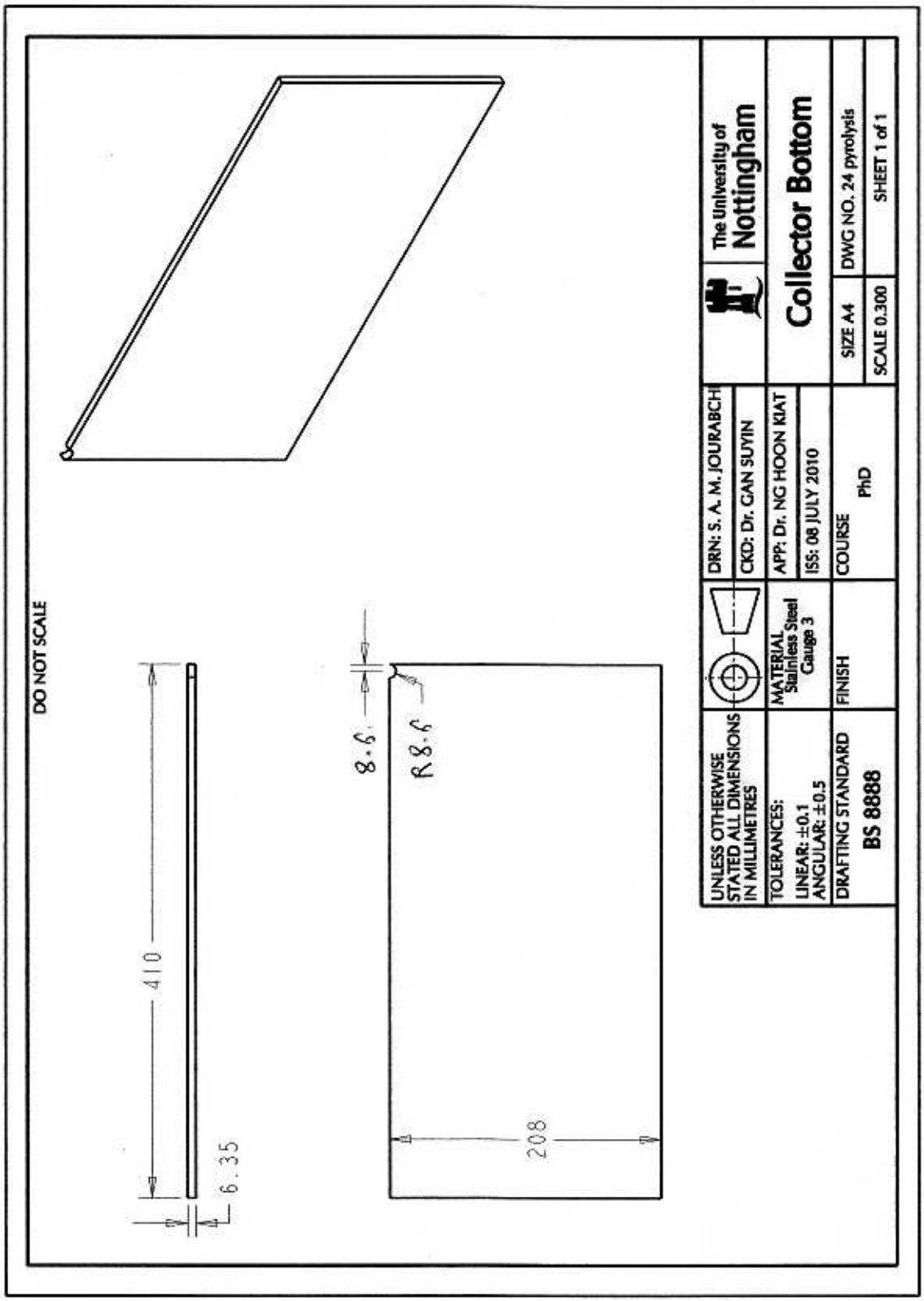
DO NOT SCALE
410
6.35
8.6
R8.6
208
UNLESS OTHERWISE STATED ALL DIMENSIONS IN MILLIMETRES
TOLERANCES:
LINEAR: ±0.1
ANGULAR: ±0.5
DRAFTING STANDARD
BS 8888
MATERIAL
Stainless Steel
Gauge 3
FINISH
DRN: S. A. M. JOURABCHI
CKD: Dr. GAN SUYIN
APP: Dr. NG HOON KIAT
ISS: 08 JULY 2010
COURSE
PhD
The University of Nottingham
Collector Bottom
SIZE A4
SCALE 0.300
DWG NO. 24 pyrolysis
SHEET 1 of 1

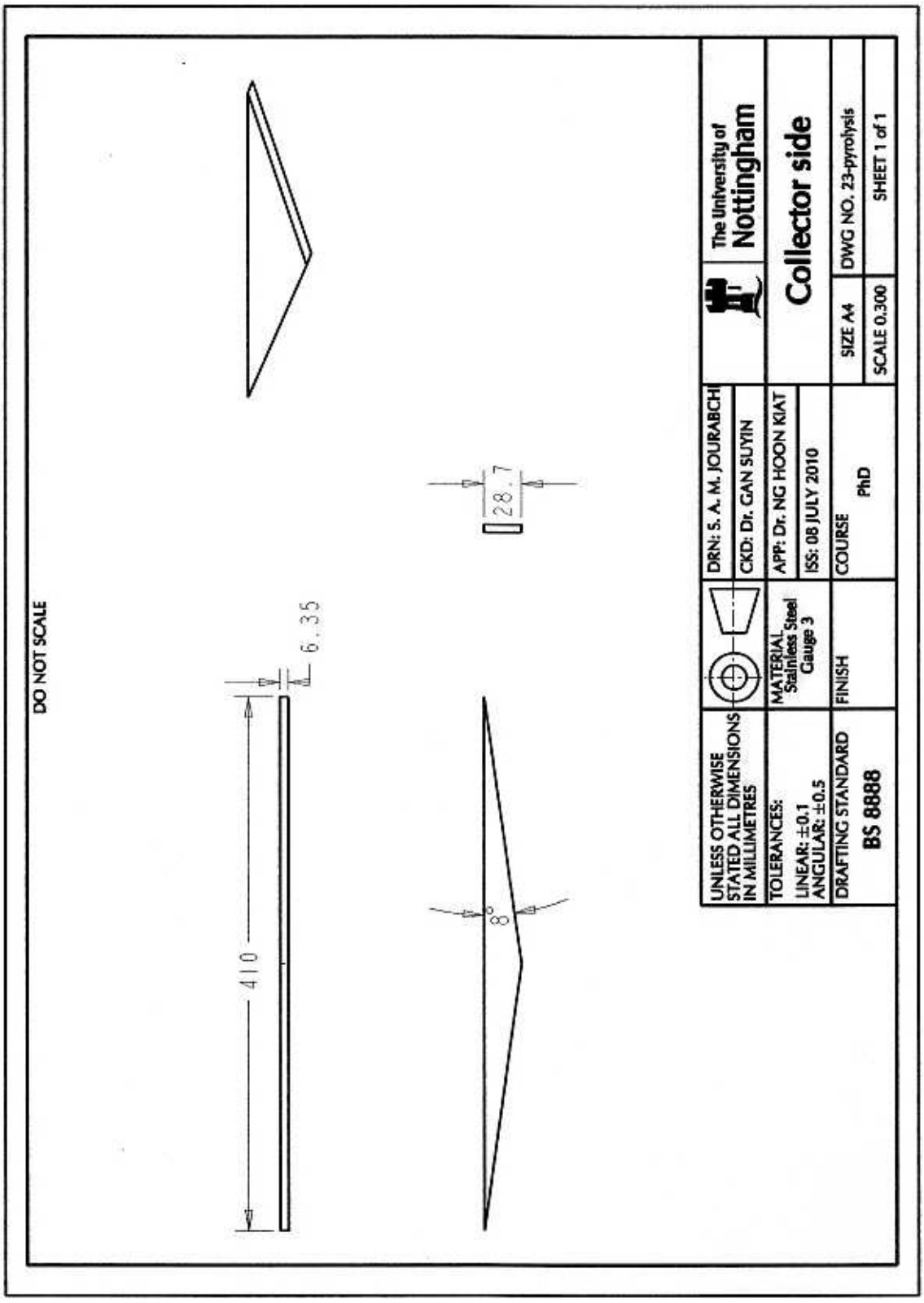
DO NOT SCALE
6.35
410
28.7
8°
UNLESS OTHERWISE STATED ALL DIMENSIONS IN MILLIMETRES
TOLERANCES:
LINEAR: ±0.1
ANGULAR: ±0.5
DRAFTING STANDARD
BS 8888
MATERIAL
Stainless Steel
Gauge 3
FINISH
DRN: S. A. M. JOURABCHI
CKD: Dr. GAN SUYIN
APP: Dr. NG HOON KIAT
ISS: 08 JULY 2010
COURSE
PhD
The University of Nottingham
Collector side
SIZE A4
SCALE 0.300
DWG NO. 23-pyrolysis
SHEET 1 of 1

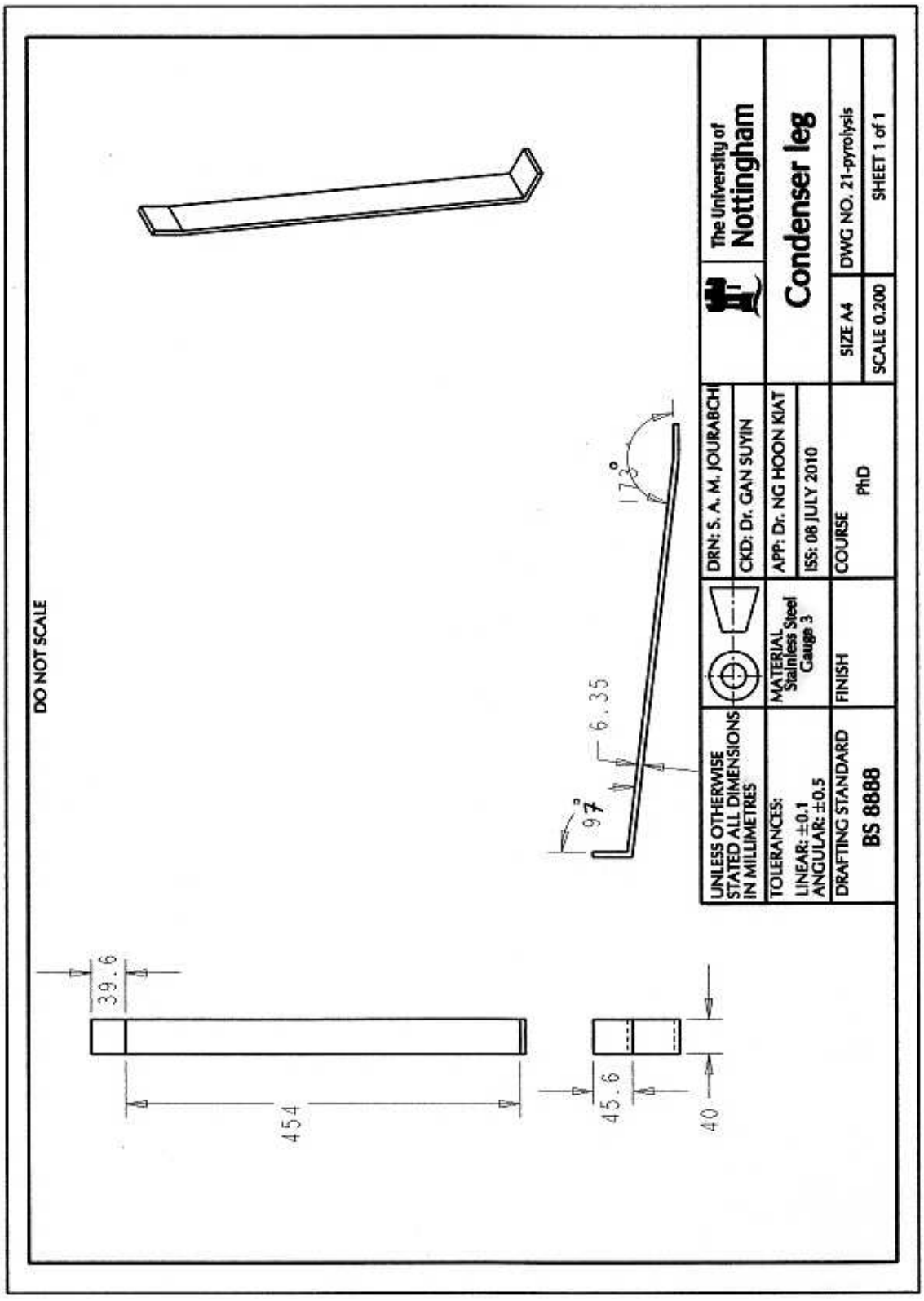
DO NOT SCALE
The University of Nottingham
Condenser leg
DRN: S. A. M. JOURABCHI
CKD: Dr. GAN SUYIN
APP: Dr. NG HOON KIAT
ISS: 08 JULY 2010
COURSE PhD
SIZE A4
SCALE 0.200
DWG NO. 21-pyrolysis
SHEET 1 of 1
UNLESS OTHERWISE STATED ALL DIMENSIONS IN MILLIMETRES
TOLERANCES:
LINEAR: ±0.1
ANGULAR: ±0.5
MATERIAL Stainless Steel Gauge 3
FINISH
DRAFTING STANDARD BS 8888
6.35
97°
173°
39.6
454
45.6
40

Convection reactor's Particle collector major parts

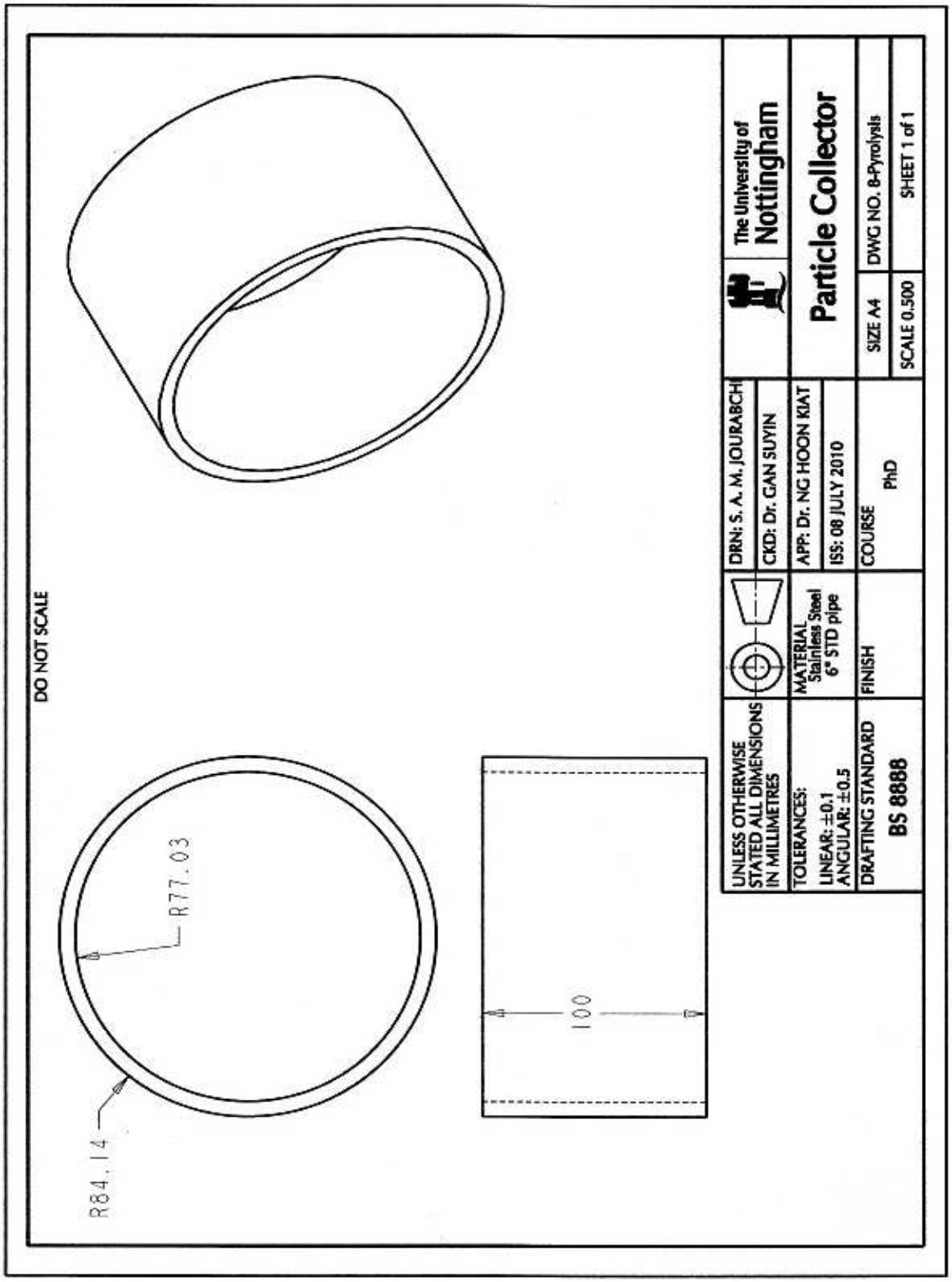

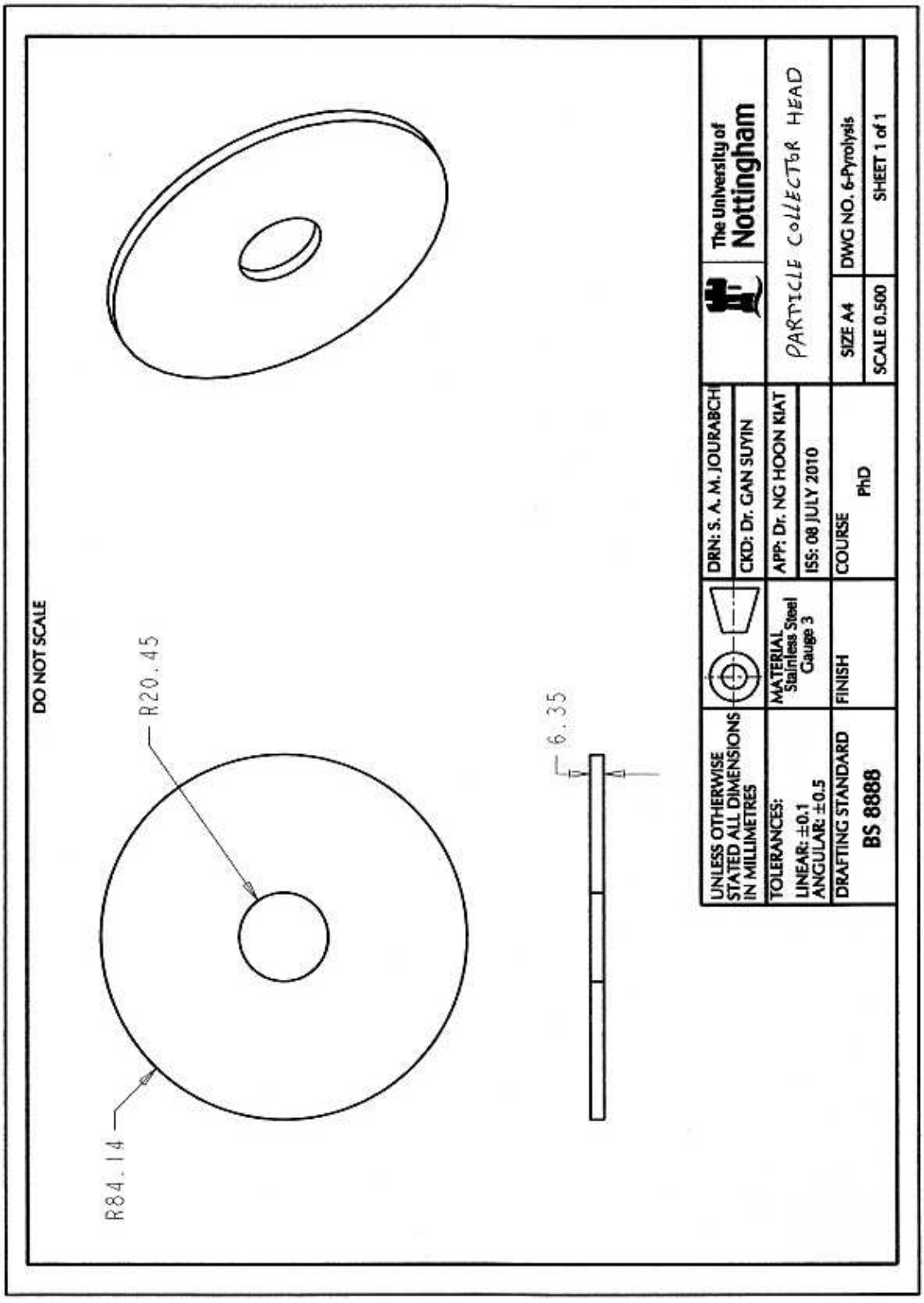
DO NOT SCALE
R20.45
R84.14
6.35
UNLESS OTHERWISE STATED ALL DIMENSIONS IN MILLIMETRES
TOLERANCES:
LINEAR: ±0.1
ANGULAR: ±0.5
DRAFTING STANDARD
BS 8888
MATERIAL
Stainless Steel
Gauge 3
FINISH
DRN: S. A. M. JOURABCHI
CKD: Dr. GAN SUYIN
APP: Dr. NG HOON KIAT
ISS: 08 JULY 2010
COURSE
PhD
The University of Nottingham
PARTICLE COLLECTOR HEAD
SIZE A4
SCALE 0.500
DWG NO. 6-Pyrolysis
SHEET 1 of 1

Convection reactor's bed major parts

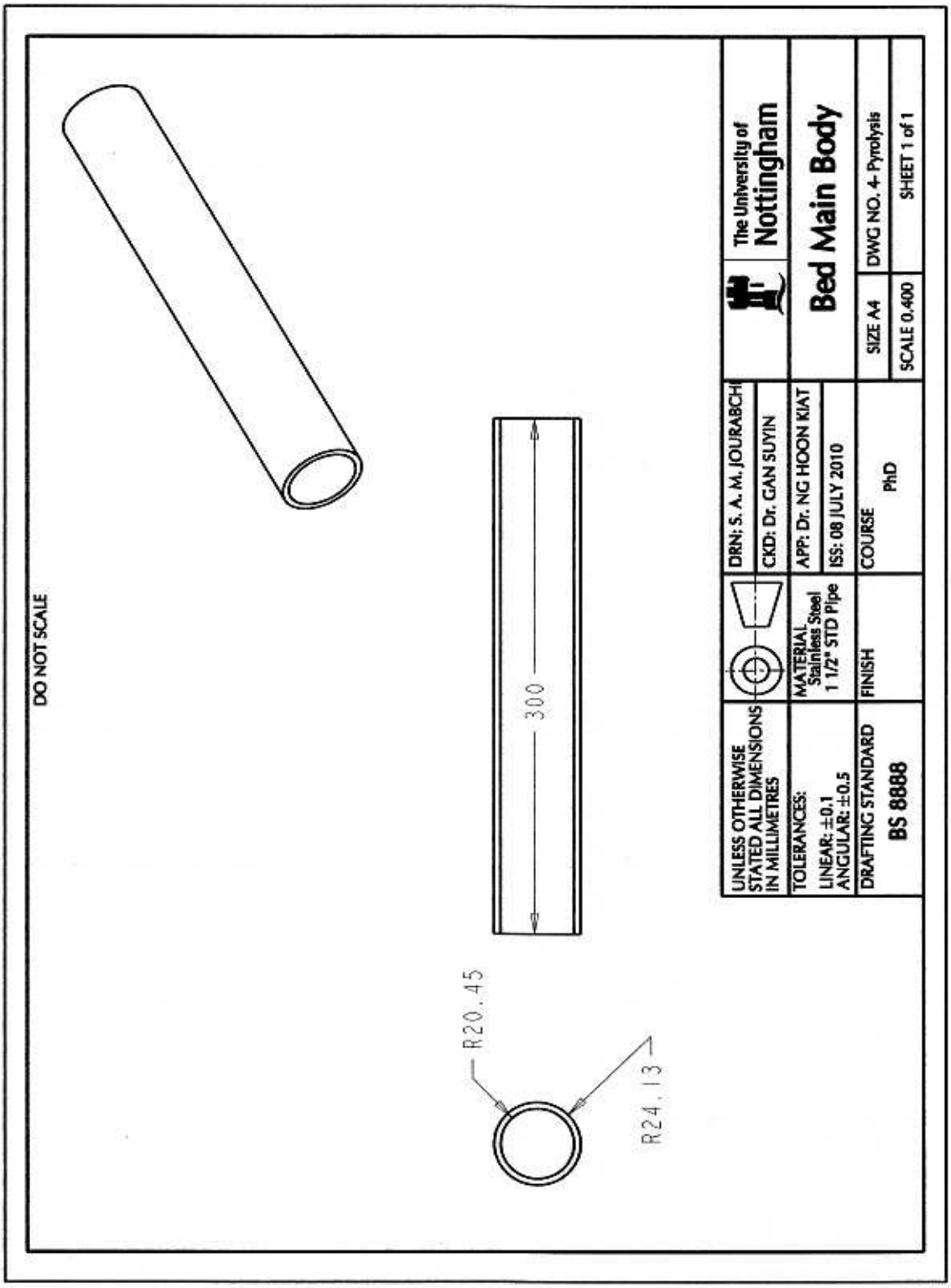

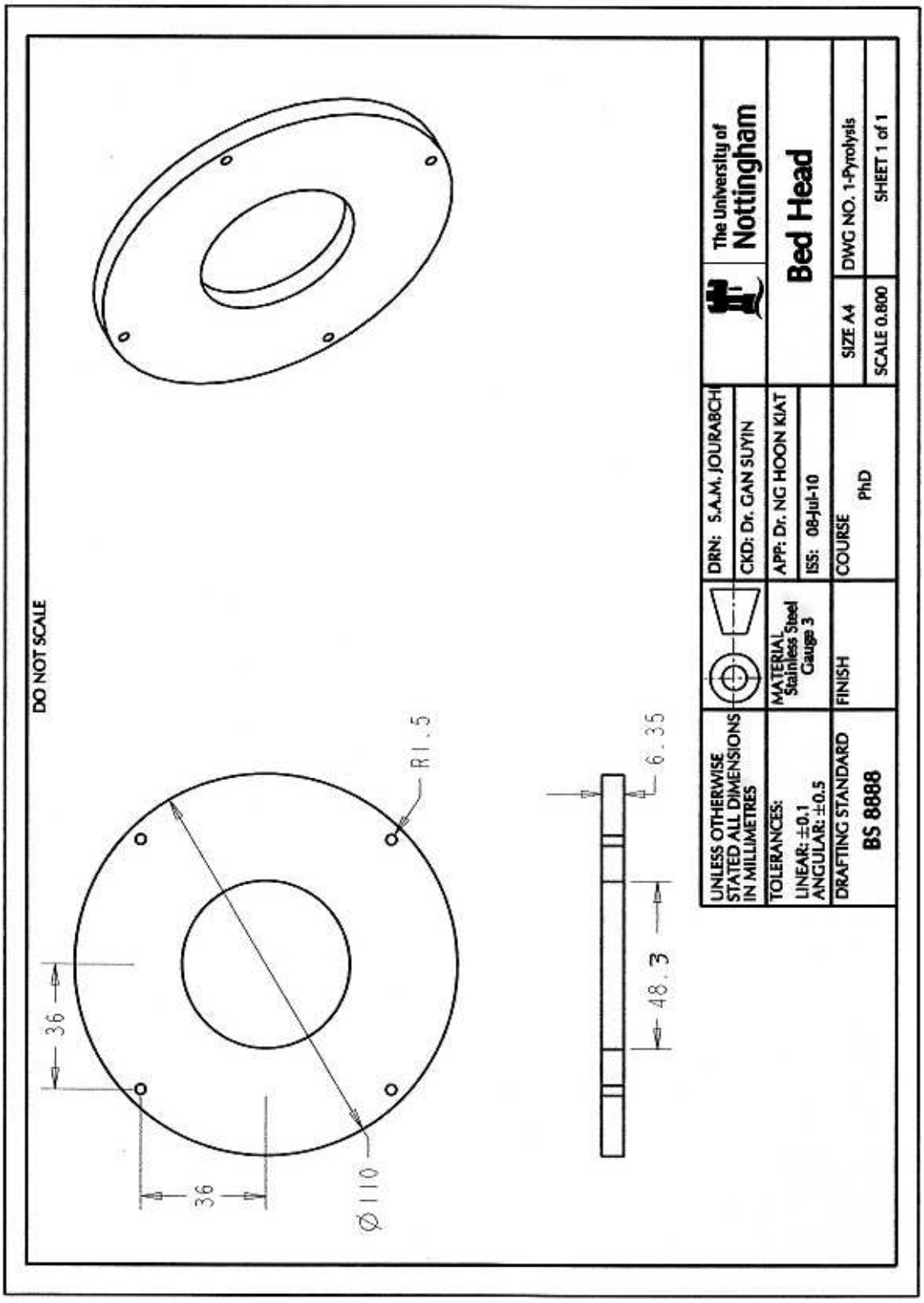
DO NOT SCALE
R1.5
6.35
48.3
36
36
Ø110
UNLESS OTHERWISE STATED ALL DIMENSIONS IN MILLIMETRES
TOLERANCES:
LINEAR: ±0.1
ANGULAR: ±0.5
DRAFTING STANDARD
BS 8888
MATERIAL
Stainless Steel Gauge 3
FINISH
DRN: S.A.M. JOURABCHI
CKD: Dr. GAN SUYIN
APP: Dr. NG HOON KIAT
ISS: 08-Jul-10
COURSE
PhD
The University of Nottingham
Bed Head
SIZE A4
SCALE 0.800
DWG NO. 1-Pyrolysis
SHEET 1 of 1

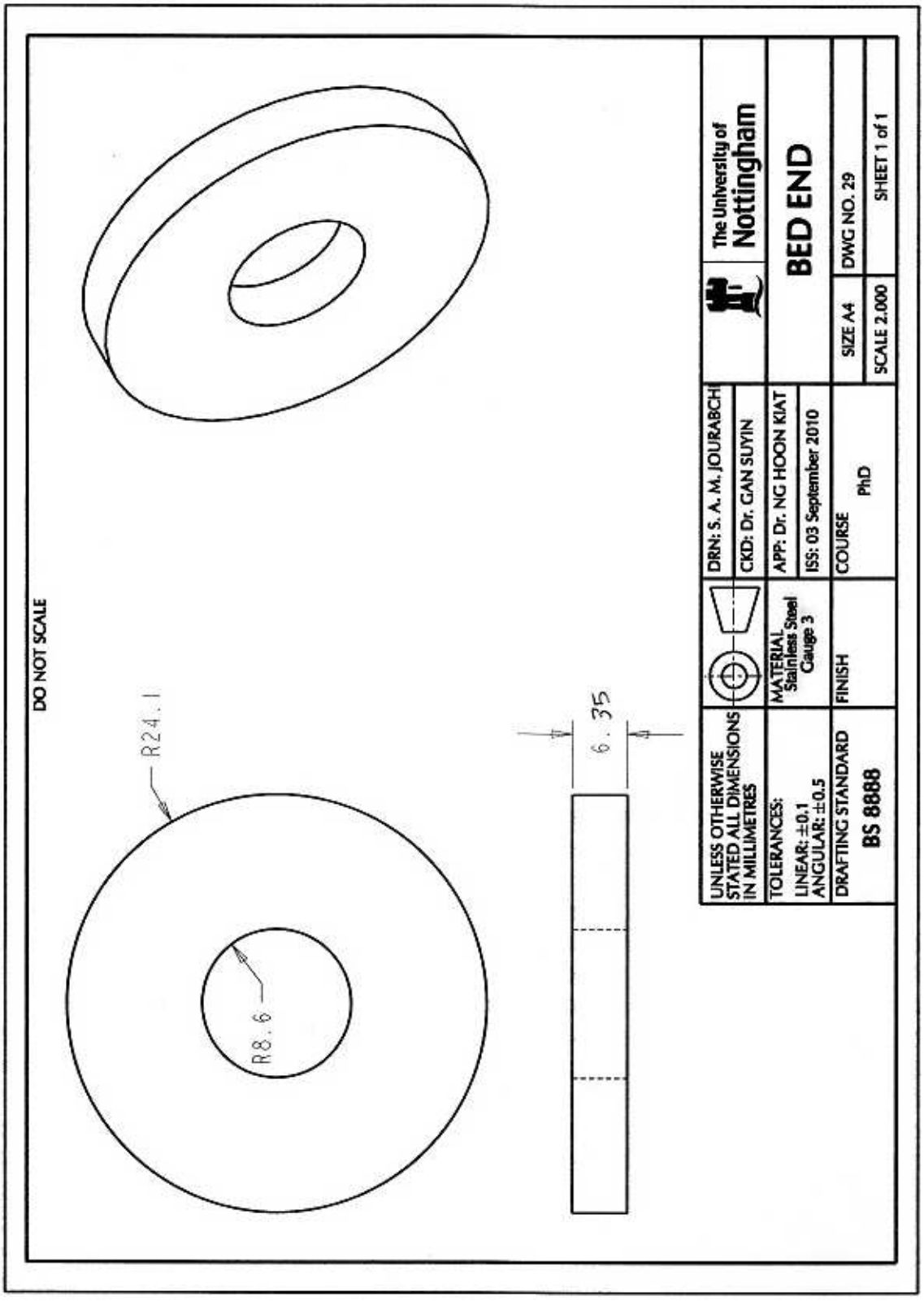
DO NOT SCALE
R24.1
R8.6
6.35
4
UNLESS OTHERWISE STATED ALL DIMENSIONS IN MILLIMETRES
TOLERANCES:
LINEAR: ±0.1
ANGULAR: ±0.5
DRAFTING STANDARD
BS 8888
MATERIAL
Stainless Steel Gauge 3
FINISH
DRN: S. A. M. JOURABCHI
CKD: Dr. GAN SUYIN
APP: Dr. NG HOON KIAT
ISS: 03 September 2010
COURSE
PhD
The University of Nottingham
BED END
SIZE A4
SCALE 2.000
DWG NO. 29
SHEET 1 of 1

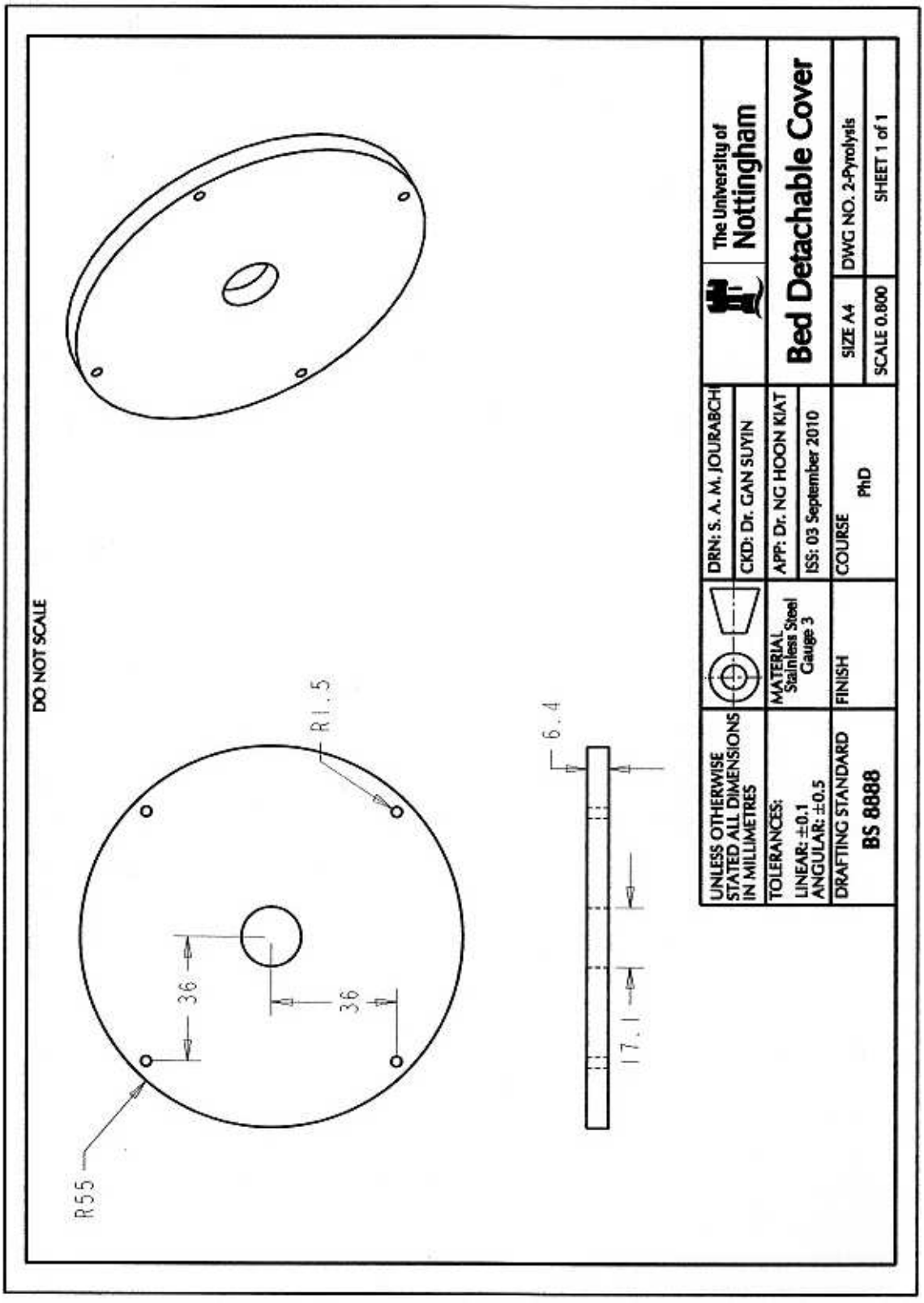
DO NOT SCALE
R55
R1.5
36
36
6.4
17.1
UNLESS OTHERWISE STATED ALL DIMENSIONS IN MILLIMETRES
TOLERANCES:
LINEAR: ±0.1
ANGULAR: ±0.5
DRAFTING STANDARD
BS 8888
MATERIAL
Stainless Steel
Gauge 3
FINISH
DRN: S. A. M. JOURABCHI
CKD: Dr. GAN SUYIN
APP: Dr. NG HOON KIAT
ISS: 03 September 2010
COURSE
PhD
The University of Nottingham
Bed Detachable Cover
SIZE A4
SCALE 0.800
DWG NO. 2-Pyrolysis
SHEET 1 of 1

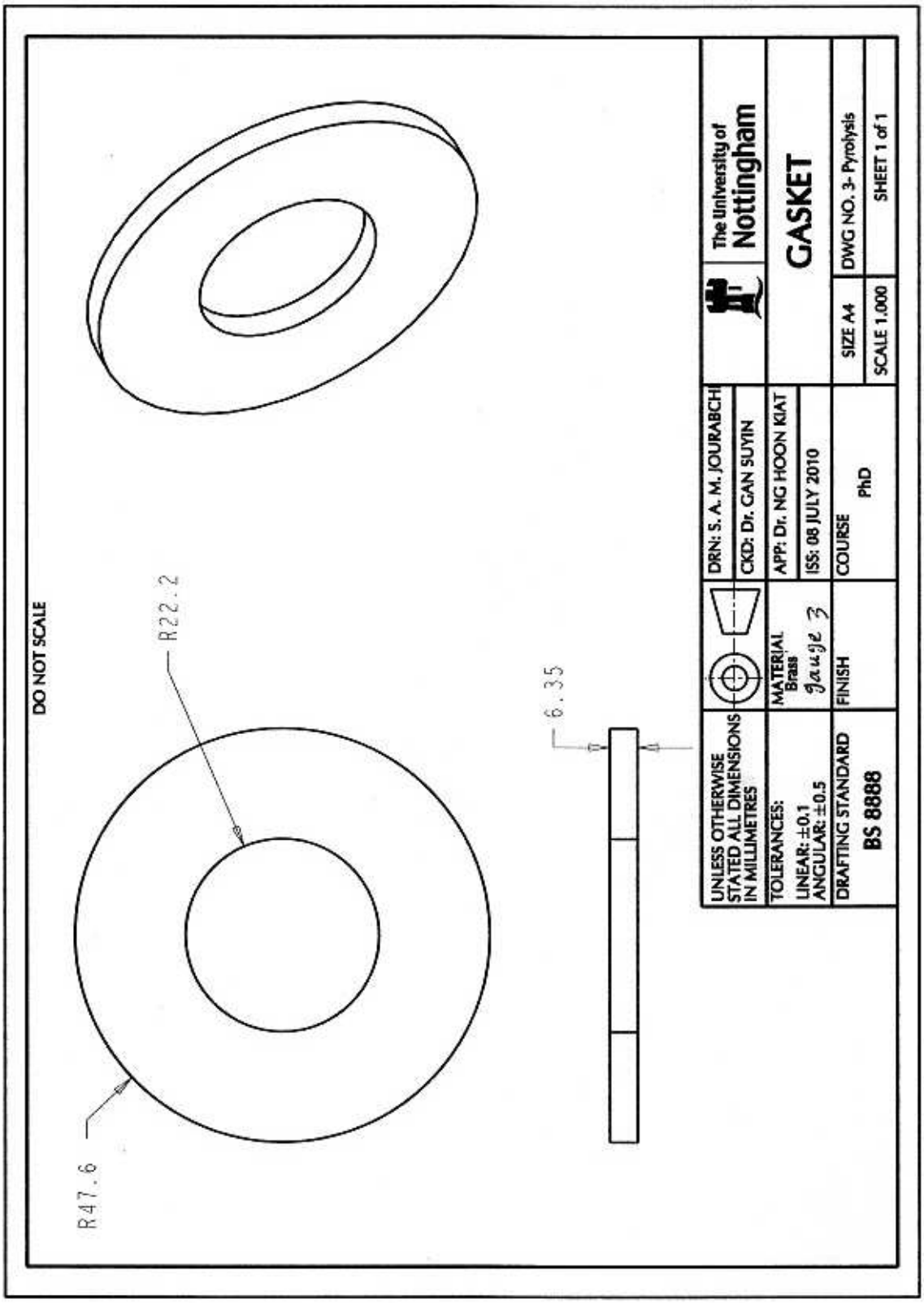
DO NOT SCALE
R22.2
R47.6
6.35
UNLESS OTHERWISE STATED ALL DIMENSIONS IN MILLIMETRES
TOLERANCES:
LINEAR: ±0.1
ANGULAR: ±0.5
DRAFTING STANDARD
BS 8888
MATERIAL
Brass
gauge 3
FINISH
DRN: S. A. M. JOURABCHI
CKD: Dr. GAN SUYIN
APP: Dr. NG HOON KIAT
ISS: 08 JULY 2010
COURSE
PhD
The University of Nottingham
GASKET
SIZE A4
SCALE 1.000
DWG NO. 3- Pyrolysis
SHEET 1 of 1

Convection reactor Pre-heater major parts

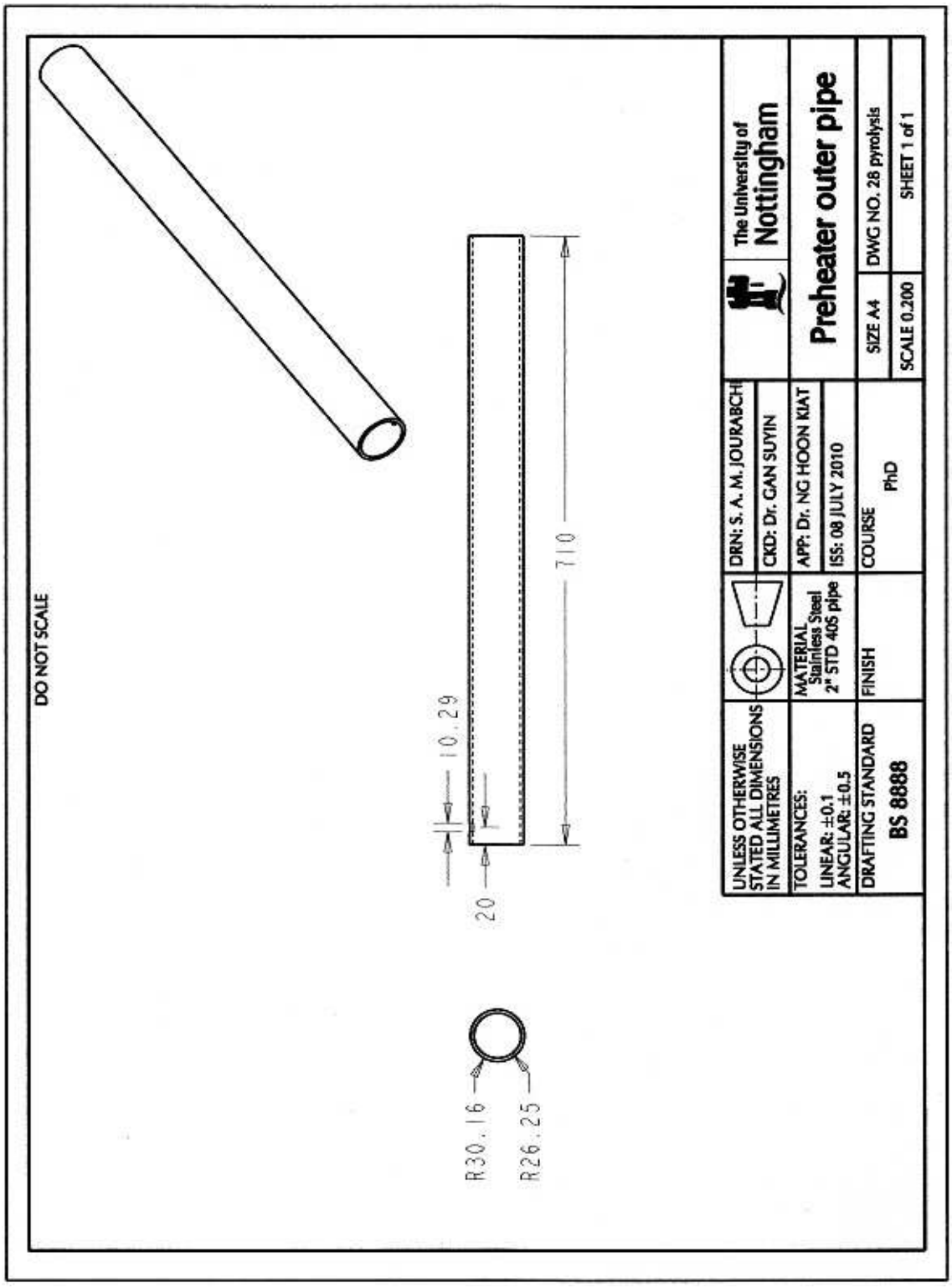

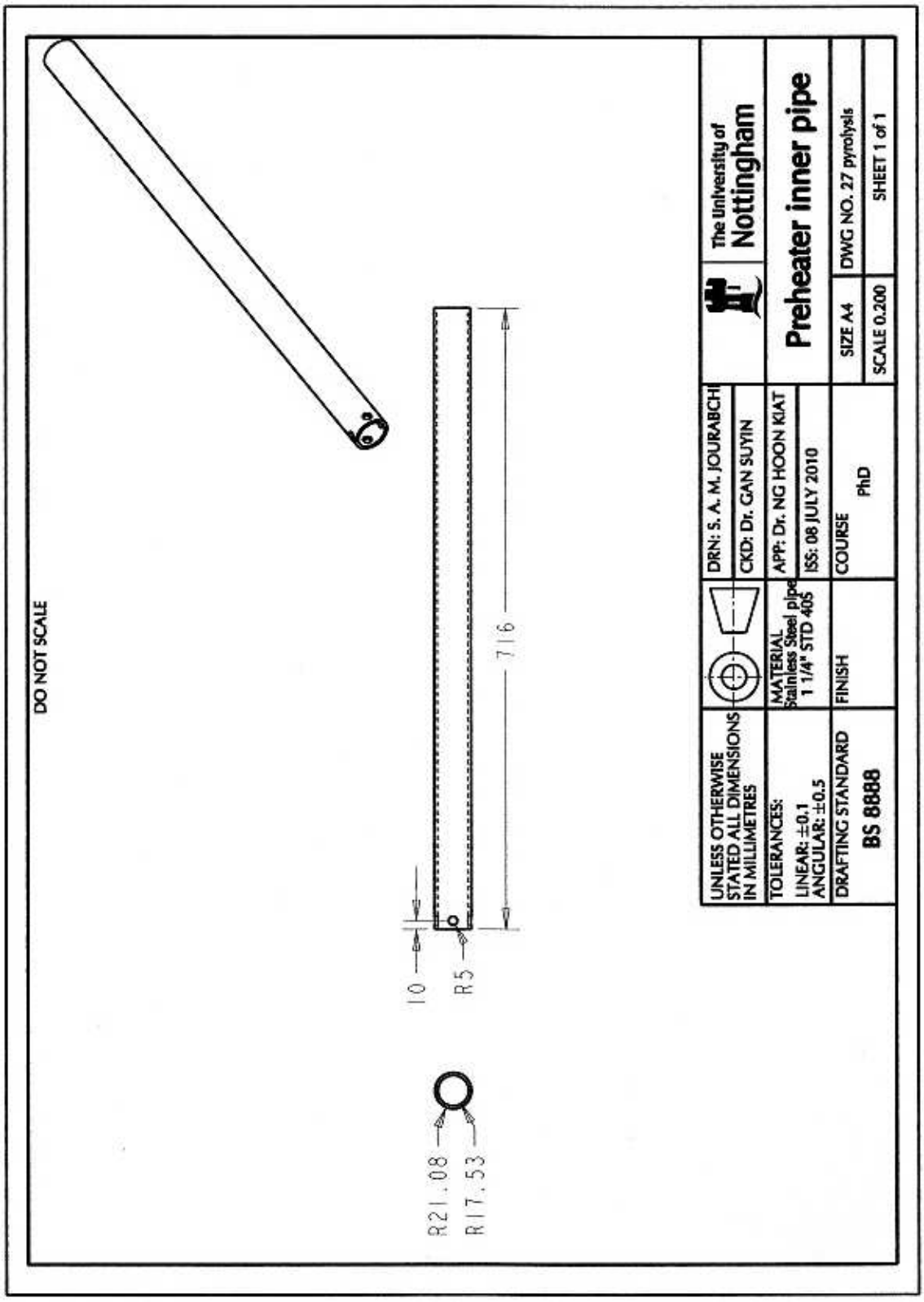
DO NOT SCALE
R21.08
R17.53
10
R5
716
UNLESS OTHERWISE STATED ALL DIMENSIONS IN MILLIMETRES
TOLERANCES:
LINEAR: ±0.1
ANGULAR: ±0.5
DRAFTING STANDARD
BS 8888
MATERIAL
Stainless Steel pipe
1 1/4" STD 40S
FINISH
DRN: S. A. M. JOURABCHI
CKD: Dr. GAN SUYIN
APP: Dr. NG HOON KIAT
ISS: 08 JULY 2010
COURSE
PhD
The University of Nottingham
Preheater inner pipe
SIZE A4
SCALE 0.200
DWG NO. 27 pyrolysis
SHEET 1 of 1

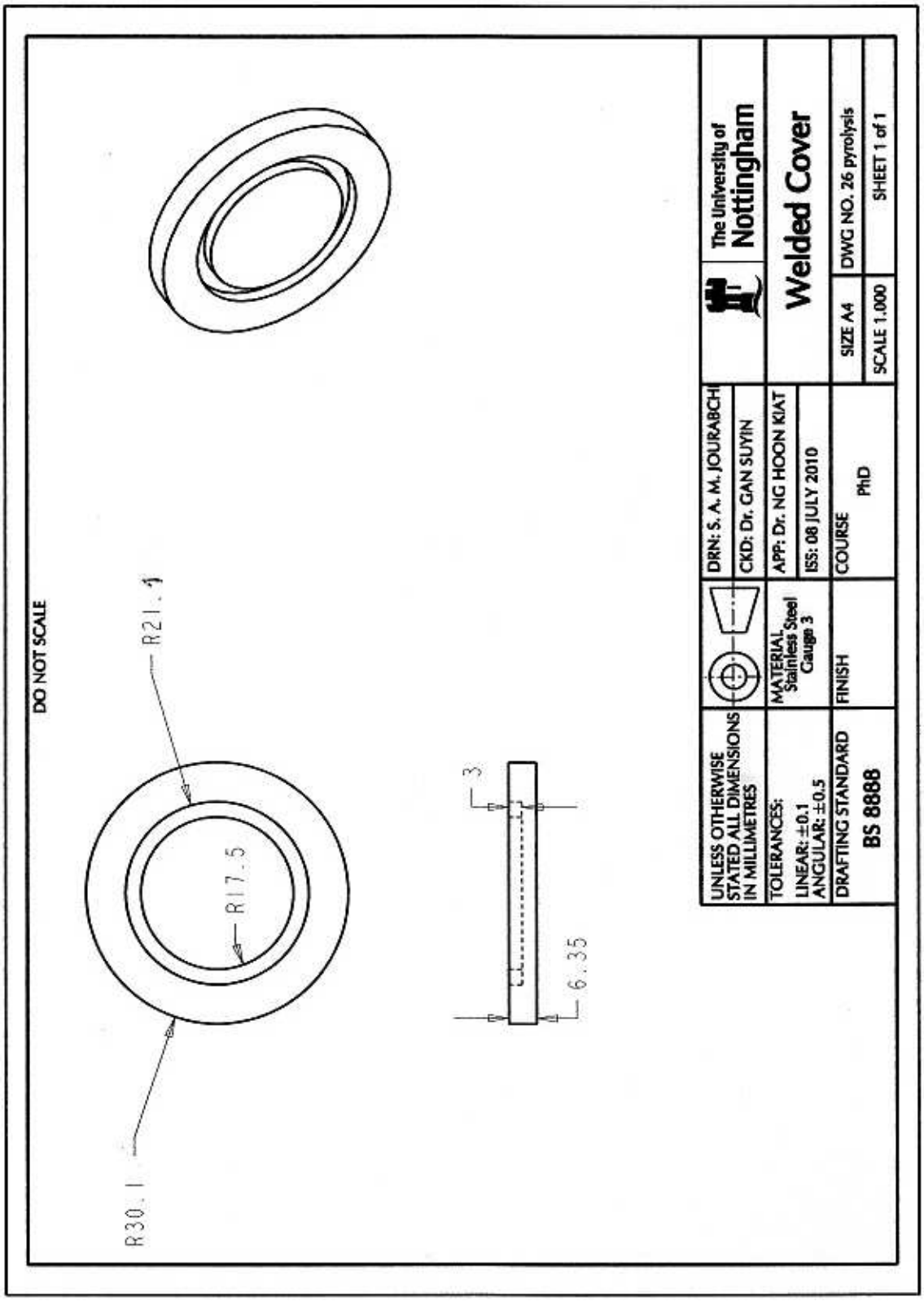
DO NOT SCALE
R21.1
R17.5
R30.1
3
6.35
UNLESS OTHERWISE STATED ALL DIMENSIONS IN MILLIMETRES
TOLERANCES:
LINEAR: ±0.1
ANGULAR: ±0.5
DRAFTING STANDARD
BS 8888
MATERIAL
Stainless Steel Gauge 3
FINISH
DRN: S. A. M. JOURABCHI
CKD: Dr. GAN SUYIN
APP: Dr. NG HOON KIAT
ISS: 08 JULY 2010
COURSE
PhD
The University of Nottingham
Welded Cover
SIZE A4
SCALE 1.000
DWG NO. 26 pyrolysis
SHEET 1 of 1

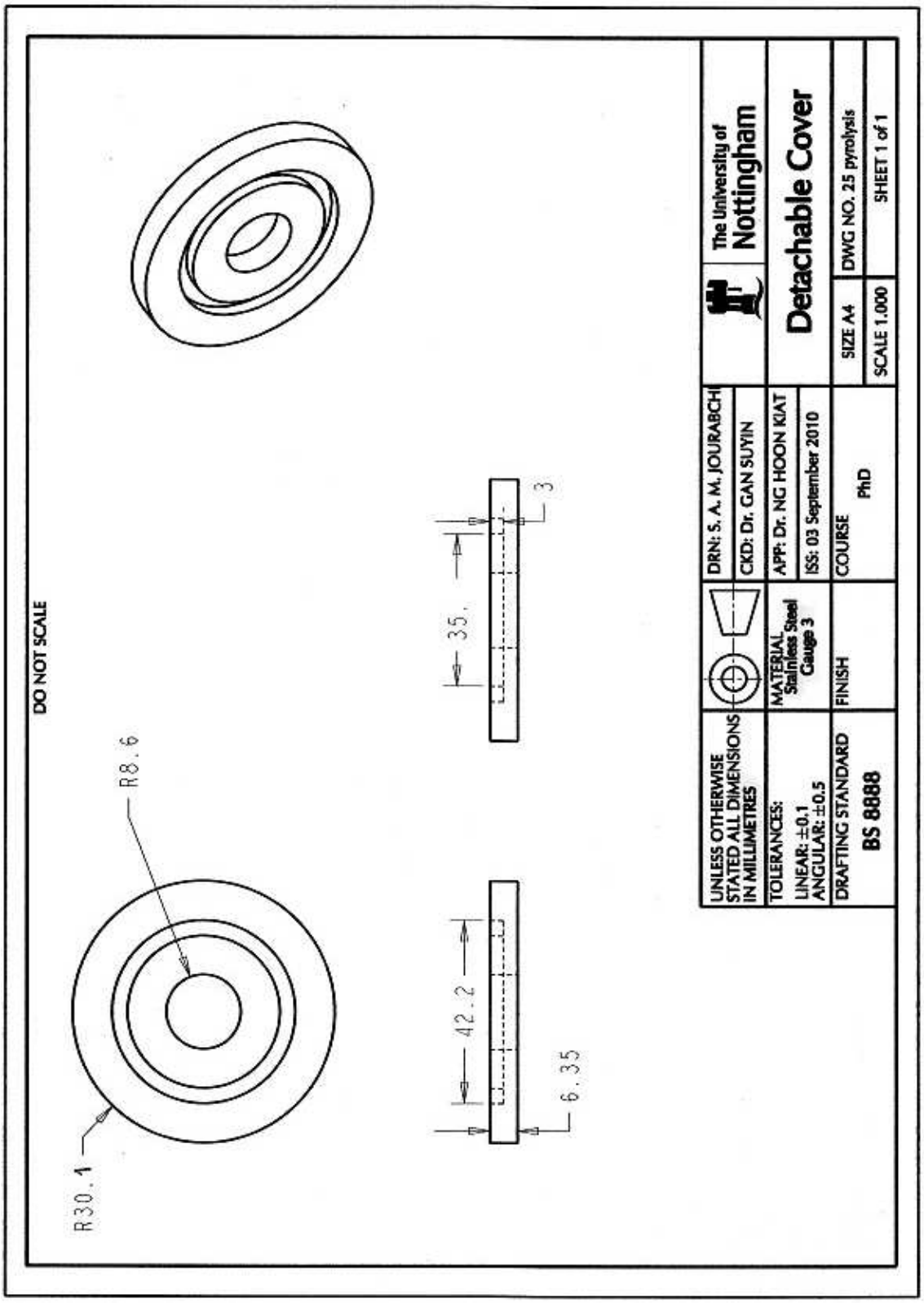
DO NOT SCALE
R30.1
R8.6
42.2
6.35
35.
3
UNLESS OTHERWISE STATED ALL DIMENSIONS IN MILLIMETRES
TOLERANCES:
LINEAR: ±0.1
ANGULAR: ±0.5
DRAFTING STANDARD
BS 8888
MATERIAL
Stainless Steel Gauge 3
FINISH
DRN: S. A. M. JOURABCHI
CKD: Dr. GAN SUYIN
APP: Dr. NG HOON KIAT
ISS: 03 September 2010
COURSE
PhD
The University of Nottingham
Detachable Cover
SIZE A4
SCALE 1.000
DWG NO. 25 pyrolysis
SHEET 1 of 1

APPENDIX C: Fabrication Process

The major fabrication steps for the designed and proposed pyrolysis system are as follows:

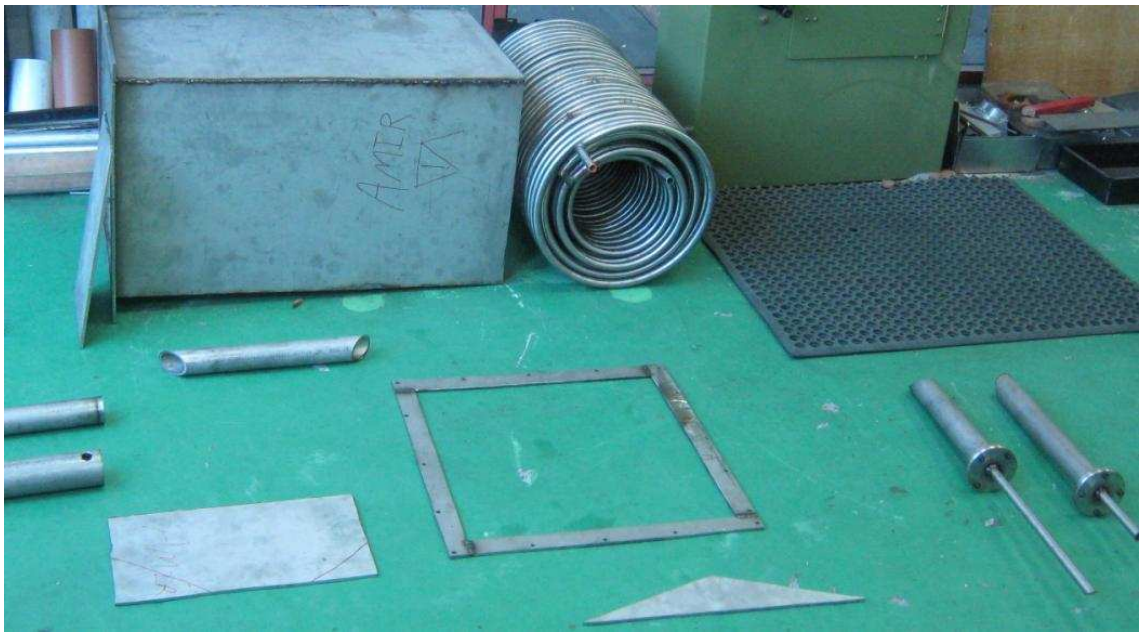

- The stainless steel pipes and sheets have been cut into desired sizes based on the drawings by using electrical saw and hand grinder.

- The sharp edges of the sized and cut steels were flattened and chamfered by hand grinder or file.

- By using the turning machine and drilling, the designed holes have been created.

- Removing the sharp edges in drilled sections was then executed.

- Most of the parts were joined by welding for permanent connections.

- The rest of the parts were joined by bolt and nuts connections.

- By using the turning machine, the main section of the designed high temperature resistant 2-way valve was fabricated.

- Some pipes and valves were joined by threading and tapping that were created by die and tapping tools.

- The bolt and nut joints were sealed by using gasket and vacuum grease and sealant.

- By using 4 bar pressured air, the system was checked for leakage and joint leakages have been sealed as mentioned in Chapter 3.

- Electronic devices such as thermocouples were joined after fabrication, and troubleshooting the system was finally initiated.